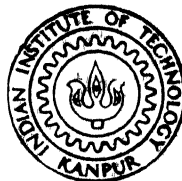


LABORATORY STUDIES ON SUPER-FLUXED IRON ORE SINTERS WITH AND WITHOUT DOLOMITE ADDITIONS

by
PENUMARTHY SIVAGOPAL



DEPARTMENT OF METALLURGICAL ENGINEERING

INDIAN INSTITUTE OF TECHNOLOGY KANPUR

SEPTEMBER 1985

MR
1985
M
SIV
LAB
TH
ME/1985/m
Si 932

LABORATORY STUDIES ON SUPER-FLUXED IRON ORE SINTERS WITH AND WITHOUT DOLOMITE ADDITIONS

A Thesis Submitted
in Partial Fulfilment of the Requirements
for the Degree of
MASTER OF TECHNOLOGY

by
PENUMARTHY SIVAGOPAL

to the

DEPARTMENT OF METALLURGICAL ENGINEERING
INDIAN INSTITUTE OF TECHNOLOGY KANPUR
SEPTEMBER 1985

ME-1985-M-SIV-LAB

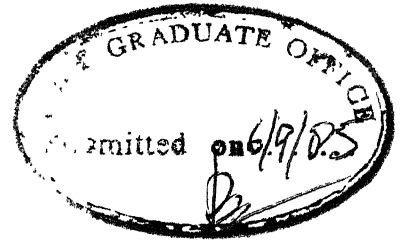
Thesis

669.141

S1 932

-1 06

91871



CERTIFICATE

This is to certify that the present work "LABORATORY STUDIES ON SUPER-FLUXED IRON ORE SINTERS WITH AND WITHOUT DOLOMITE ADDITIONS" by Mr. P. Siva Gopal has been carried out under my supervision and has not been submitted elsewhere for a degree.

Date : 6/9/85

N.K. Batra
(N.K. Batra)
Assistant Professor
Department of Metallurgical Engineering
Indian Institute of Technology
Kanpur-208016 (U.P.)

RECEIVED
DEPARTMENT OF METALLURGICAL ENGINEERING
INDIAN INSTITUTE OF TECHNOLOGY
KANPUR
20/9/85

Acknowledgements

I wish to acknowledge my indebtedness to Dr. N.K. Batra for his help and guidance without which, this work would not have been so exhaustive and yet so brief.

I sincerely thank our laboratory assistants Mr. D.P. Tripathi and Mr. A. Sharma for their cooperation and cordiality throughout the period of this work and the help they extended to me. I thank my friends and colleagues of our Pyrometallurgy laboratory Mr. A.K. Patjoshi, Mr. Praveen Kumar, Mr. Prabhat Tewari, Mr. A.K. Pandey, Mr. G.G. Krishna Murthy, and many others who have given me an opportunity to share their nice company and also the problems whenever faced by me. I extend my sincere thanks to Mr. A.V.V. Satyanarayana for his help in my thesis proof reading and the company he has given me during my stay in IIT Kanpur. My thanks to Mr. Negi who helped me in the welding work of my thesis.

Last but not least a special word of appreciation is given to the typist Mr. Raj Khanna for typing this entire thesis.

Words cannot reveal my appreciation for them, however hard I may try with pen and express my appreciation & thankfulness symbolically.

Author

CONTENTS

	Page
List of tables	... (i)
List of figures	... (ii)
Abstract	... (iii)
Chapter 1	
1.1 Introduction	... 1
Chapter 2 LITERATURE REVIEW	... 4
2.A. Mineralogical study in iron ore sintering	... 4
2.B. Effect of sinter basicity on strength properties	... 9
2.C. Reducibility measurements; Effect of basicity of sinters	... 13
2.D. Effect of Magnesium oxide addition on properties of sinter	... 18
Chapter 3 PLAN OF WORK	... 21
Chapter 4 EXPERIMENTS	... 24
4.1 Materials	... 24
4.2 Equipment	... 24
4.3 Procedure	... 28
Chapter 5 RESULTS	... 33
Chapter 6 DISCUSSION	... 61
6.1 Effect of Moisture on bulk density and permeability	... 61
6.2 Forced draft sintering	... 62
6.3 Reducibility of iron ore sinters	... 68
6.4 Model for shaft reduction of iron ore	... 70

Chapter 7 PROCESS ANALYSIS OF SINTERING

Chapter 8

8.1 Summary and conclusions ...

8.2 Recommendations ...

Chapter 9 APPENDIX

REFERENCES ...

LIST OF TABLES

	Page
1. Degree of reduction of sinter minerals after reduction for 40 minutes in pure CO at 850°C	... 16
2. Source and analysis of materials	... 24
3. Results of crucible studies of oxide mixtures, heated at 1298°C for 1 hour	... 37
4. Results of ^{the} quantitative analysis of raw materials by weight loss method, after heating to specified temperatures	... 38
5. Results of forced draft sintering ^{unit} unit ^{2 (rm) sintering}	... 39
6. Pressure responses in various stages of sintering	... 40
7. Results of reducibility test ^{experiments}	... 51
8. Results of shatter test ^{experiments}	... 59
9. Porosity values calculated for different mixes of cold model studies	... 63
10. Results of reducibility tests	... 76
11. Overall heat balance in sintering.	...

LIST OF FIGURES

	Page
1. Schematic diagram of mineral formation processes of Matsuno study ...	6
2. Chemical compositions of oxide mixtures and their micro structures after heating at 1400°C for 5 mins. in air ...	7
3. Variation in sinter minerology with basicity ...	8
4. Variation of strength with basicity of the self fluxing sinters in the range of 1-3.5 ...	11
5. Variations of sinter strength & production rate with basicity ...	12
6. Reducibility curves for different minerals as a function of time ...	15
7. Schematic diagram of sintering unit ...	25
8. Schematic diagram of reducibility apparatus ...	26
9. Bulk density - Moisture plot ...	36
10-18. SIN I - SIN X 's temperature & pressure responses as a function of time ...	41-50
19-25. Plots of H ₂ flowlet flow rate vs. time from RED 1 to RED 7 ...	52-58
27. Yield ^{and} peak temperature plots for various sinters experiments st ...	67
26. X-ray diffraction patterns of A1, B1 and D1 compounds ...	60
28. Fe-H-O and Fe-C-O equilibrium diagrams ...	69

ABSTRACT

Iron ore sinters with and without calcite and dolomite additions were produced by setting up a forced draft sintering unit in the laboratory. The scientific studies such as the pressure and temperature response measurements to record the progress of sintering by the strength and reducibility determinations have been carried out by performing a large number of experiments. The cold model studies in the determination of the bulk density and permeability of the bed were performed to get information about the porosity and nature of the bed as influenced by the presence of water, fluxes and coke in the bed. The mechanism of bond formation during sintering was studied separately by heating various mixtures of iron ore, calcite, dolomite, sand and graphite materials in a crucible to a high temperature of 1200-1300°C. The quantity of the liquid slag formed and hence the yield and strength of the sintered mass depended upon the temperatures attained by the bed during sintering. The maximum temperatures attained were more when the sintering was carried out at the speed of 0.9-1.0 cm/min compared to 0.5-0.7 cm/min. It was confirmed that good sinters could be produced when the bed reached the temperature of 1150-1200°C in case of fluxed or super-fluxed sinters. The temperatures of around 1200°C were possible only in those cases where fluxes decomposed ahead of the sinter zone so that the calcination of the flux did not absorb heat during

combustion of carbon in the sinter zone. For acid sinters good strength and yields were obtained only when the bed material reached temperature of around 1300°C during the sintering process. The yield ~~in~~ sintered mass was found to be around 50% and the effective yield around 40% in most of the experiments.

Mathematical models based on overall and zonal thermal balances have been developed to describe the process variables which affect the quality and the rate of sintering. Calcite material is known to decompose at slower rate compared to dolomite material so that the expected peak temperatures in the bed are low when large quantity of calcite is added in the sinter mix and the effective yield will be poor.

A mathematical model is developed to describe the reduction behaviour of iron ore in the shaft by H_2 gas. This can be used to estimate the exit gas composition and the degree of reduction as a function of time. The experimental results carried out at 750°C matched with the theoretical predictions if $100\text{--}150^{\circ}\text{C}$ loss in temperature of bed due to cooling by H_2 gas is allowed. Presence of fayalite ($2\text{FeO}.\text{SiO}_2$) in the bed material posed problems in the removal of last 10-30% of the oxygen in the material.

INTRODUCTION

In an integrated steel plant, fines of various raw materials (like Iron ore, limestone, coke, dolomite etc.,) are generated during their mining, transport and comminution stages to the sizes of the requirement. Utilization of these fines becomes a vital factor in view of the economy of the iron and steel industry and also from the view point of environmental pollution. Various processes for agglomeration have been tried in the past three decades but sintering and pelletization were found to be more suitable for the iron and steel industry. Sintering is considered to be a better process among the two, as it yields higher productivity, gives better reducibility, lowers coke rate in a blast furnace, eliminates the need of fluxstone charging and gives better silicon and sulphur control in the hot metal. Sintering is basically the process of incipient fusion of fines to make an agglomerated synthetic mass which possesses sufficient strength to withstand the blast furnace conditions and sufficient porosity to maintain the permeability of the bed inside the blast furnace. They are produced by applying suction at the bottom of the sintering pan or bed leaving the top open. The incoming air (precisely O_2 in the air) reacts with the carbon in coke to produce heat and high temperature for fusion. The fusion zone moves from top to bottom during the sintering

process while the bed itself moves from left to right in an industrial sinter strand.

Sinters may be classified into three types . acid sinters, self-fluxed sinters and super-fluxed sinters. Acid sinters are those which are produced from the iron ore and coke fines without any addition of fluxes. Fluxed sinters are those in which flux has been added to the mix just to nullify the burden acids so that it provides the same basicity ($\frac{\text{CaO} + \text{MgO}}{\text{SiO}_2}$) ratio as desired in the final blast furnace slag. Super-fluxed sinters are those which have very high basicity ratios ($\frac{\text{CaO} + \text{MgO}}{\text{SiO}_2} > 3.0$), they have found applications both in iron making and steel making stages.

The desirable properties of the sinter for its use in blast furnace include high Fe content of the product, good room temperature strength, good strength under high temperature reducing conditions, and good reducibility. These properties are known to be influenced by the process parameters such as the nature and size distribution of raw materials, moisture content, fuel content, speed of sintering, ignition etc., The important scientific studies are due to the bond formation between the particles. The bonding in case of sintering of the metal powders is a physical bond i.e., the bridging of particles in the sinters, but in the case of iron ore sinters the bond is not only physical but also chemical in nature. For acid sinters, the primary liquid formed is due to the formation of low MP fayalite (2 FeO SiO₂) phase while for fluxed and superfluxed sinters, the formation of dicalcium ferrites, or calcium diferrites prevent the

formation of wustite acid then contribute to high reduction strength. It has been found¹ that among the ferrites, CF_2 is most reducible while C_2F is most irreducible.

Attempts have been made in the recent past to replace CaO by MgO ². These resulted in the formation of magnessio-spinels and suppression of the formation of Ca-Ferrites as well as hematites, and dicalcium silicates. The inclusion of MgO as a constituent in the sinter³, is mainly intended to obtain a blast-furnace slag containing 6-14% MgO to achieve optimum slag conditions in terms of good flowability and easy sulfur removal. The main effects of mineralogical phases with special reference to MgO addition in superfluxed sinters are discussed in this thesis. The experiments were mostly conducted in the modified system of the existing forced draft iron ore sintering unit in the laboratory⁴. Suggestions for improved performances for the industrial prediction of superfluxed iron ore sinters are included by developing the process models to describe the sintering process.

CHAPTER-II

LITERATURE REVIEW

2.A. Mineralogical study in Iron ore sintering

Self fluxing sinters may consist of several kinds of minerals such as iron oxides, calcium ferrites, calcium silicates, glassy slags etc., Their formation in the sinters vary with basicity and type of flux added. These minerals in the sinters are found to affect the metallurgical properties of sinters such as mechanical strength at room temperature, reducibility, degradability during reduction at around 550 C.

Ekertorp⁵ presented a nice review of agglomeration of iron bearing minerals. He discussed different factors influencing the form and speed at wave passing through a sinter bed, and the importance of heat exchange process, high reducibility and good strength attainment by the formation of calcium ferrites in high-lime sinters. The porous and open structure of low-fuel sinter according to Rist⁶ shows a microstructure wherein the iron oxide remains in its original form and is not recrystallised from a melt, as would be the case at higher temperatures. It has also been found that the Fayalite ($2\text{FeO} \cdot \text{SiO}_2$) occurred only in siliceous feeds with high fuel contents. Fumio Matsuno⁷ have recently reported extensive study on mineral changes during sintering. He made mixture of fine powders with

basicities of 0.6 to 5.0 consisting of 80% hematite, slaked lime, and quartz which were rapidly heated to 900 °C to 1400°C and cooled in air. The process of the formation of minerals during rapid heating was examined. They presented a schematic diagram of mineral formation processes of 80% Fe_2O_3 -CaO-SiO₂ system as shown in Fig. 1. It was studied that assimilation of quartz and the melt of calcium ferrite proceeds in the following three steps.

- (a) Molten silicate slag with low basicity is formed around quartz, and quartz dissolves into the melt.
- (b) Molten silicate slag reacts with molten calcium ferrite and hematite precipitates at the boundary of the two melts.
- (c) Hematite is divided into particles by molten silicate slag, and the reaction between the two melts continues until the assimilation completes even if the temperature is comparatively low.

After the completion of the reaction mentioned above characteristic microstructures are formed according to the basicities. The minerals formed with the mixtures of basicity lower than 1.6 consist of glassy silicate and secondary hematite or granular hematite originated from calcium ferrite, those having basicity greater than 2.0 consist of calcium ferrite and dicalcium silicate. Hematite particles coarsen as the temperature increases, and some of them change into magnetite particles

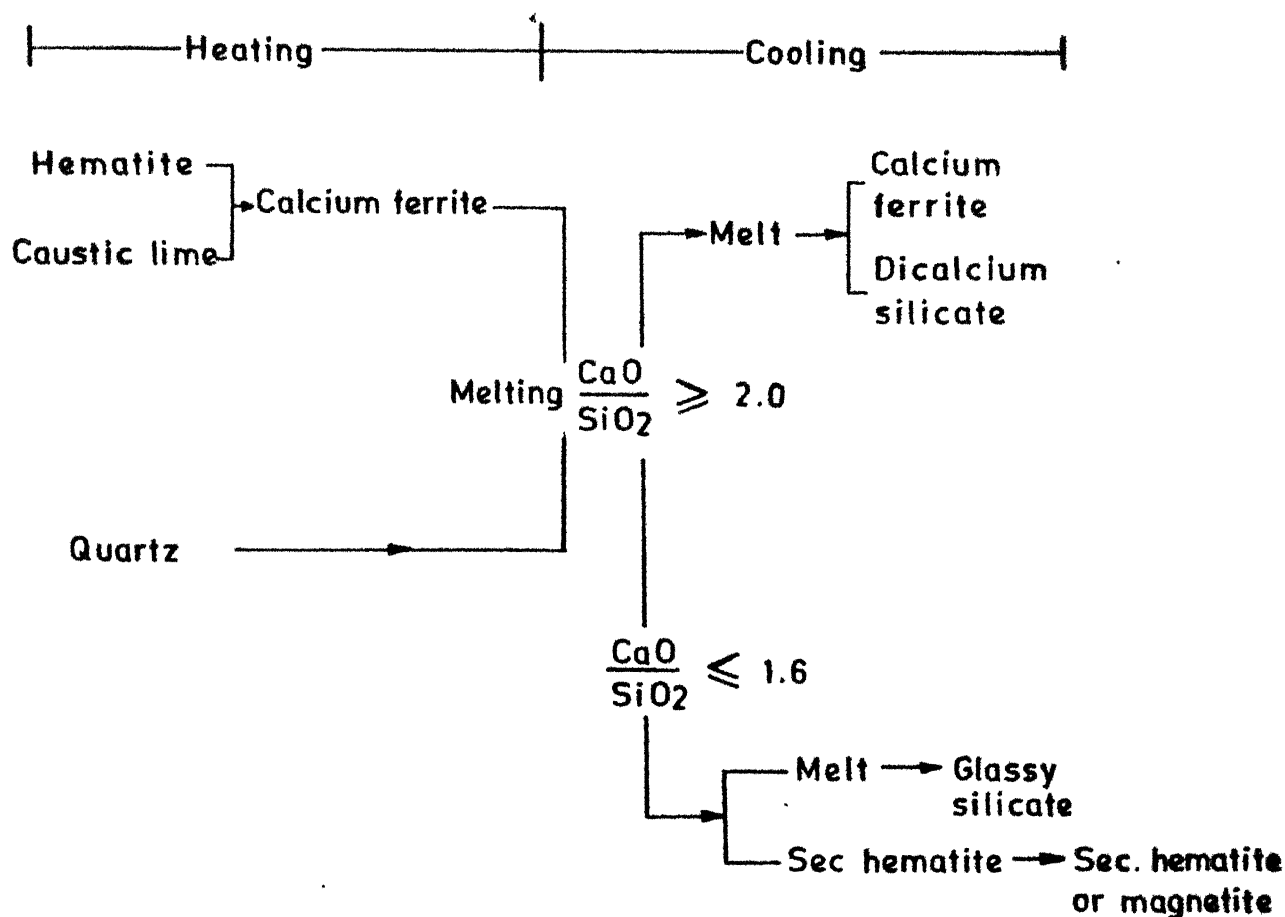
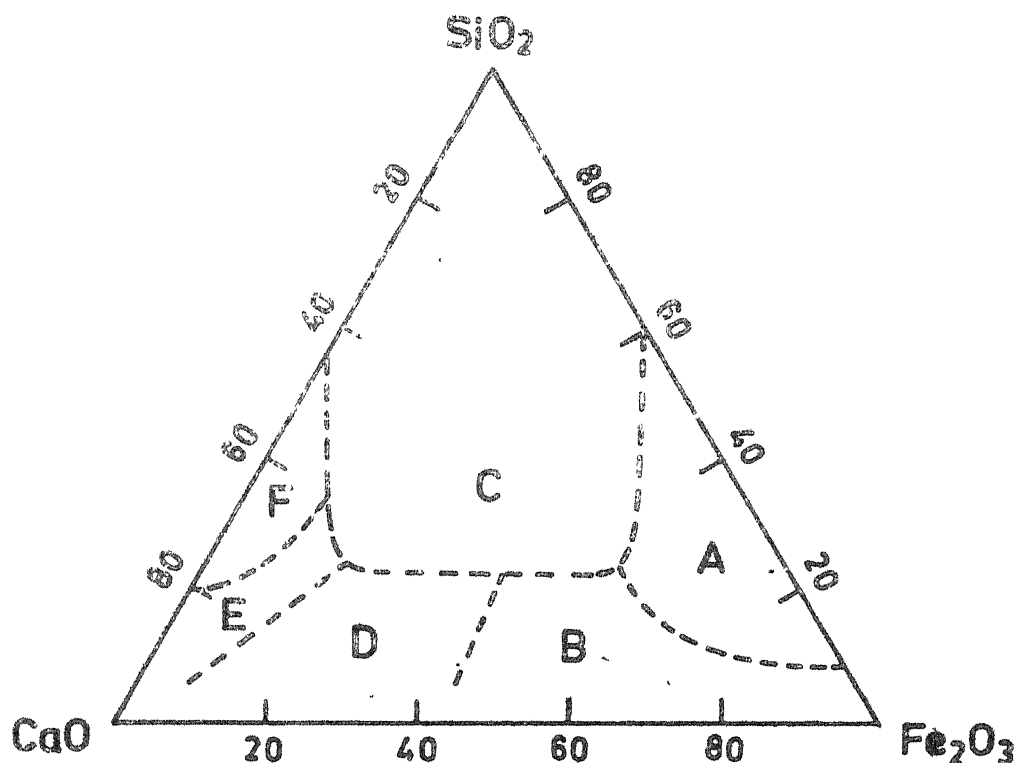


Fig.1 Schematic diagram of mineral formation processes of mixtures 80% Fe_2O_3 - CaO - SiO_2 system ⁽⁷⁾

which has larger coarsening rate than hematite. Chemical compositions of examined oxides by Matsuno after heating at 1400°C for 5 mins. in air are shown in Fig. 2. Sinter mineralogy changes with basicity⁸. As shown in Fig. 3, when CaO increases the coke rate for sinter plant decreases due to the formation of low melting CaO-Fe₂O₃ phase. As silica content increases, may be due to coke ash and iron ore, it yields more glassy slag. It has been reported that dolomite additions promote magnetite formation by substitution of Mg²⁺ for Fe²⁺ in the magnetite lattice. Increase in MgO content shifts the mineralogical changes to the right in Fig. 3.

2.B. Effect of sinter basicity on strength properties

Glassy slag and dicalcium silicates are presumed to be detrimental to the mechanical strength, because the former is brittle and the later has the allotropic transformation with a larger volume change. During reduction of the sinters (at around 550°C) of the self-fluxing type, the carbon deposition in the sinters resulting from CO gas was considered as the cause for the degradation of sinters⁷. However it has been found that degradation takes place during reduction in H₂ gas. This is considered to occur due to the larger volume change resulted from reduction of hematite to magnetite. ~~With the addition of lime dust strength deteriorates.~~ With an increase in MgO content strength again deteriorates. In general increased



- A - Hematite + Magnetite + Glassy slag
- B - Calcium ferrite + Magnetite + Dicalcium silicate
- C - Glassy slag
- D - Dicalcium silicate + Calcium ferrite
- E - Dicalcium silicate + Glassy slag
- F - Monocalcium silicate + Glassy slag

Fig. 2 Chemical compositions of oxide mix. and their microstructures after heating at 1400°C for 5 minutes in air.⁽⁷⁾

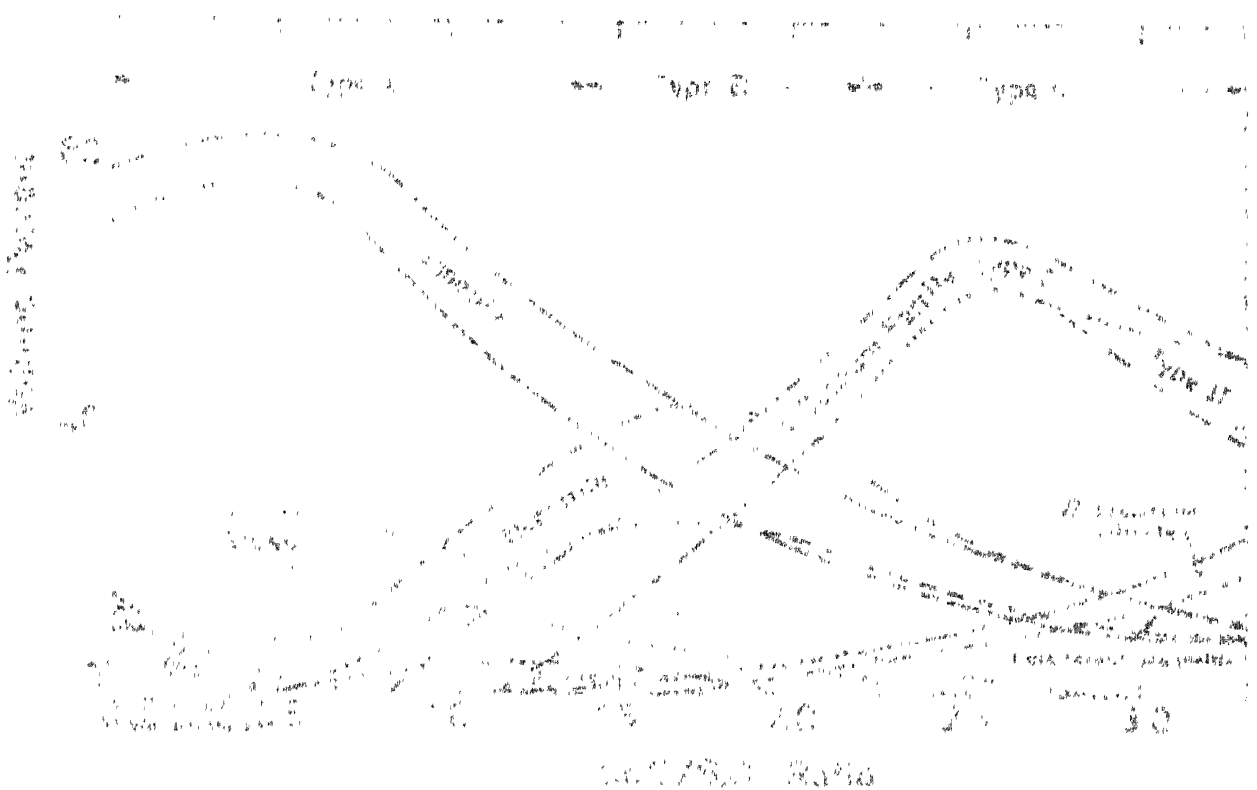


Fig. 2. Relationship between refractive index and change in viscosity (8)

Type A: up to 1.4 CaO/SiO_2 ratio

Type B: 1.4 to 2.2 CaO/SiO_2 ratio

Type C: greater than 2.2 CaO/SiO_2 ratio

MgO, CaO addition contributes to lower sinter cold strength³. However for sinters in the lower basicity range, small MgO additions have a beneficial effect. For CaO-rich sinters the presence of ferrites is the main strength contributing factor and for MgO-rich sinters the precipitation of olivines in the glass matrix contributes to higher strength of sinters. Presence of large slag pools and/or the precipitation of dicalcium silicates appear to have deteriorious effect on the strength of sinters. Mazanek³ investigated the properties of self fluxing sinters in the basicity range of 1.0 - 3.5. According to him strength of sinter varies with basicity as shown in Fig. 4. The low strength of sinter of $B \approx 1.4-2.2$ is connected with the presence of calcium orthosilicate, β -2CaO.SiO₂. The allotropic transformations of β -2CaO.SiO₂ on the cracking of the sinters is also confirmed by Mazanek. Sintors of basicity above 2.2 are satisfactory; the presence of large amounts of plate stick and needle shaped ferrites and the presence of 3CaO.Fe₂O₃ favour the strength of these sinters.

Testing of laboratory sinters made from Lackawanna⁹ mixes had shown that little change in tumbler strength or net production rate would occur as the basicity ($B = \frac{\%CaO + \%MgO}{\%SiO_2 + \%Al_2O_3}$) increased from the self-fluxing level of 1.0 to a super-fluxing level of 2.3. Further testing showed that as basicity goes from 2.3 to 4.0, sinter strength goes up but sinter production

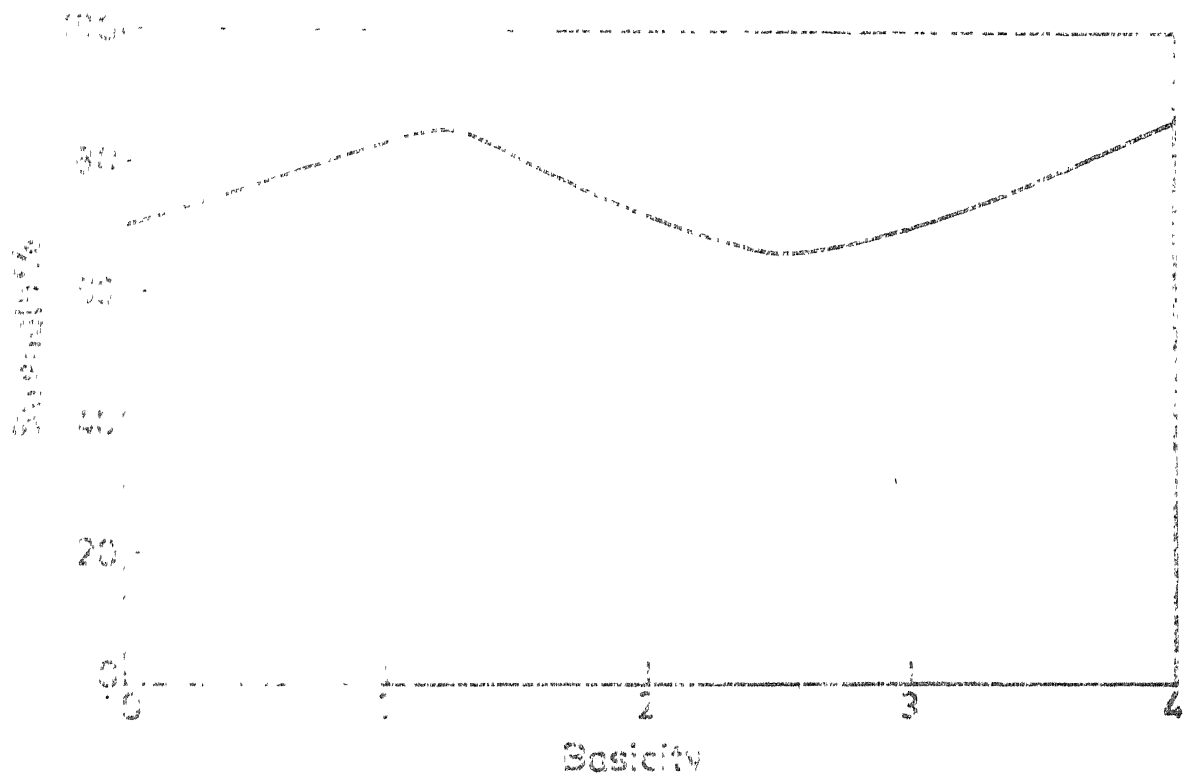


Fig. 4. Plot of strength as a function of basicity in the Mazanek et al study. (9)

decreases rapidly (Fig. 5). Mineralogical studies showed that dicalcium ferrite ($2\text{CaO} \cdot \text{Fe}_2\text{O}_3$) bonds provides the major strength mechanism for super-fluxed sinter compared with iron oxide bridging in the self-fluxed range. In Lackawanna plant the super fluxed burden in J-blast furnace was increased from 12 % (in Feb. 1967) to 53 % (in April 1967) and at the same time the pellet burden was reduced from 85% to 47%. During this period hot metal production increased from 2823 to 3035 tpd and coke consumption decreased from 941 to 914 lb per ton of hot metal. The amounts of raw fluxstone charged to the D/F was reduced from 531 in Feb 1967 to 0 lb per THM in April 1967.

2.c. Reducibility measurements: Effect of basicity on reducibility of sinters

To determine the thermodynamic characteristics of reduction processes, it is essential to form or attain a state of equilibrium. In heterogeneous systems i.e. gas-solid or -liquid phases, the moment of attaining equilibrium is determined by variations in the pressure or volume of a gaseous phase, variations of the mass of reacting phases, on heating or cooling curves etc. The most common methods for analysis of reduction processes are those with the participation of a gaseous phase. They may be termed as static and dynamic methods.

Static Method Measured quantities of a substance to be tested and a gaseous phase are held in a sealed apparatus at specified values of temperature and pressure. Samples of gas are taken

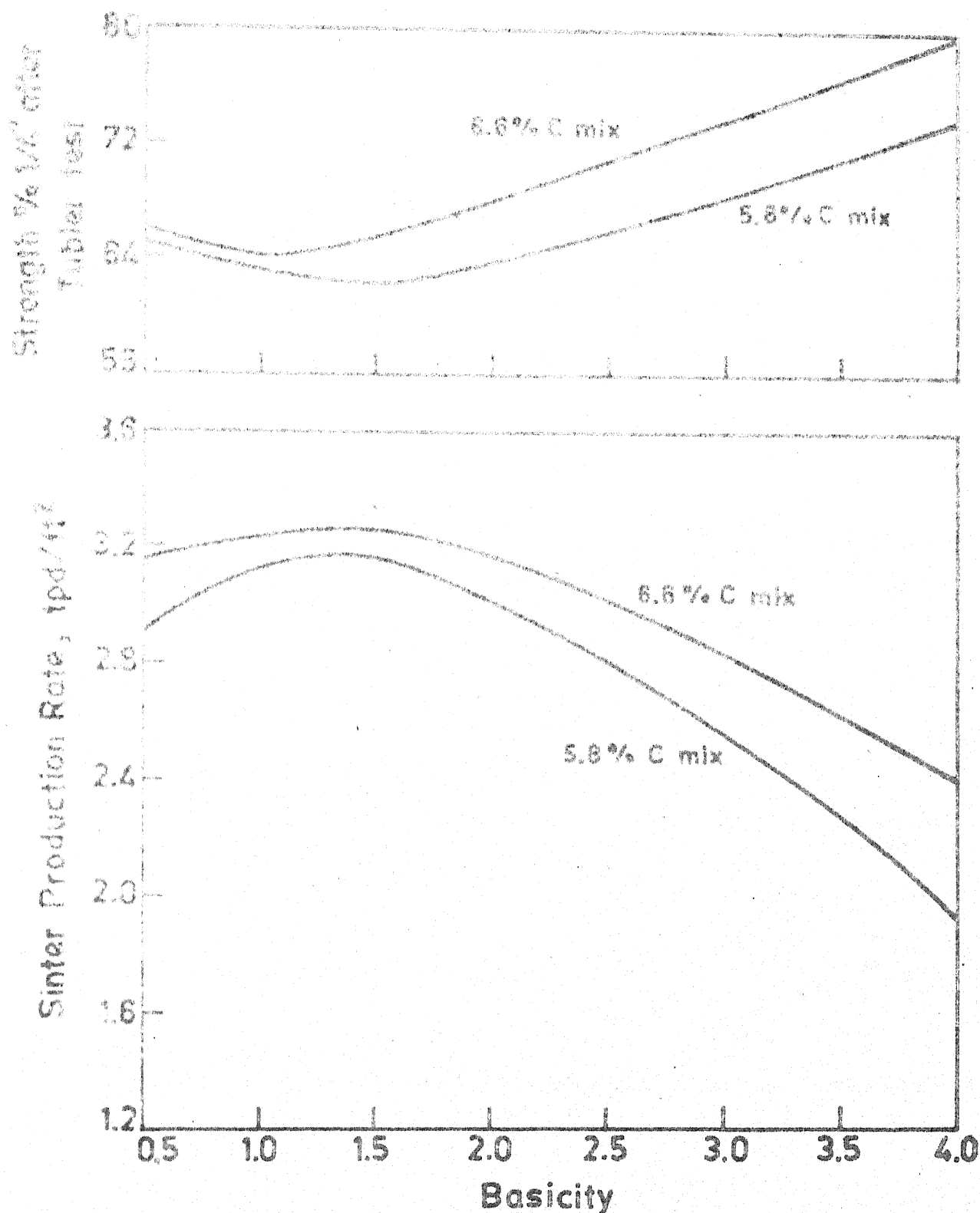


Fig. 5 Effect of basicity on strength and production rate of Lackawanna sinters. ⁽¹⁰⁾

off and analysed in regular time intervals. It is taken that a state of equilibrium is attained when the results of analysis of a number of successive samples are identical.

Dynamic Method In this method, a gas is caused to flow over the solid surface at such a speed which is sufficient to form a state of equilibrium during the time of passage of the gas over or through the solid surface. The subsequent analysis of gaseous phase gives direct equilibrium values.

Apart from the above mentioned ones there is another method called circulation method in which a gas flows over the solid surface and a continuous chromatographic analysis of the gas phase is done by the variations of heat conductivity, interference properties etc. In a study of the kinetics of oxides by gases the rate of reduction is judged upon by variations in the mass of a sample, ~~is done in case of~~ gravimetric methods measuring the weight loss continuously with time.

The reduction behaviour of oxide compounds with iron oxides^M has often been studied because of its importance in connection with sinters and pellets but no fundamental clarification has yet been achieved of the sub-processes which occur. Most of the investigations in which the reduction rate of such phases have been measured suffer from the fact that the porosity and surface area of the specimens under investigation have not been determined precisely. Some of the results of measurements with

various kinds of minerals are given in Fig. 6 and Table 1.

3. Matnabe¹⁰ concluded the following from his studies :
~~concluded~~

(a) Calcium ferrites rich in iron oxide and also the compound $\text{CaO} \cdot \frac{1}{2}\text{Fe}_2\text{O}_3 \cdot 2\text{Fe}_2\text{O}_3$ are equally reducible as hematite ores or more reducible.

(b) Dicalcium ferrite and the silicate $\text{CaO} \cdot \text{FeO} \cdot \text{SiO}_2$ are less easily reducible.

The reducibility of self fluxing sinter has been reported¹¹ to change according to the basicity in the same manner as the mechanical strength. It is confirmed that the reducibilities of sinters containing much iron oxides and calcium ferrites are larger than those containing silicate minerals. Mazanek reported that the reducibility goes down between 1.5-2.2 basicity sinters and again increases with further increase in basicity. The reason for the former effect is explained due to the decrease of Fe_2O_3 content and increase of dicalcium ferrite, and for the latter effect due to the rise of mono-calcium ferrites, $\text{CaO} \cdot \text{FeO} \cdot \text{Fe}_2\text{O}_3$.

The reducibility of the two binary ferrites which are rich in lime has been studied by Schenck et al¹². Edstrom has studied the reduction of $\text{CaO} \cdot 2\text{Fe}_2\text{O}_3$ and observed that reducibility was roughly same for $\text{CaO} \cdot \text{Fe}_2\text{O}_3$ and $\text{CaO} \cdot 2\text{Fe}_2\text{O}_3$. Panigrahy et al¹³ reported a negative influence on the reducibility of

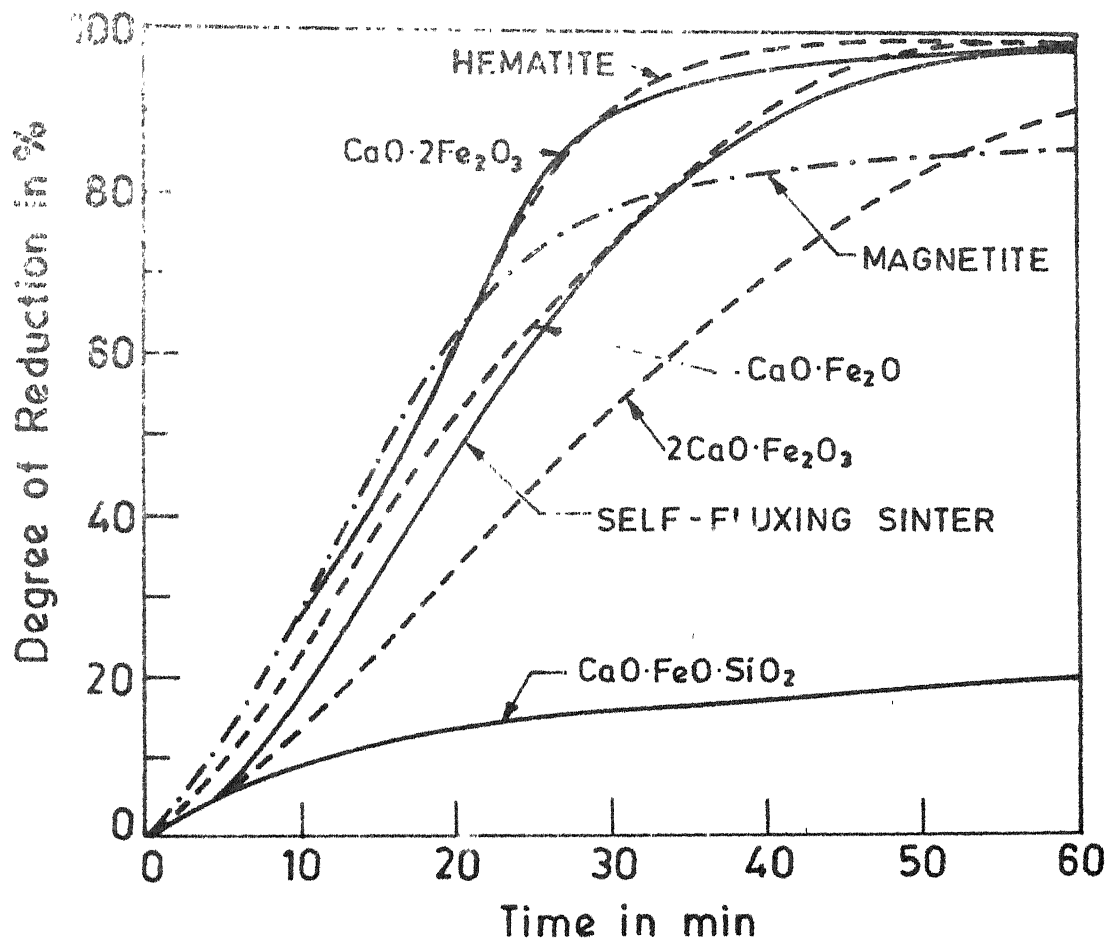


Fig. 6 Reducibilities of various ores and sinter constituents in hydrogen at 800°C, according to Watanabe.

Table 1 : Degree of reduction of sinter minerals after reduction for 40 minutes in pure CO at 850°C (17)

R_{sinter}	%
Fe_2O_3	49.4
$\text{CaO} \cdot \text{Fe}_2\text{O}_3$	49.2
$2\text{CaO} \cdot \text{Fe}_2\text{O}_3$	25.5
$\text{CaO} \cdot 2\text{Fe}_2\text{O}_3$	58.4
$3\text{CaO} \cdot \text{FeO} \cdot 7\text{Fe}_2\text{O}_3$	59.6
$\text{CaO} \cdot \text{Al}_2\text{O}_3 \cdot 2\text{Fe}_2\text{O}_3$	57.3
$4\text{CaO} \cdot \text{Al}_2\text{O}_3 \cdot \text{Fe}_2\text{O}_3$	23.4

sinters that are prepared by MgO additions. He further concludes that the drop in reducibility could be explained by the decrease in hematite and Ca-Ferrite content and subsequently the increase in magnetite phase which has lowered reducibility. The higher amount of FeO in the slag phase which forms poorly reducible silicates and the dendritic magnetites are not easily accessible to the reducing gases because of the surrounding slag layer. At high basicity indices, $B = 1.6$ and 1.9 where sinter structure is marked by a continuous ferrite frame, the sinters show very high reduction Degradation Index even without MgO addition, in spite of hematite being present. MgO stabilises magnetite as magnesian spinel formation suppresses the Ca-ferrites and hematites to form. It is been confirmed¹³ that sinters with basicity above 2.5 say in the range of 2.5 - 4.5 the reducibility is seen to have considerable improvement. Similar results were obtained by Hazanek, R.A. Limons et al, S. Watanabe. The higher the basicities of the sinter, the greater is the ferrites it contains, the higher is the CaO present in the olivine $(CaO)_x \cdot (FeO)_{2-x} \cdot (SiO_2)$ and lesser the free magnetite. All these three effects gives rise to marked increase in reducibility values.

2.D. Effect of magnesium oxide addition on properties of sinter

Dolomite additions to the sinter mix are done to increase MgO content of the sinter. ~~This MgO replaces CaO in the basicity index.~~ It has been observed that the addition of dolomite lowers

reducibility¹⁴, increases the strength and improves reduction strength of the sinter. The charging of dolomite through the sinter burden also improves ~~the~~^{the} performance. An increase MgO content of the sinter decreases the amount of calcium ferrites, even in sinters with a low FeO content. It also brings about an increase in the content of MgO bearing olivines and the appearance of almost irreducible pyroxene and ferromonticellite $[Ca(Fe, Mg) SiO_4]$. This was confirmed by A. Chatterjee et al. MgO contents below 4.5% do not influence the mineral constituent of the specimen, because MgO easily replaces the Fe⁺⁺ ions in the space lattice of the olivines and pyroxenes. MgO stabilizes magnetite. This stabilization is the key factor of the lowering of reducibility of sinter upon MgO addition. The effect of MgO on the mineralogical composition⁷ of the sinter is such that the phases present in Fig. 3 are displaced to the right. That is, at any particular basicity, increasing the MgO content increases the magnetite and decreases both the hematite and calcium ferrite contents. Additions of dolomite must be compensated for the sinter mix by an increase in the addition of coke breeze. Unlike limestone, dolomite has the tendency of increasing the temperature of initial melt formation. It was noted that pockets of poorly sintered material existed with dolomite addition and ~~is likely to hinder the flow of air compared with that in poorly sintered material.~~^{ed} The slower progress of flame front results in a longer sintering period. The reasons for this effect are

as the following :

- (1) Replacement of CaO by MgO leads to an increase in liquidus temperature of the melt phase.
- (2) As more MgO replaces CaO the slag phase progressively becomes SiO_2 -rich resulting in higher values of melting point and viscosity of the slag.
- (3) The porosity increased with increased replacement of CaO by MgO. Moreover while the high CaO-bearing sinters exhibited uniform distribution of pores, the sinters with increased MgO content showed variable distribution.
- (4) Poor mechanical strength.

The fall in production as discussed above for the case of sinters in the range of self and superfluxed basicity range (B = 1.3-1.9) is because of crystal size of flux materials, increased melt viscosity, poor mechanical strength and high porosity due to MgO additions. It was also concluded in Panigrahy's paper that one should take care in choosing proper fluxes, in particular in selecting dolomites of the correct crystal size, and using dunites wherever they are economically attractive as the MgO bearing source.

CHAPTER-III

PLAN OF WORK

The conventional sintering unit is a downdraft pan sintering unit with a circular detachable grate leading to a blower for suction of air through the sintering mix. The limitations of this unit to carry out any scientific studies are as the following .

1. Pressure drop measurements during sintering are not possible.
2. Correct positioning of thermocouples inside the sinter bed is not possible.
3. Total bed height is usually small.
4. Maintaining a constant air flow in such units is not possible due to changes in the permeability of the bed during the process of sintering.

Rao¹⁶ designed a forced draft sintering unit in which air was constantly supplied from a compressor at a predetermined rate for his scientific studies on the production and testing of super fluxed iron ore sinters. Temperature responses could be measured by putting the thermocouples in the bed from the top and pressure responses measured by using a manometer. This setup too suffered from the following difficulties :

1. The size of the unit was small, because of which studies were limited to bed heights of 20 cm or less.
2. Facilities were not provided for the measurement of pressure drop across a section of the sinter bed during the progress of the sintering process.
3. There was no provision for the measurement of the exit gas temperature.

Considering these difficulties into account a new set-up was designed and fabricated in the laboratory.

For measuring the reducibility of iron ore sinters for comparison purposes, a new setup was designed in this work.

Pure hydrogen gas was made to flow through the material which ^{was} is heated to different temperatures in a furnace. H_2O in the product was removed and the quantity of the remaining H_2 in the gas was determined using a flow meter. For better understanding and evaluation of results, a few crucibles studies were conducted where the mixtures of Iron ore, calcite, coke, dolomite etc., in various proportions ^{were} are heated to $1300^\circ C$ in a silicon carbide furnace.

Thus the whole work can be classified into the following parts :

1. The quantitative analysis of calcite, dolomite limestone, and coke brecced used in the present work by weight loss measurements.

2. Cold model studies to determine the bulk density and permeability of the bed as a function of moisture content.
3. Modifying the existing forced draft sintering unit so as to record 3 temperature and 2 pressure responses measurements during the progress of sintering.
4. Designing and fabrication of reducibility apparatus.
5. Production of acid sinters, fluxed sinters and super fluxed sinters with and without dolomite additions.
6. Crucible studies to study the bond formation between the various oxides.
7. X-ray diffraction study of the sintered products of the crucible studies.
8. Shatter tests to determine the strength of the sinters produced.
9. Evaluation and tabulation of results.
10. Recommendation for improved performances in the industry based on the results of present study.

CHAPTER-IV

EXPERIMENTS

4.1 Materials

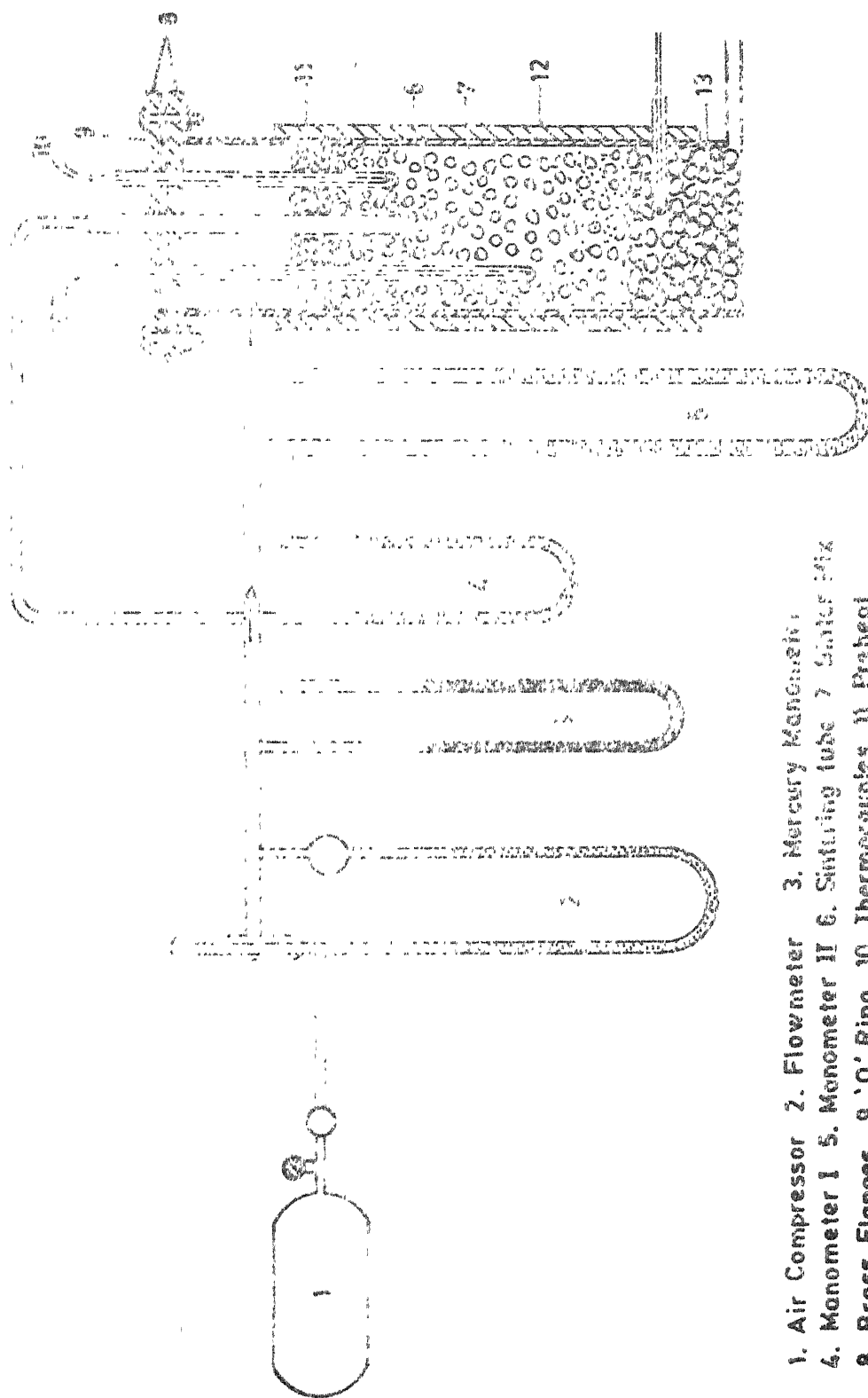
The source and analysis of raw materials used in the present study are given in ^{the} Table ~~2~~ ^{below}. The chemical analysis of coke breeze, dolomite, calcite and sand was determined in the laboratory. The results are given in the next chapter.

Table 2 : Source and analysis of materials

Sl.No.	Material	Source	Size
1.	Iron ore (65.6% Fe, 1.3% SiO ₂)	TISCO, Jamshedpur	0.15 mm to 2.36 mm
2.	Coke breeze	Local Market	0.4 to 2.36 mm
3.	Dolomite	-do-	0.15 to 2.36 mm
4.	Calcite	-do-	0.15 to 2.36 mm
5.	Sand (98% SiO ₂)	Ganga river sand from foundry laboratory	0.15 to 0.4 mm
6.	Graphite (99.9%)	Laboratory	Powder

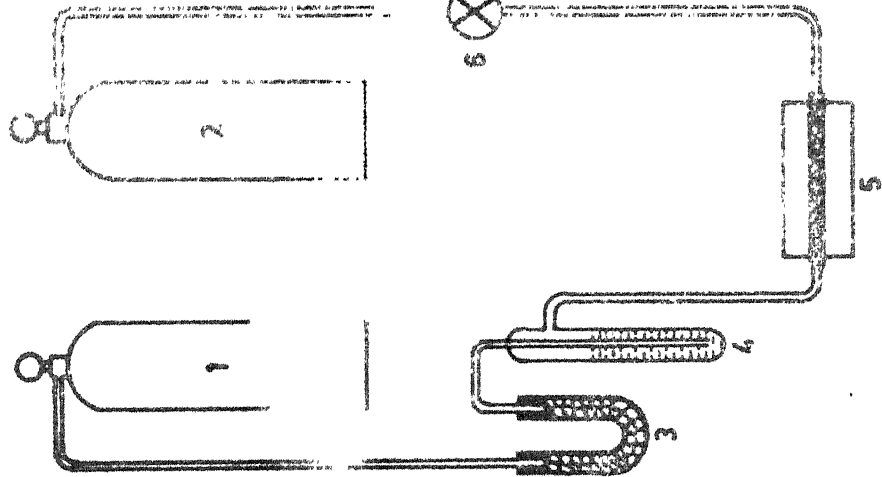
4.2 Equipment

~~This is a~~
4.2.1 Forced draft sintering unit : The ~~system was made air~~
tight with the help of an O-ring in the top flange. The ends of
probes for temperature measurements inside the bed and just
below were sealed. The unit consisted of a mild steel tube of



1. Air Compressor
2. Flowmeter
3. Mercury Manometer
4. Manometer II
5. Manometer I
6. Sintering tube
7. Gate
8. Brass Flanges
9. 9'0" Ring
10. Thermocouples
11. Preheat
12. Insulation
13. Refractory Chips

Fig. 7 Schematic diagram of sintering unit.



1. H_2 Cylinder, 2. N_2 Cylinder 3. U-Tube 4. Bubblers with H_2SO_4 5. Copper gauze burner 6. Two way cock 7. Flowmeter 8. Quartz Tube 9. Furnace 10. Thermocouple (Copper Alloy) 11. Gas flow and 12. Gas flow 13. H_2O Removing tube with CaCl_2 14. Flowmeter 15. Soap Bubblemeter 16. Cooling water

Fig. 8 Schematic diagram of reducibility test apparatus.

3 cm diameter and 65 cm length with inlet and outlet connections as shown in Fig. 7.

The following equipments were needed to run the experiment using this units :

1. Air compressor of $10 \text{ dm}^3/\text{hour}$ capacity.
2. Capillary flow meter; it was calibrated with the help of a wet-test meter.
3. Calibrated Chromel/Alumel and Pt/Pt - 10% Rh thermocouples, on the side of equipment.
4. - Two digital potentiometers to record temperature responses in mV in the range of $0.00-55.00^\circ$.
5. One double key switch.
6. Mercury and ethyl Pthalate manometers to measure pressure responses.
7. One oven for drying raw materials before use.
8. One stop watch to record time.

4.2.2 Reducibility apparatus : The schematic diagram of the apparatus used for determining the reducibility of the iron ore or iron ore sinters is shown in Fig. 8. It consisted of 15 mm ID, 1 meter ¹⁵⁴length quartz tube with leak proof inlet and outlet connections for the flow of H_2 gas. The following equipments were needed to conduct the experiments.

1. Capillary flow meters,
2. Resistance furnace capable of reaching 900°C .

3. Temperature controller with relay switch.
4. ~~Cromel~~, Alumel thermocouple.
5. Gas train to purity H_2 gas.
6. H_2O condensation tube.
7. Digital potentiometer.
8. Stop watch.
9. Soap bubble meter.
10. Measuring cylinder.
11. Chemical balance.

4.2.3 Silicon carbide furnace for crucible studies : A muffle silicon carbide furnace was used for crucible studies. 40 Amps, oil cooled transformer was used to supply power to four 18 mm dia. Silicon carbide rods. The furnace is controlled by a pt/pt : 10% Rh thermocouple connected to an on-off recorder and temperature was measured using another thermocouple connected to the digital potentiometer.

4.3 Procedure

4.3.1 Forced Draft sintering unit : The following procedure was adapted in carrying out the experiments .

1. Check the system to be air tight by pressurising it first with air supply, close ^{ing} the exit end ^{and} cut off the air supply. Any leaks in the system can be observed by the drop in the pressure in the system as recorded by the manometers.

2. Feed the steel tube with ceramic pieces to the predetermined depth and place a mild steel wire mesh on top of the refractory chips.
3. Weigh the quantities of the dry iron ore, calcite, dolomite, coke breeze in the suitable proportions and add the necessary amount of water to it. Mix them thoroughly in a drum.
4. Add the prepared sintering mix to the unit and determine the permeability of the green mix by closing the lid and recording pressure drop across the bed for a fixed flow rate of air.
5. Remove the top lid and add the preheat burden consisting of iron ore (300 g) and coke breeze (40 g).
6. Add charcoal and saw dust over the preheat burden so as to give a 2 cm thick layer in the sintering unit.
7. Now ignite the bed with a match stick.
8. Pass air at the rate of 10-20 cc/sec and cover the top of the unit with a refractory asbestos sheet if necessary to increase the intensity of combustion of charcoal in the top layer.
9. Measure the temperature of the ignition of the bed, close the top lid and adjust the air flow rate to the desired level.
10. Record the various pressure and temperature responses at regular intervals of one minute till the temperature of

the bed has cooled to 600°C and the peak in the exit gas temperature has been obtained.

11. Stop the supply of air from the compressor and allow the bed to cool down to room temperature.
12. Measure the permeability of the cold sinter by recording the pressure drops across the bed for the fixed flow rate of air.
13. Open the top lid and take out the sinter from the unit.
14. Weigh the amount which is sintered to size grade of 15 mm and weigh the unsintered mass separately.
15. Subject the sintered material to further tests such as shatter tests and reducibility determination.

4.3.2 Crucible studies . These studies are conducted in the following steps.

1. The amounts of iron ore, calcite, sand, dolomite, graphite etc., in suitable proportions are taken into alumina crucibles and the same are weighed.
2. These crucibles are placed inside the furnace at 1200 °C or 1300 °C for one hour.
3. Crucibles are then removed carefully and allowed to cool in air.
4. Crucibles along with the material is weighed again to record any loss in weight of material on heating.
5. The materials are collected by breaking the crucibles if necessary and subjected to further tests and examinations.

4.3.3 Reducibility test : The procedure of this test is as follows :

1. Fill the quartz tube with broken refractory chips upto the middle of the tube and place a steel wire mesh over it.
2. Add the weighed material of iron ore or sinter over the mesh in the quartz tube.
3. Insert the quartz tube carefully in the furnace tube and make the inlet and outlet connections for the flow of gases.
4. Put the furnace on and wait till desired temperature is reached.
5. Pass H_2 gas at a known flow rate to flush the apparatus for 15 minutes.
6. Start passing the purified H_2 gas at a constant rate and note down the flow rate of H_2 in the outlet with the help of flow meter and the soap bubble apparatus at regular intervals of time.
7. When H_2 in the exit gas has reached a constant value for a long period, stop the experiment and allow the furnace to cool.
8. Take out the amount of H_2O collected in the copper bubbler after each experiment and measure its volume.
9. Remove the reduced iron ore or sinter material from the quartz tube carefully and determine its weight.

4.3.4 Determination of shatter strength . A fixed weight of .15 mm sinter material is dropped once from the height of 2 meters on a 12 mm thick mild steel plate. The percentage retained in 4.7 mm size is assumed as the shatter index in the present work.

4.3.5 X-ray studies : 3-5 gms of a compound is crushed in an agate and pestle and the powdered mass is subjected to the X-ray diffraction using Cu-K_{α} and Cr-K_{α} radiations.

CHAPTER-V

RESULTS

This chapter describes the results of all the experiments carried out in this study.

5.1 Cold model studies

The measured bulk densities of the iron ore and sinter mix materials as function of the moisture content are given in Fig. 9. The pressure drop across the bed of a sinter mix as a function of moisture content of the mix is also plotted in Fig. 9 itself. From these results, the moisture content was kept at 7 pct. in all further experiments ~~on the sintering~~ ^{Sintering} of iron ore.

5.2 Crucible studies

Table 3 summarizes the details of experiments carried out on heating of the oxide mixtures in the silicon carbide furnace, and the observations recorded.

5.3 Quantitative analysis of raw materials

The results of the weight loss determination on heating of the carbonate materials and the coke at different temperatures are mentioned in table 4. Coke breeze is found to contain 38 pct. ash and 4 pct. moisture. Weight losses on heating of carbonate materials at a temperature less than 900°C are due to the decomposition of $MgCO_3$. The loss of 4.15 gm on heating of 20 gm of dolomite material at 850°C. would give its MgO content as 18.86 pct.

i.e., $(\frac{4.15}{44} \times \frac{40}{20} \times 100)$. The weight loss due to the decomposition of dolomite and calcite materials on heating at 980°C suggest that dolomite contains 30.8 pct. CaO and calcite contains 54.22 pct. CaO. Calcite used in the present study is thus at least 90 pct. pure.

5.4 Sintering of iron ore in the forced draft sintering unit

The details of all the experiments carried out in the sintering unit are given in table 5 alongwith the weight measurements of the product after the experiment. The measured temperature and pressure responses during the progress of sintering in these experiments ^{are} shown in Figs. 10 to 13. The pressure drop measurements across the bed in the empty reactor, in the green mix, during sintering and after sintering are summarised in Table 6 for better comparison of the bed permeability at different stages of the sintering process in each experiment.

5.5 Reducibility study

The results of the experiments on the shaft reduction of iron ore, manufactured iron ore sinters and the crucible heated products by H₂ gas are summarised in Table 7. The measured flow rate of H₂ gas at the outlet of the reducibility apparatus are plotted against time are shown in Figs. 19 to 25 for these experiments. The area under the curve in each experiment gives the total amount of H₂ that has escaped out of the system, and by difference the amount of H₂ that has reacted with iron ore can

be determined by taking the difference in the flow rates of H_2 in the inlet and the outlet of the apparatus and the exit gas composition can be determined in taking the ratio of the two flow rates.

5.6 Shatter test

The sintered masses from the experiments of the forced draft sintering of various iron ore mixes were subjected to the shatter tests as described in section 4.3.4 and the results are summarised in table 8.

5.7 X-ray diffraction

The diffraction patterns for the A1, B1 and D1 crucible compounds are schematically shown in Fig. 26.

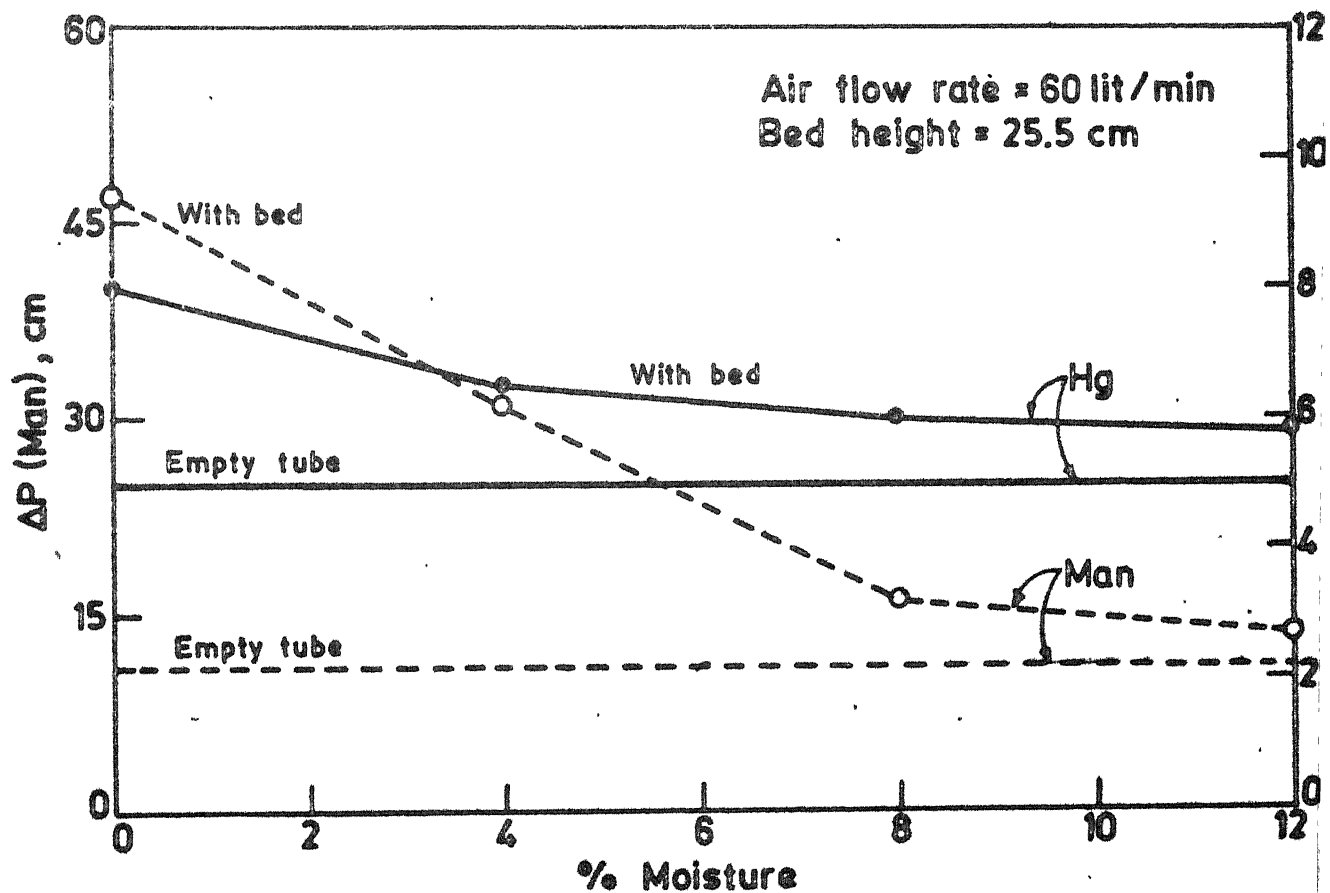
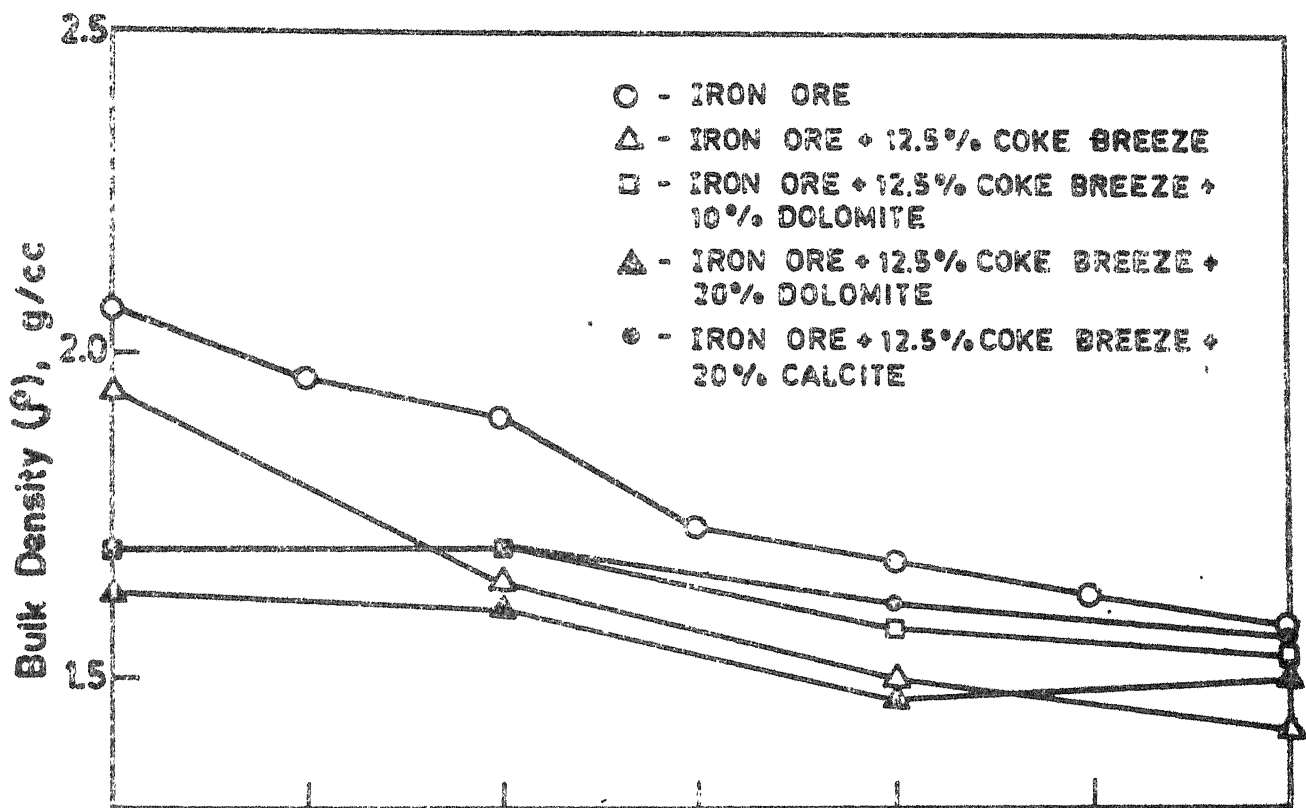


Fig. 9 Bulk density and ΔP Vs moisture plot.

Sample	Quantities of materials in the mix before heating				Observations after heating the mix
	Iron ore (g)	Calcined calcite (g)	Calcined dolomite (g)	Graphite (g)	
A	20	-	5	-	Bonding occurred with porous fused mass
B	20	5	-	-	Excessive melting shrinkage observed
C	13	-	-	-	No Bonding
D	13	-	5	1.5	Good Bonding with shrinkage observed
E	-	10	-	-	Weak Bonding; most of the material unreacted
F1	20	5	-	-	No bonding
F2	20	5	5	-	Good Bonding with shrinkage
G	20	5	5	1.5	Melting and shrinkage
H1	60	-	15	-	Porous fused mass observed
B1	50	15	-	-	Shrinkage observed
D1	50	-	20	6	Shrinkage observed

Temperature of heating }
for F1 & G

Temperature for the rest - 1300 C

Table 4 : Results of quantitative analysis of raw materials

Raw material	Temperature	Weights		Wt.loss (g)	% loss
		Initial (g)	after heating(g)		
Coke breeze	105	1.000	0.960	0.04	4
	900	1.000	0.3799	0.62	62
Dolomite (dry)	735	20	19.80	0.20	1.0
	850	20	15.85	4.15	20.75
	980	100	55	45	45
Calcite (dry)	735	20	19.79	0.21	1.05
	850	20	19.88	0.12	0.6
	980	100	57	43	43

Particulars	SIN I	SIN II	SIN III	SIN IV	SIN V	SIN VI	SIN VII	SIN VIII	SIN IX
Iron ore (g)	1500	1500	1500	1500	1500	1500	1500	1500	1500
Calcite (g)	-	-	150	150	300	-	-	300	-
Lolomite (g)	150	300	150	-	-	300	-	-	-
Coke breeze (g)	190	190	190	190	190	190	190	190	190
Water (cc)	105	105	105	105	105	105	105	105	105
Led height (cm)	25	25.3	27	25	25.5	25	26	25.5	25
Air flow rate (l/min)	40	40	40	40	40	40	60	60	60
Expected weight of sinter (g)	1640	1740	1740	1620	1740	1560	1730	1730	1560
Weight of unsintered mass (g)	800	350	900	720	775	1300	875	900	520
Weight of sinter (g)	820	830	850	920	145	290	655	735	1010
Yield (per cent)	50	50.6	49.13	56.8	25.5	18.6	50	45.3	64.7
(CaO , Ca), SiO_2	1.14	2.28	2.38	1.24	2.48	0	2.28	2.43	0
FeO , CaO	0.61	0.61	0.22	0	0	0	0.6	0	0
Sintering rate (cm/min)	0.65	0.317	0.75	0.65	0.59	0.40	0.866	1.19	0.85

Table 5 : Forced draft sintering results

Experiment	Empty Reactor			Green Mix			During sintering			After sintering		
	Hg cm	Man 1 cm	Man 2 cm	Hg cm	Man 1 cm	Man 2 cm	Hg cm	Man 1 cm	Man 2 cm	Hg cm	Man 1 cm	Man 2 cm
SIN I	2.8	5.5	-	-	-	-	3-8	5.6-12	-	3	5.6	-
SIN II	3	5.5	-	3.2	6.9	-	3-3.8	6.5-12.8	-	3	6	-
SIN III	2.8	5.5	-	3	6	-	3.2-4	7.5-12.5	-	3	7	-
SIN IV	3	5.5	-	3	5.8	-	3-3.5	5.3-10.5	-	3	5.5	-
SIN V	2.8	5.5	5.8	3	6.4	11	4-5.8	3.4-30	21-40	4	3.4	21
SIN VI	2.8	5.5	6	3.4	6.5	14	3.5-5	6.5-9	15-28	3	5.5	7.5
SIN VII	5.4	10.5	11	6.4	11.5	21.5	7-8	11.5-30	27-60.5	7	11.5	27
SIN VIII	5	11.5	12.5	5.3	11.5	10	5-8	5.5-17.5	15.5-41	5	5.5	12.5
SIN IX	5	11.5	11.5	5.4	13	13	5-6.5	6-14.5	12.5-30.5	5	12	14
+ 2												

Table 6. Pressure responses in various stages of sintering

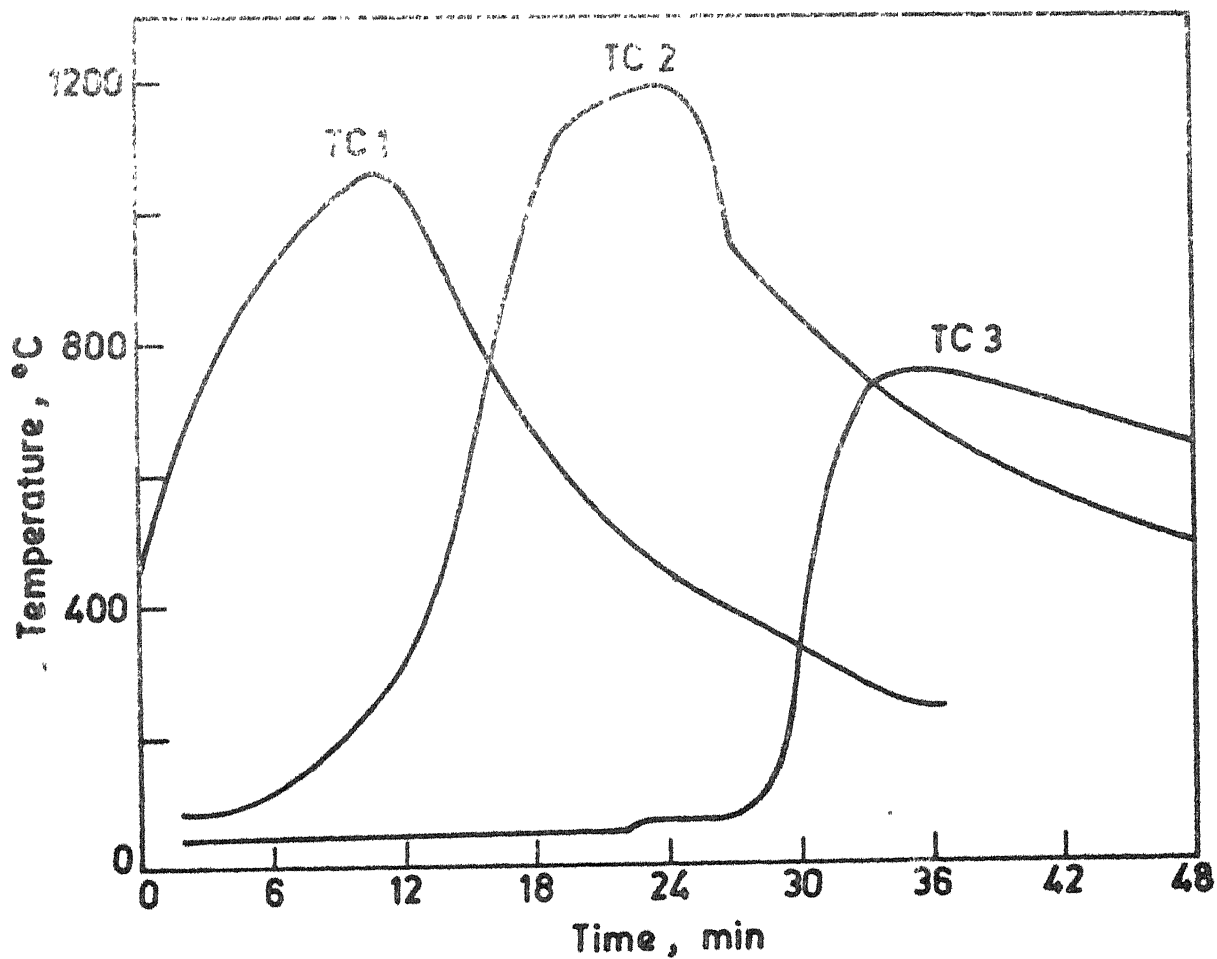
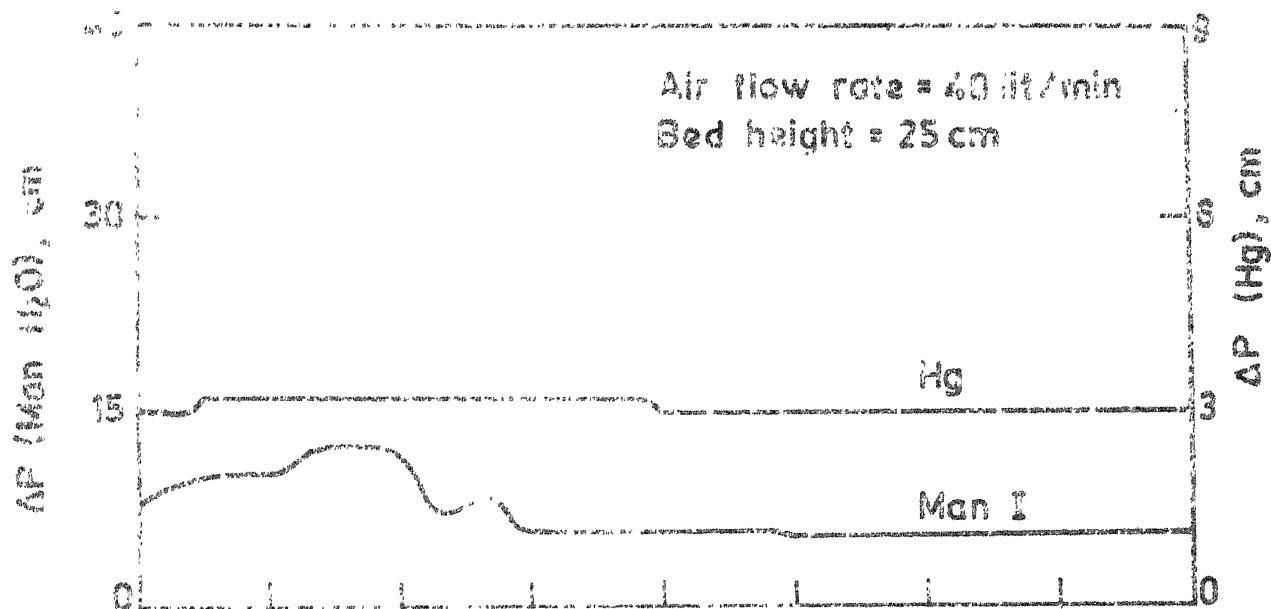


Fig.10 Plots of pressure and temperature in SIN I against time.

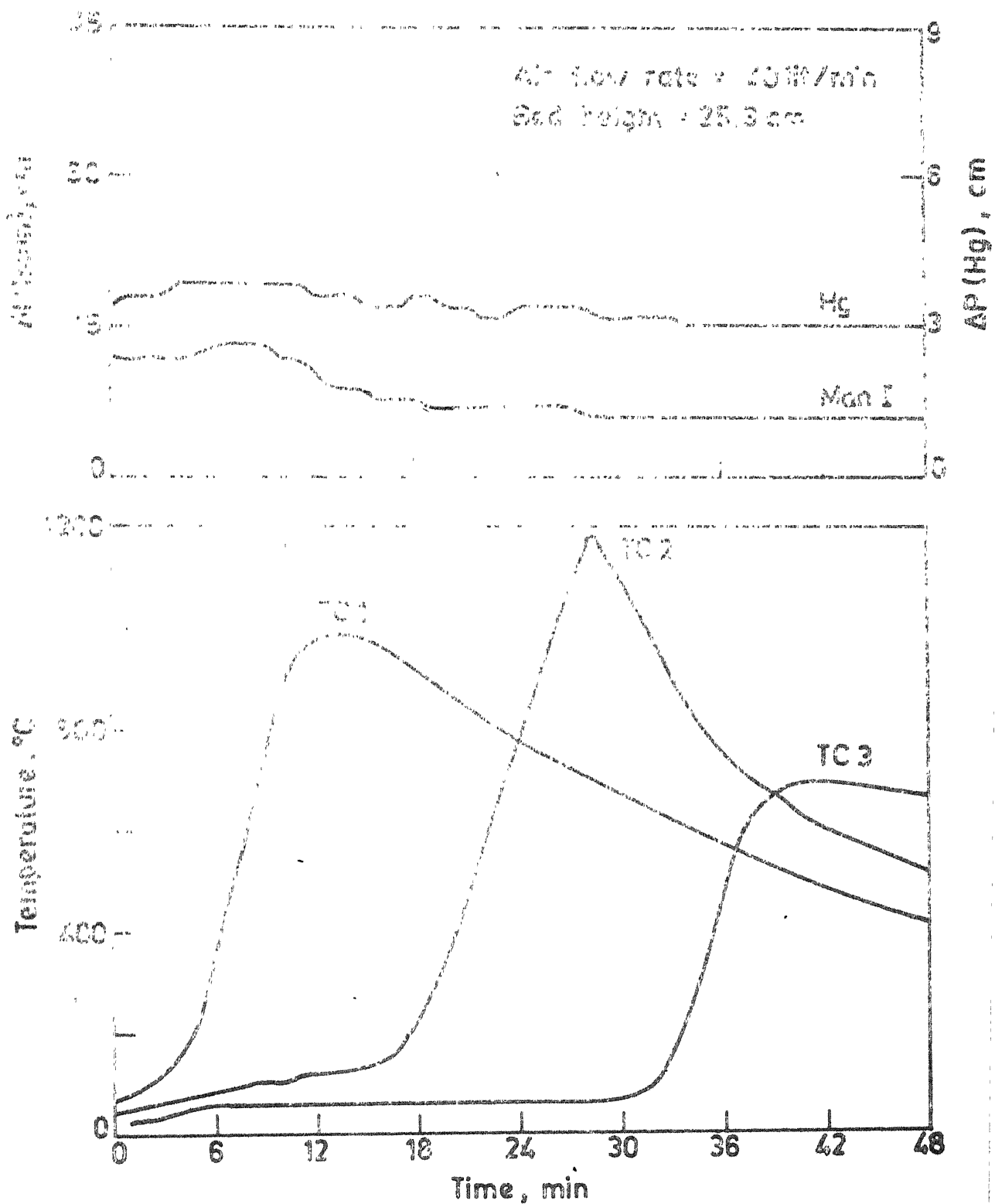


Fig. 11 Plots of pressure and temperature in SIN II against time.

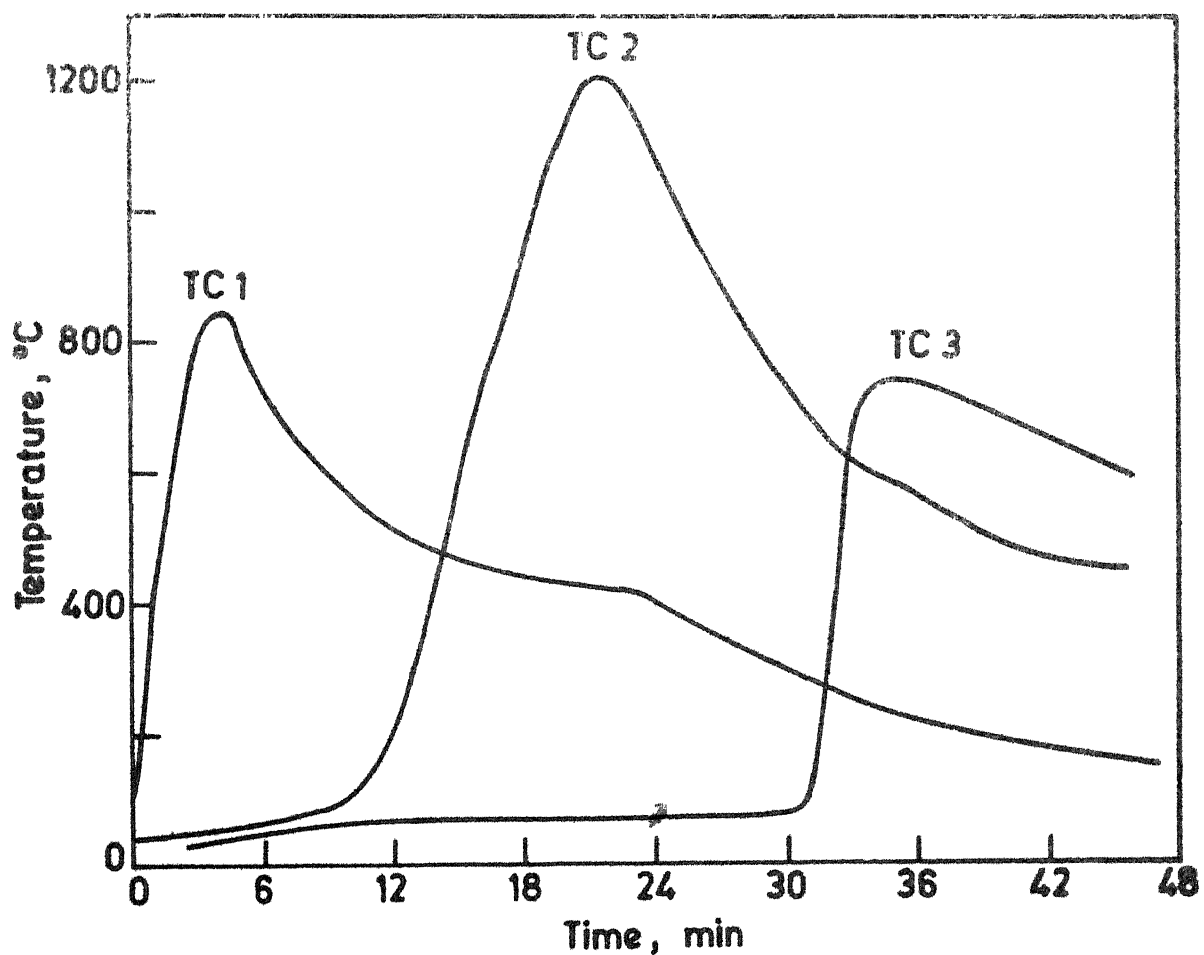
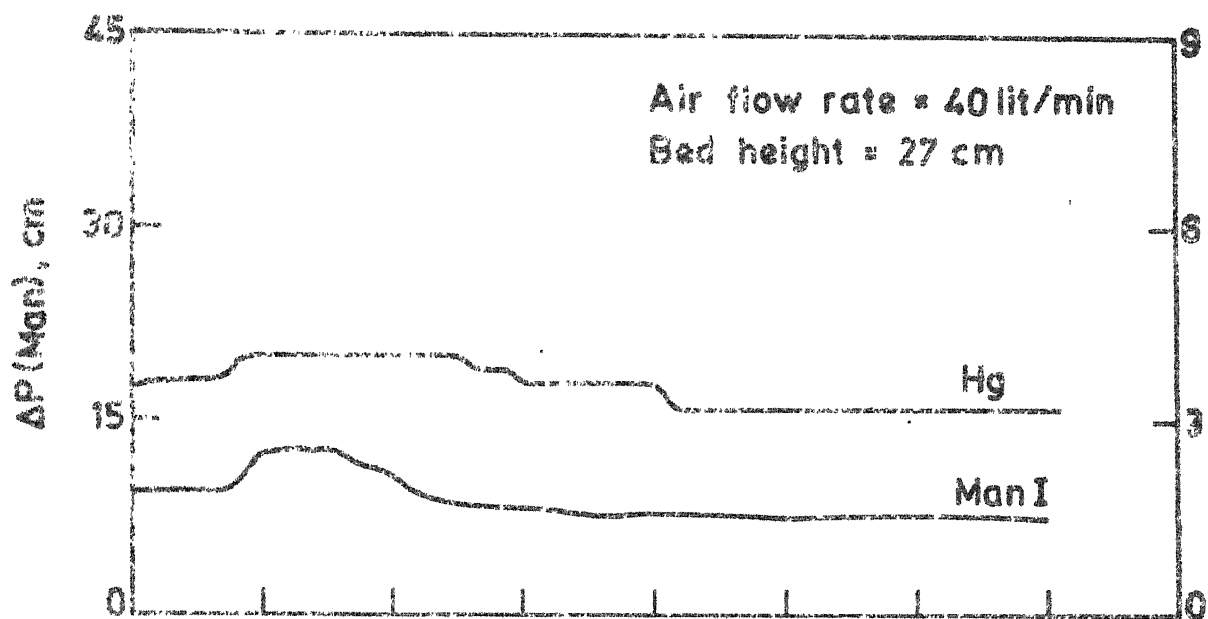


Fig.12 Plots of pressure and temperature in SIN III against time.

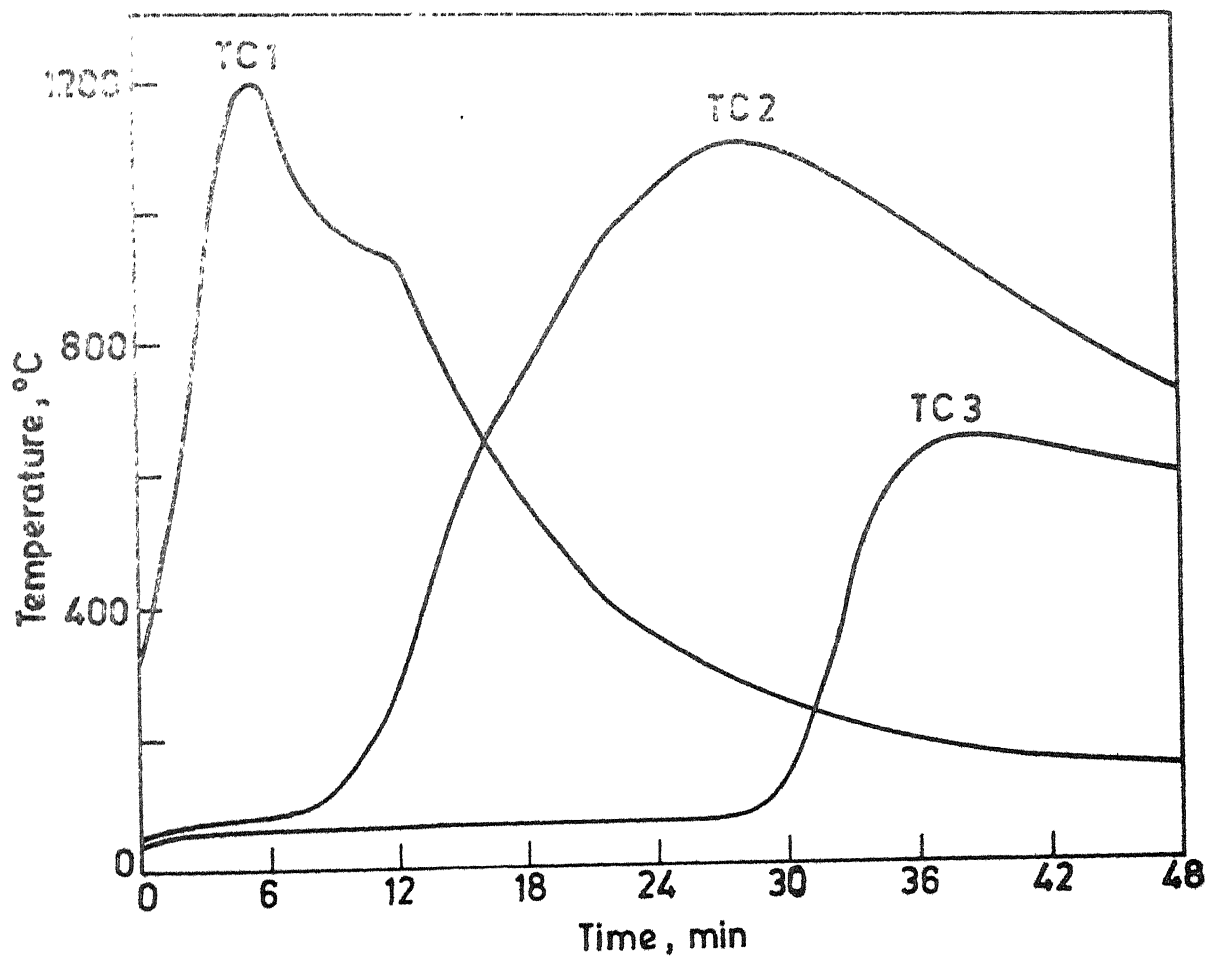
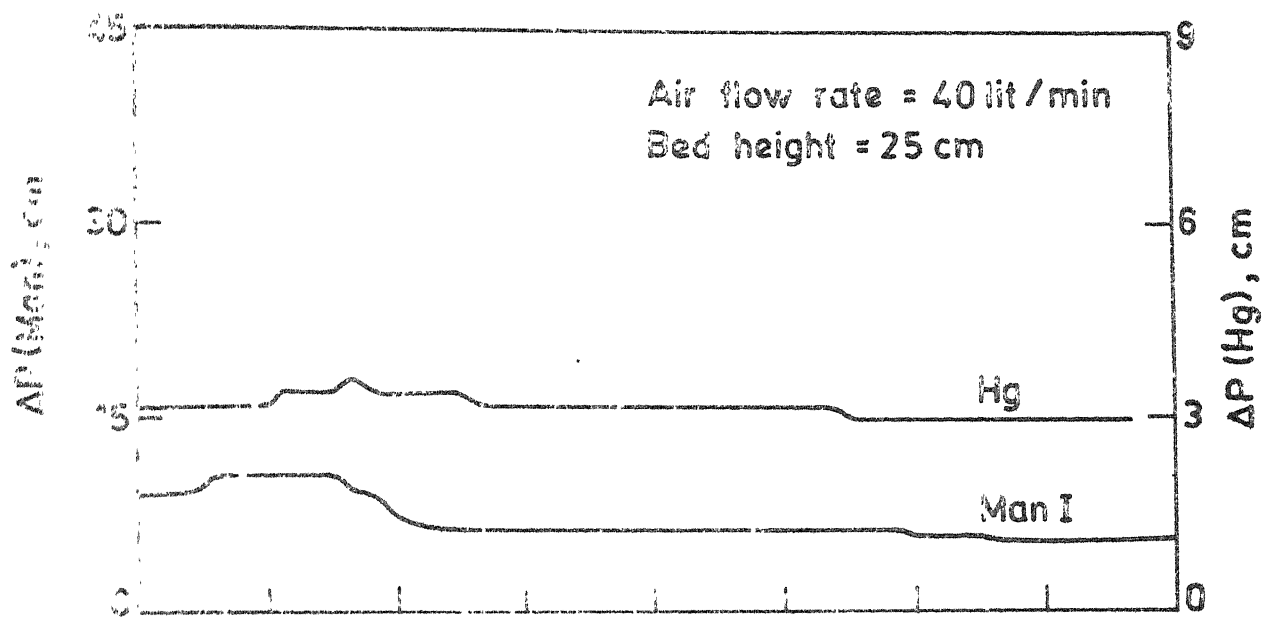


Fig.13 Plots of pressure and temperature in SIN IV against time.

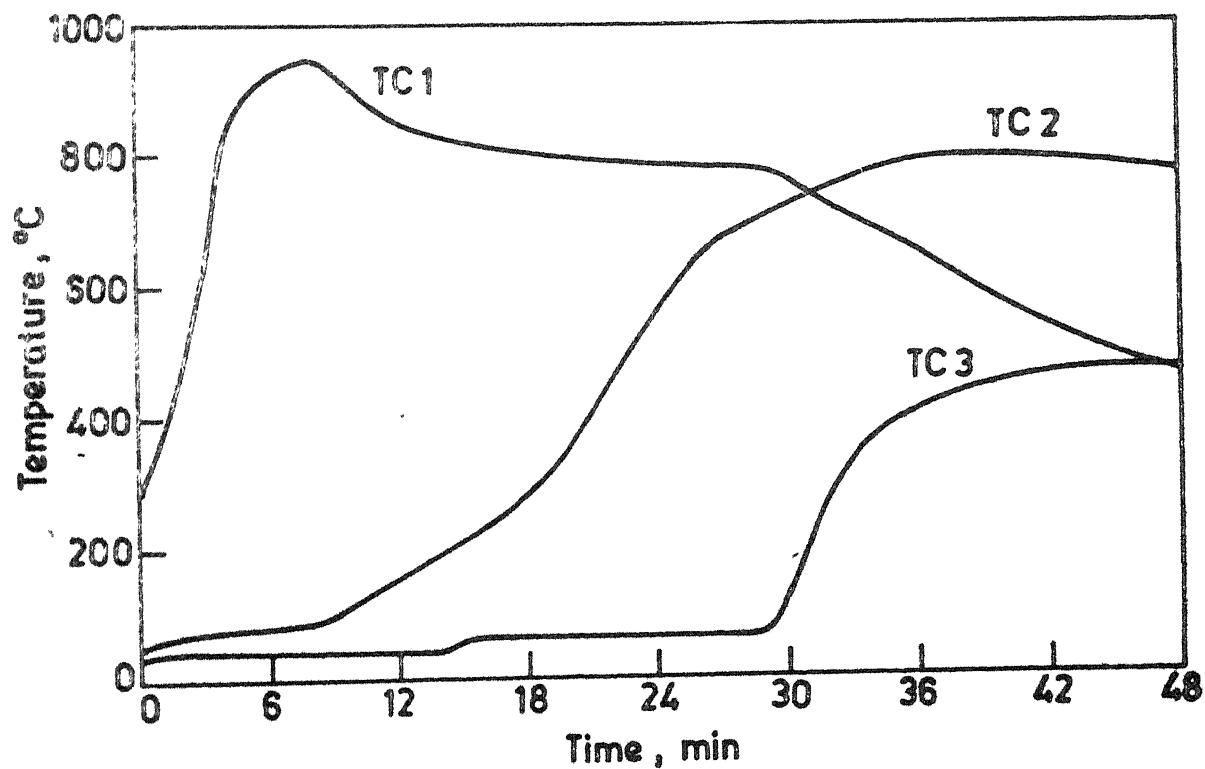
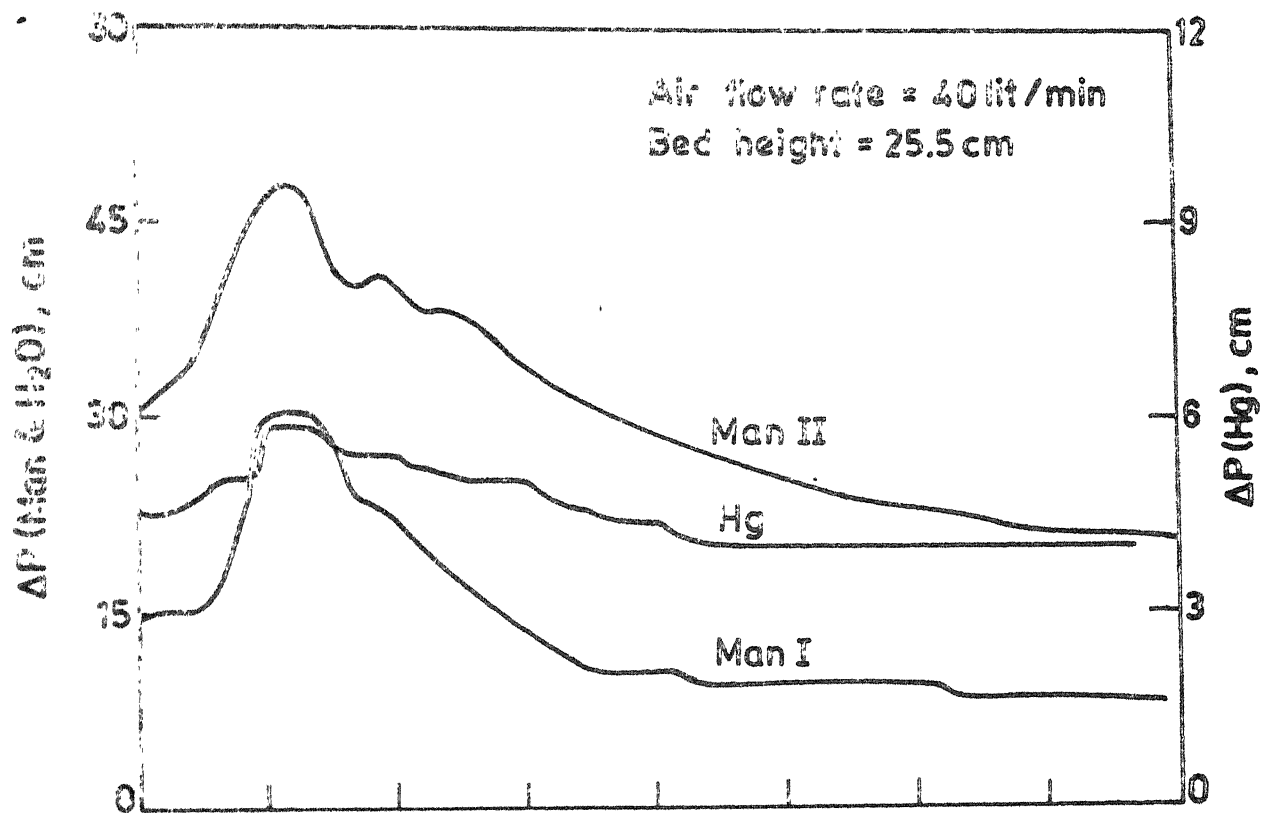


Fig.14 Plots of pressure and temperature in SIN V against time.

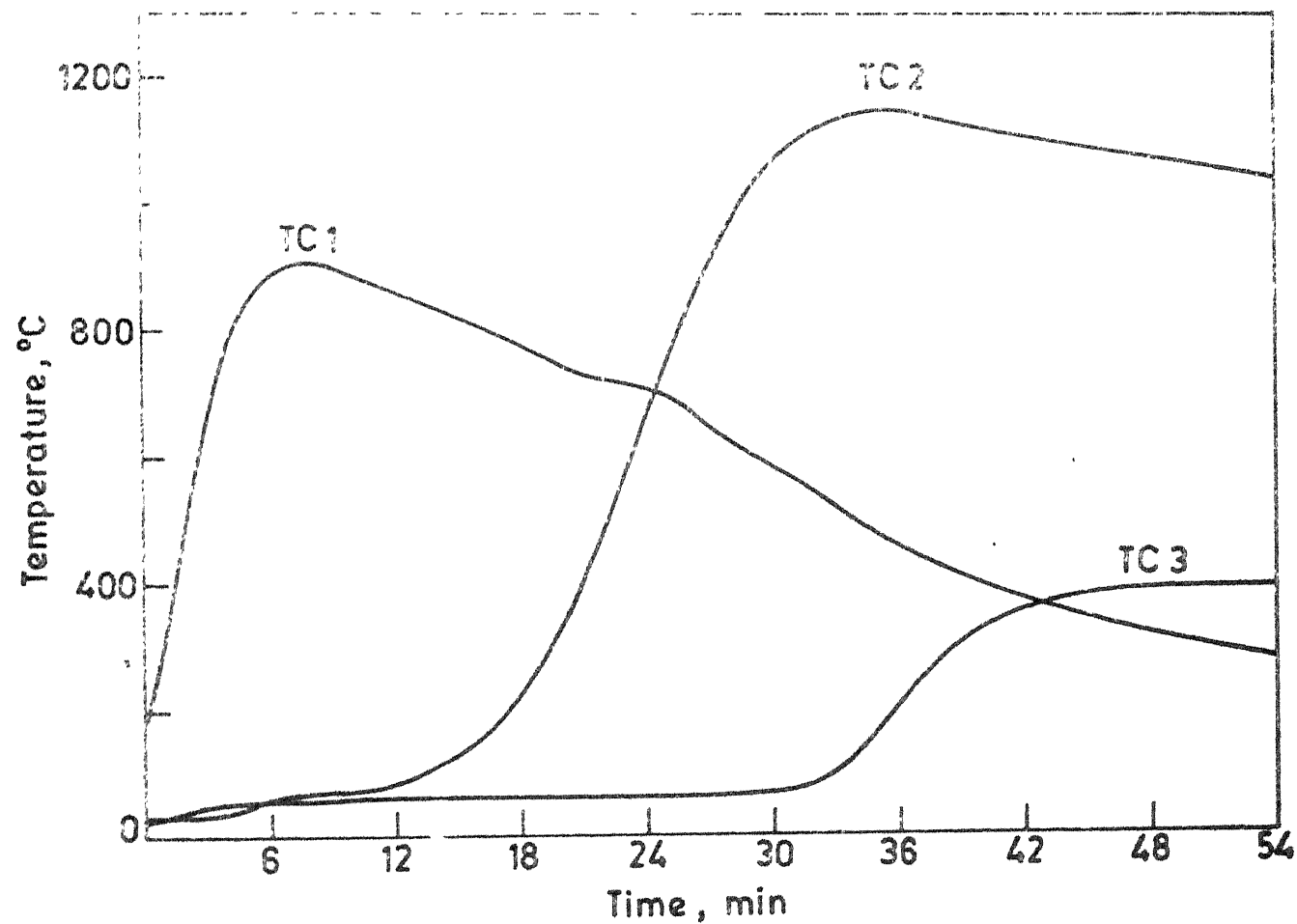
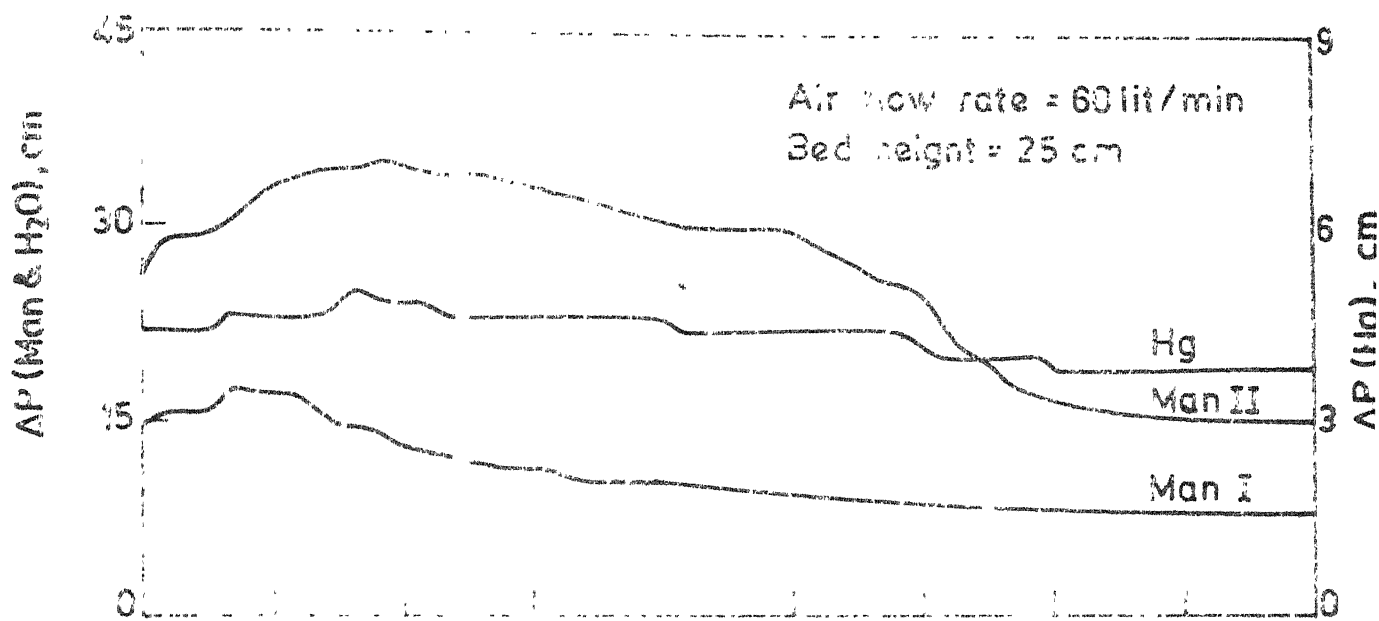


Fig.15 Plots of pressure and temperature in SIN VI against time.

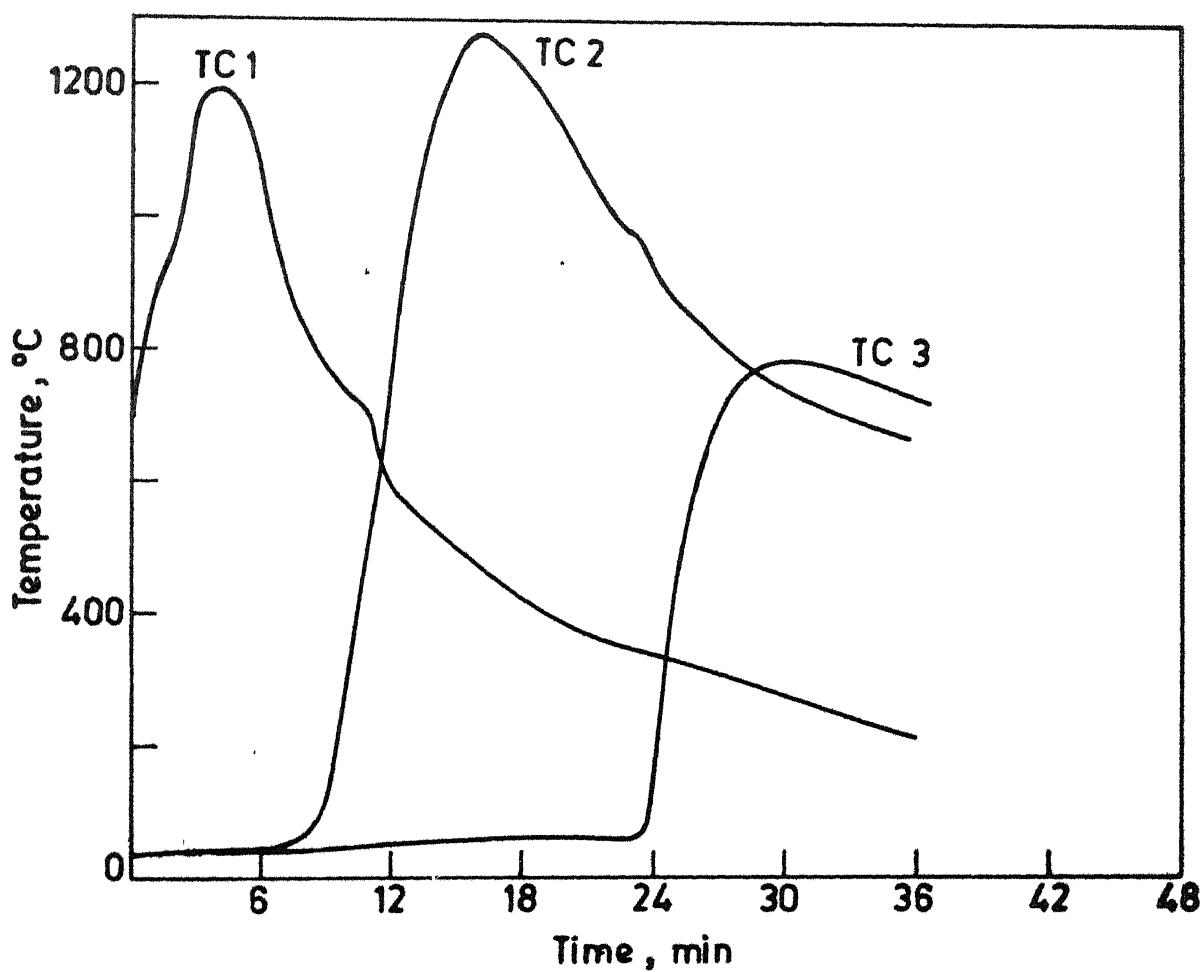
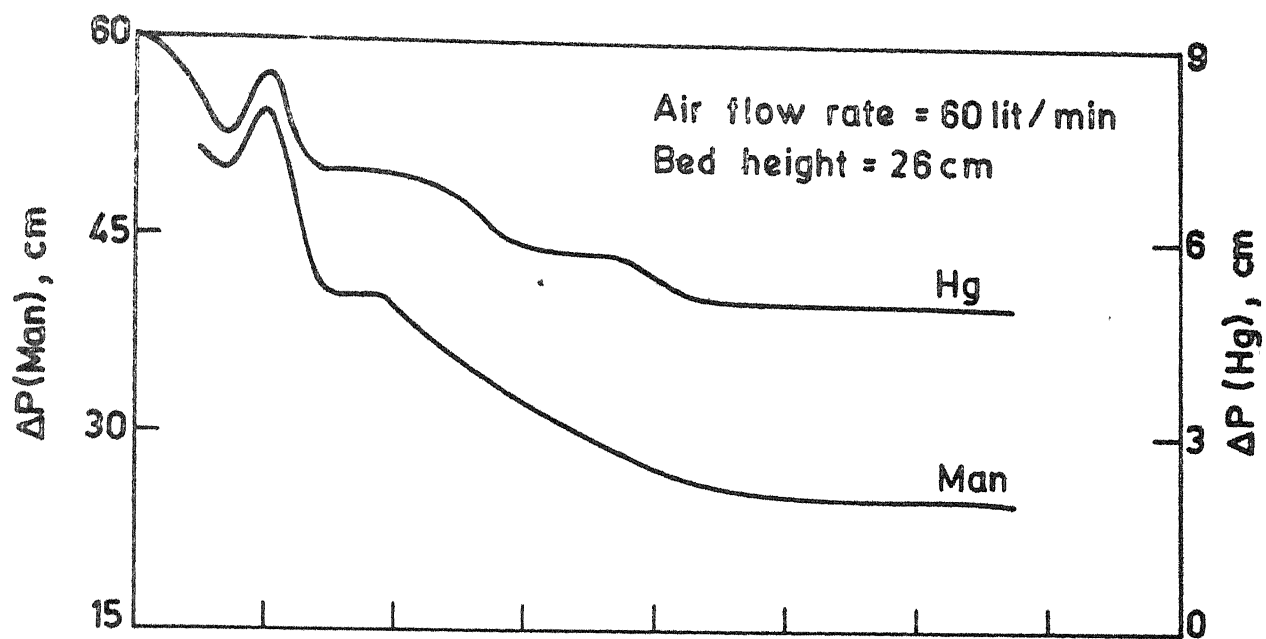


Fig. 16 Plots of pressure and temperature in SIN VII against time.

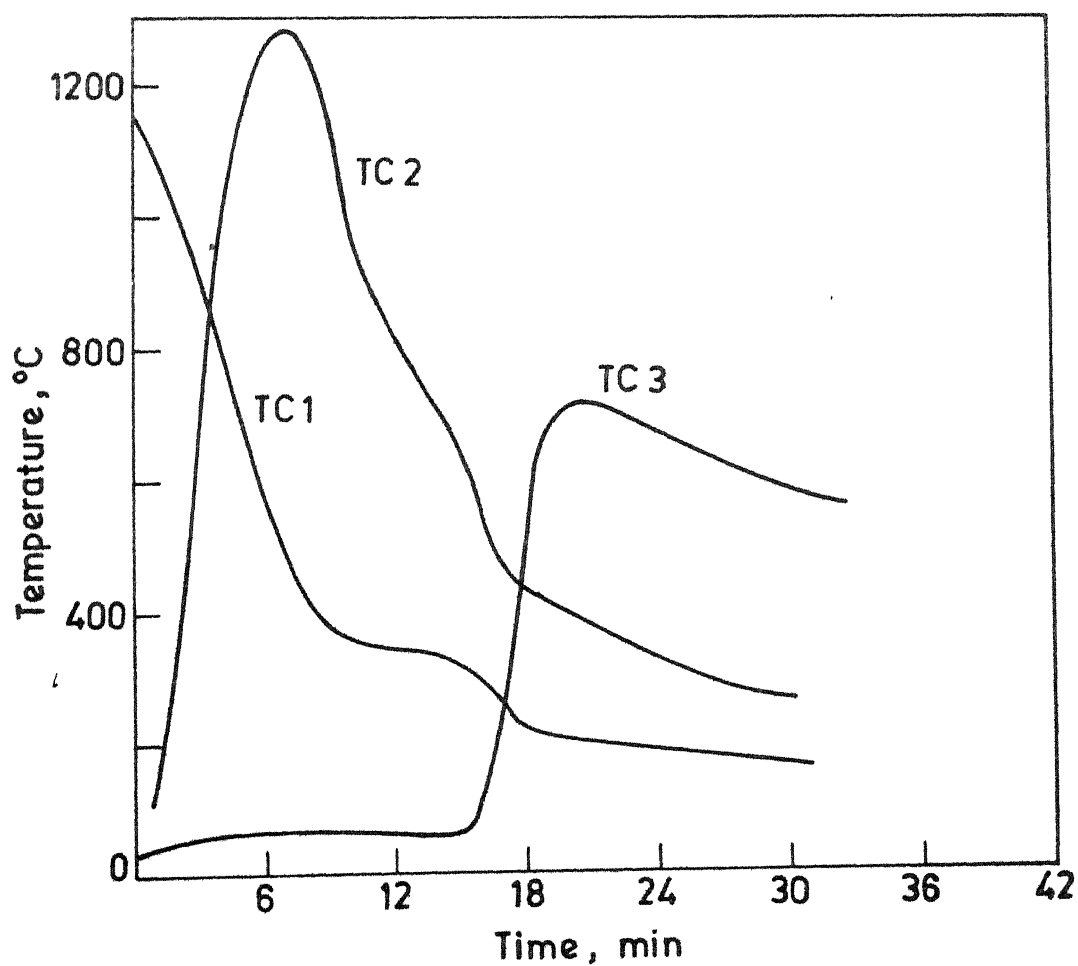
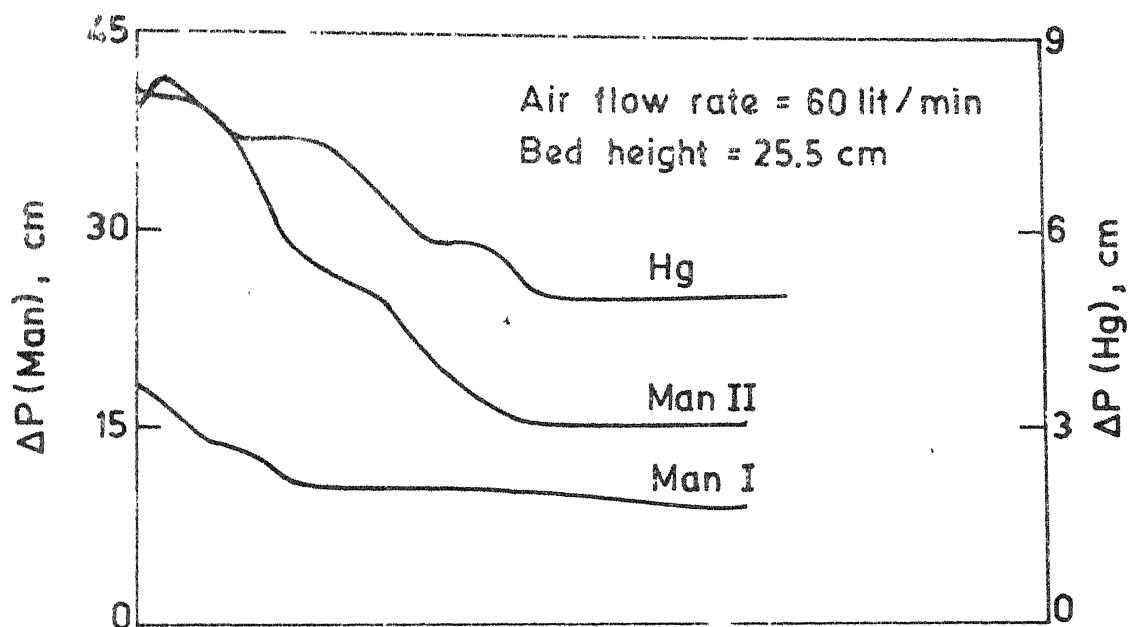


Fig. 17 Plots of pressure and temperature in SIN VIII against time.

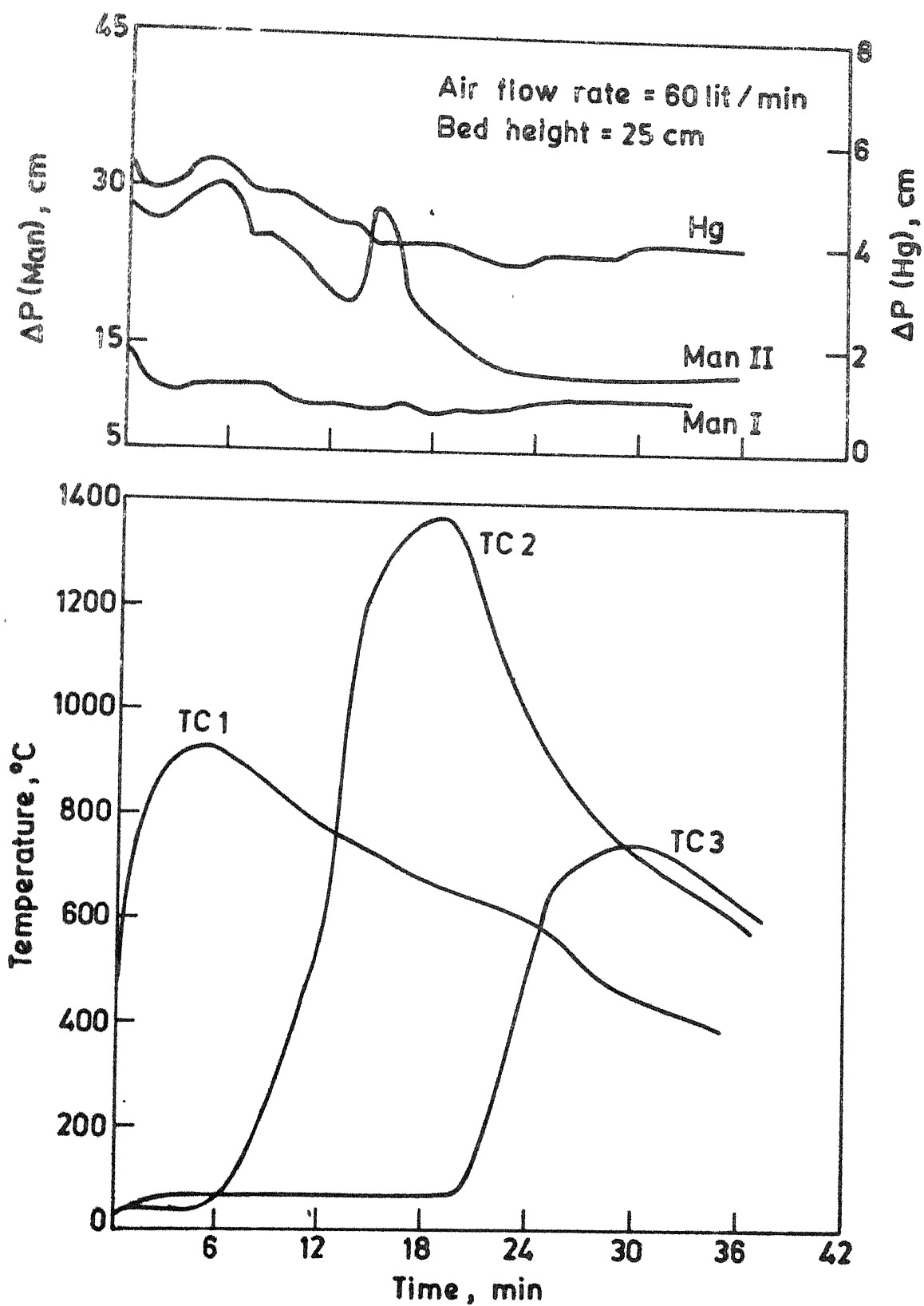


Fig.18 Plots of pressure and temperature in SIN IX against time.

Experiment	Material	Initial weight(g)	Bed height cms	Time of expt. (min.)	Final weight (g)	Weight loss (g)	Amount of H ₂ collected in the trap (cc)
RED1	I/ore	50	12.5	90	35	15	-
RED2	Crucible A1	30	8.0	80	25	5	4
RED3	Crucible B1	50	12.5	60	44	6	6
RED4	Crucible D1	20	6	60	18	2	2
RED5	SIN X	50	13.0	135	40	10	10.5
RED6	SIN IX	50	13.0	125	40	10	10
RED7	SIN VII	50	113.0	140	39	11	12

Temp. 750°C; Size range = 0.15 to 2.36 mm ; For RED 1 H₂ Flow rate = 880 cc/min.

Rest expts = 440 cc/min.

Table 7 : Reducibility test results

U. S. ARMY
GENERAL LIBRARY
A 91871

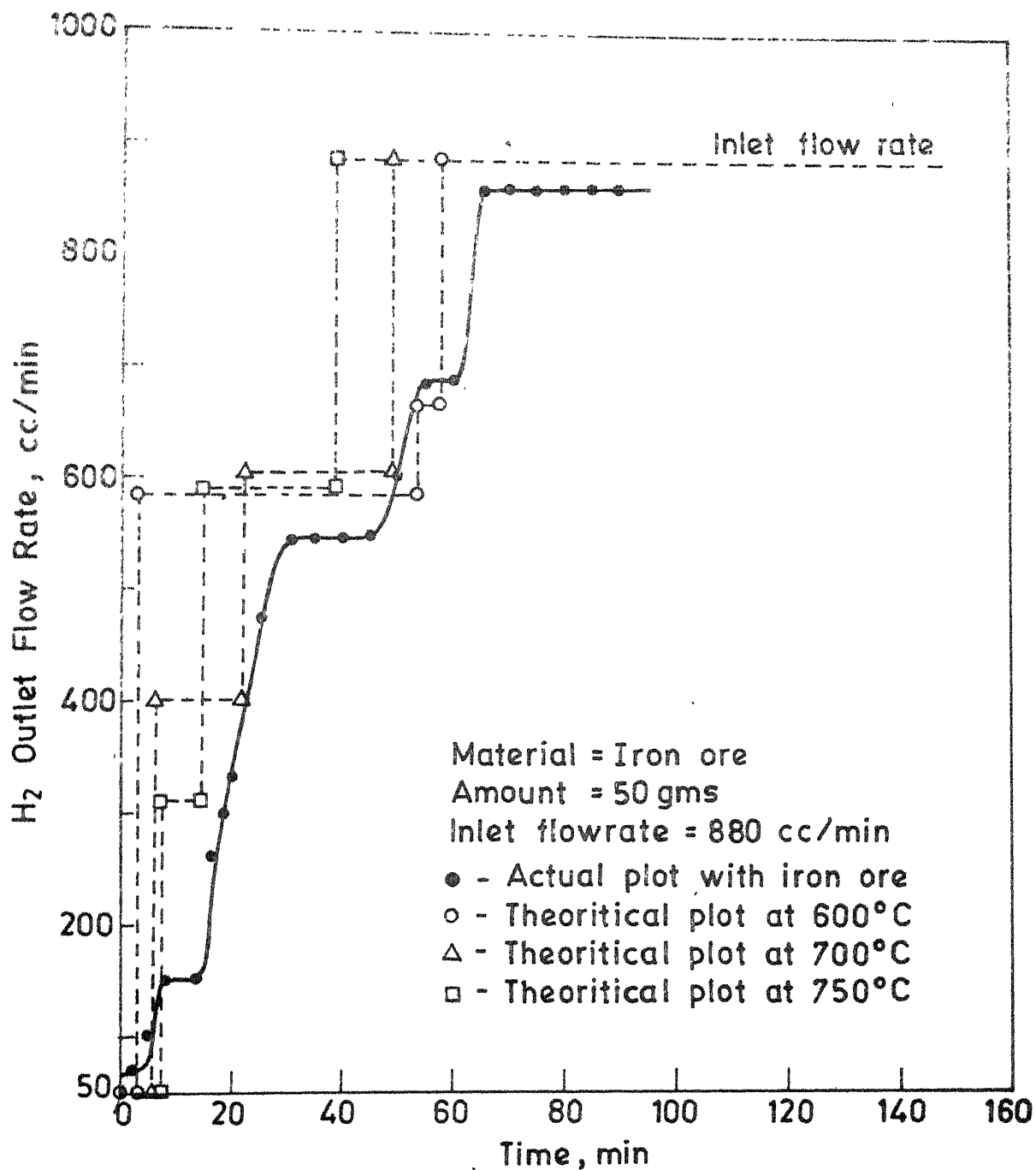


Fig.19 Plots of outlet flowrate of H₂ in RED 1 against time.

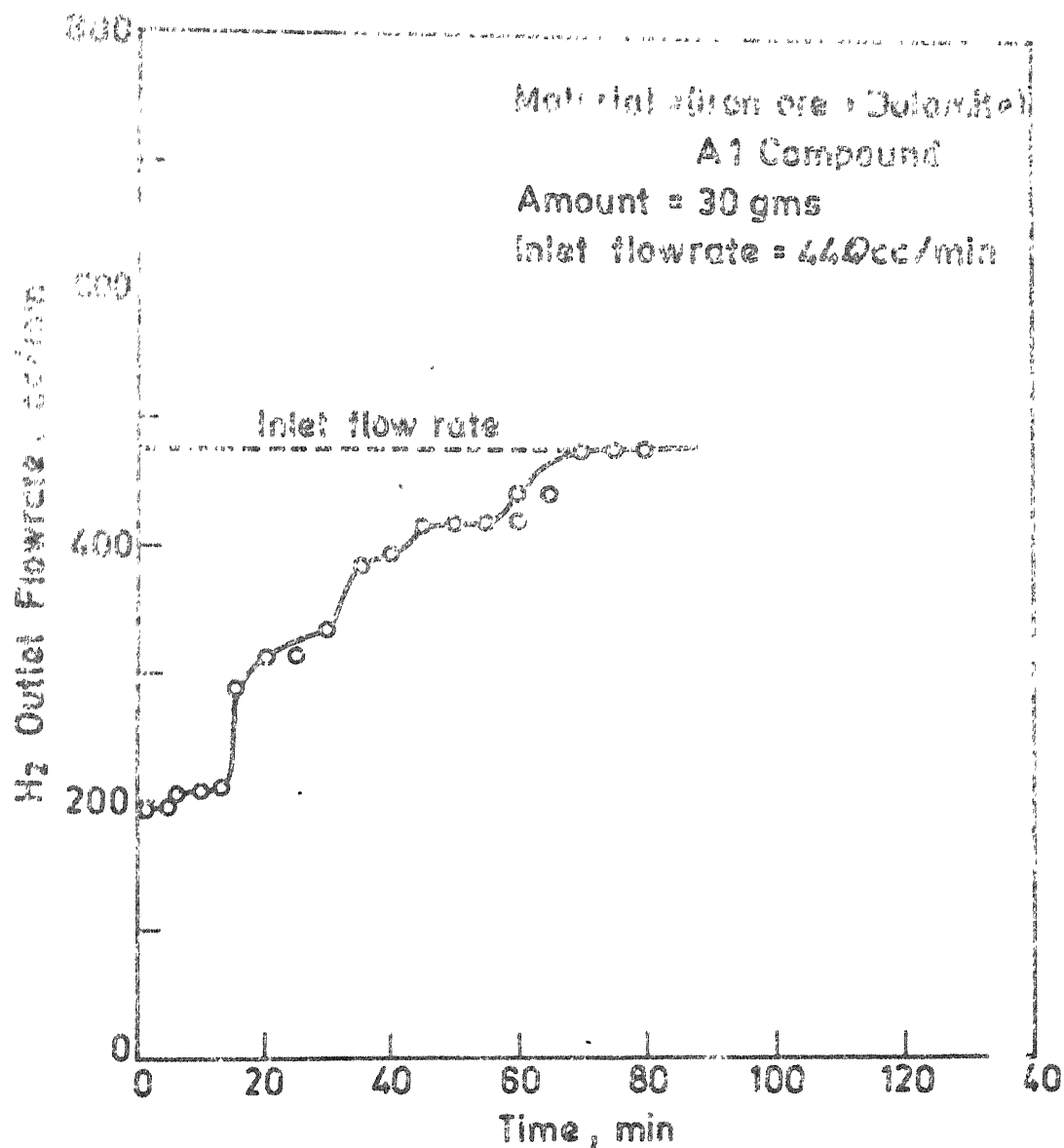


Fig. 20 Plot of outlet flowrate of H₂ in RED 2 against time.

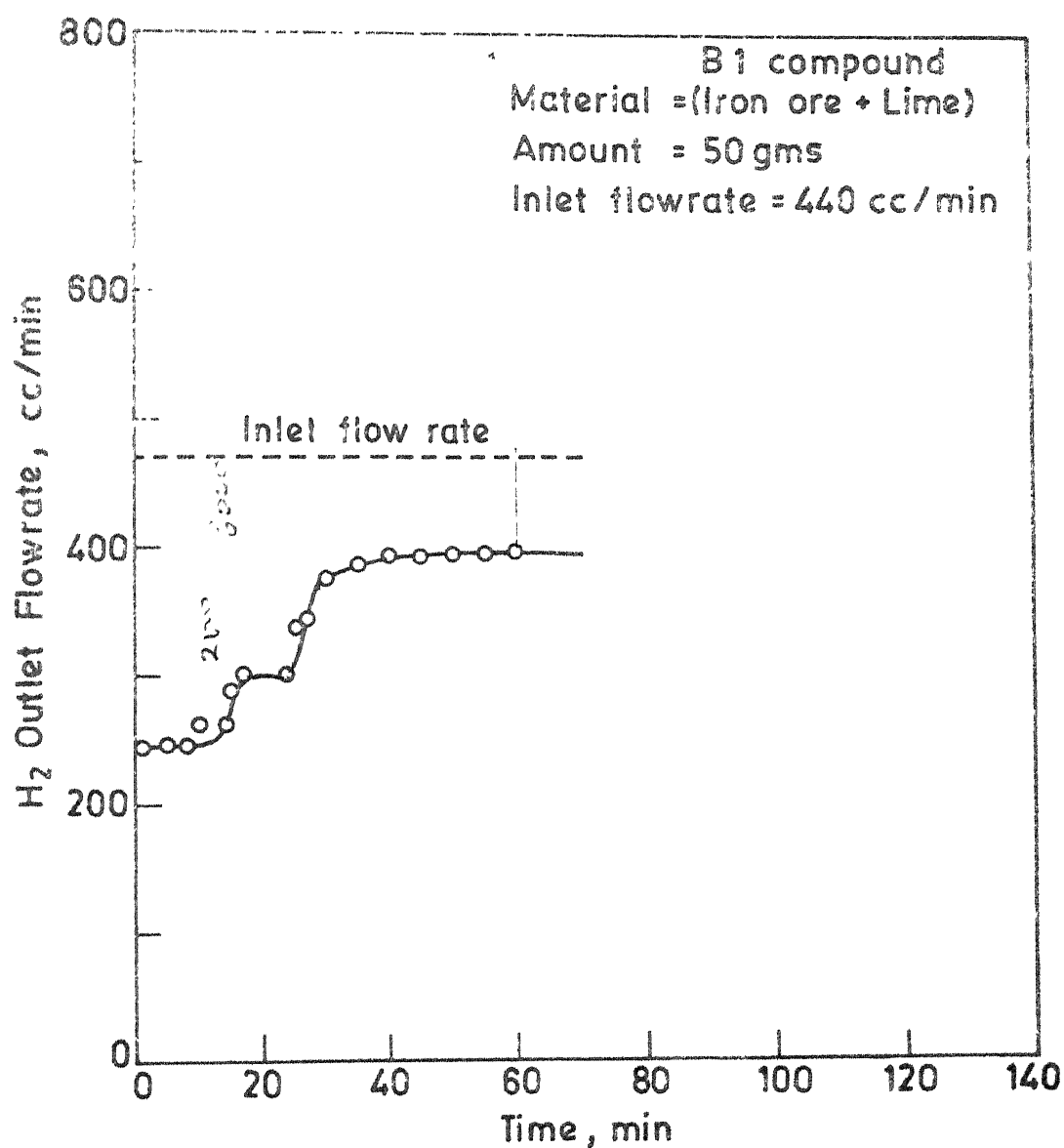


Fig. 21 Plot of outlet flowrate of H₂ in RED 3 against time.

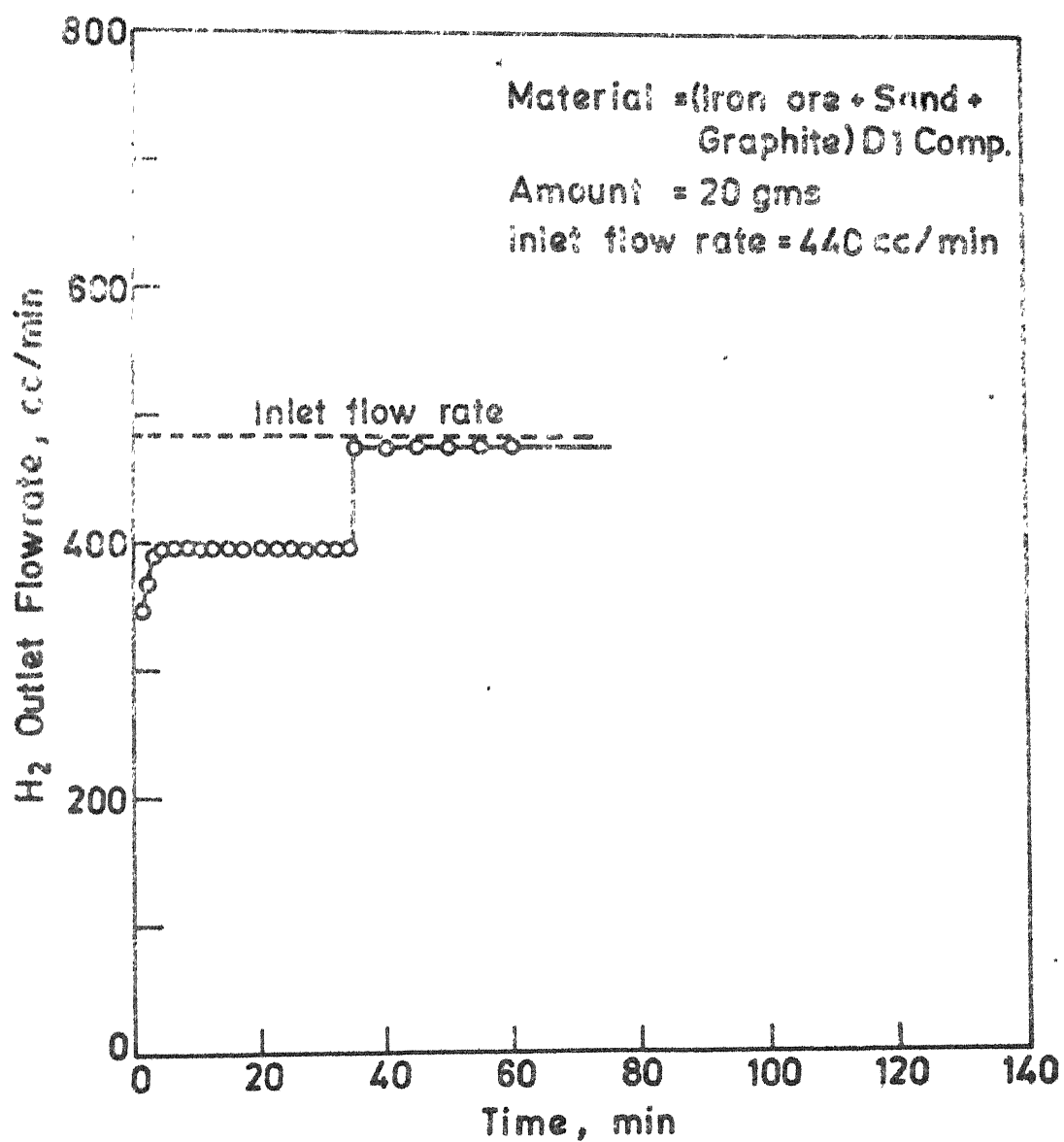


Fig.22 Plot of outlet flowrate of H₂ in RED 4 against time.

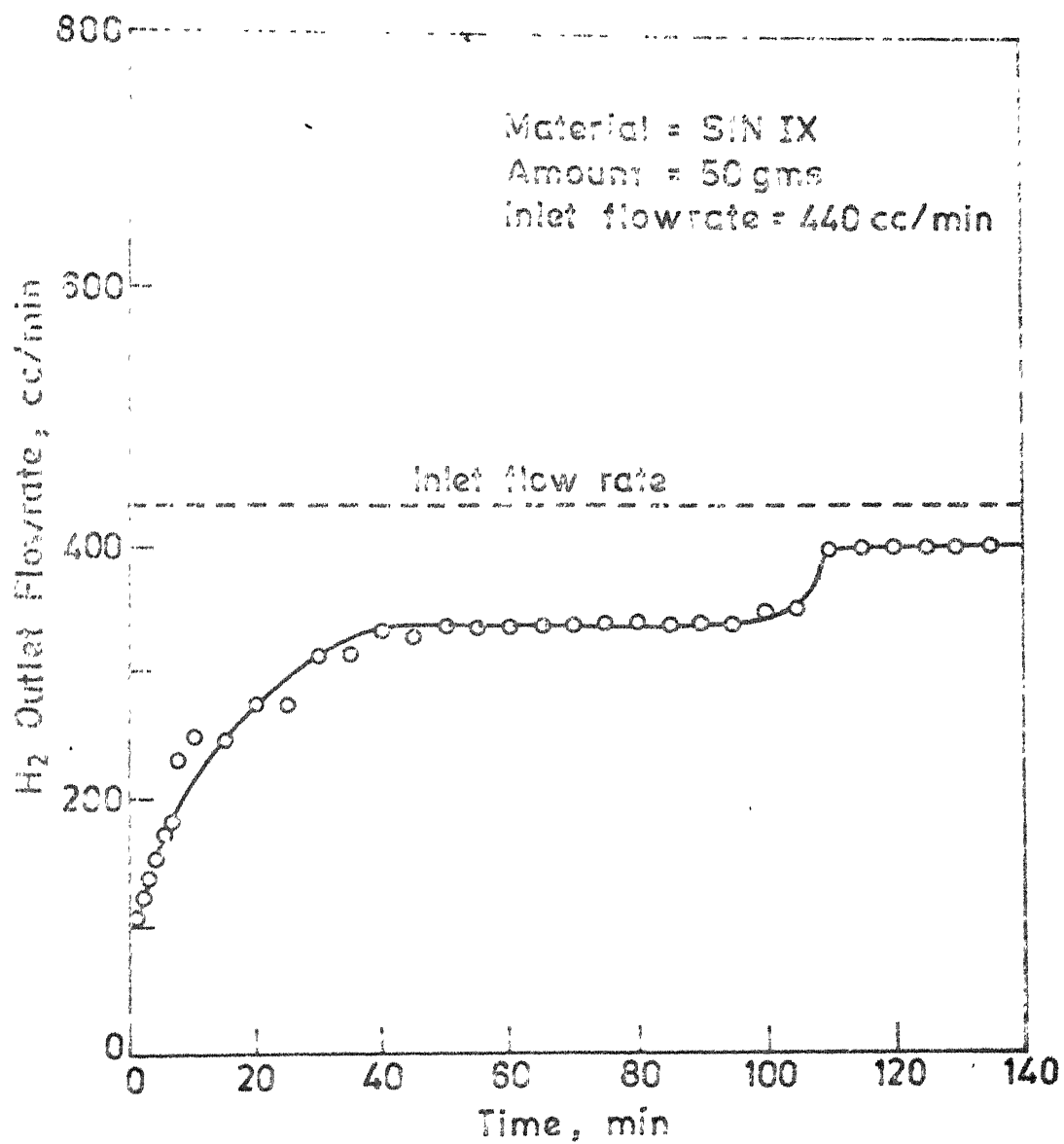


Fig. 23 Plot of outlet flowrate of H₂ in RED 5 against time.

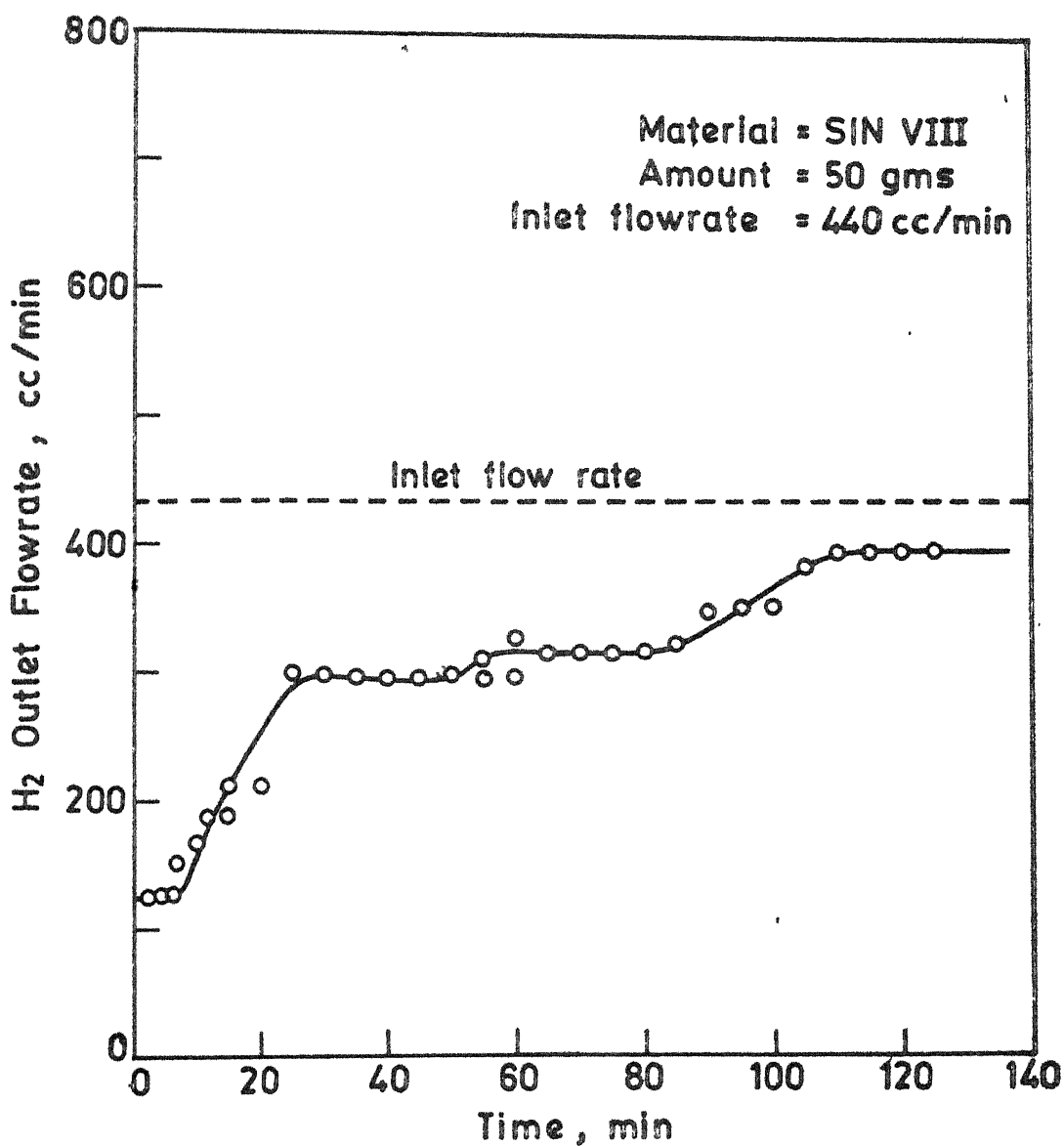


Fig. 24 Plot of outlet flowrate of H₂ in RED 6 against time.

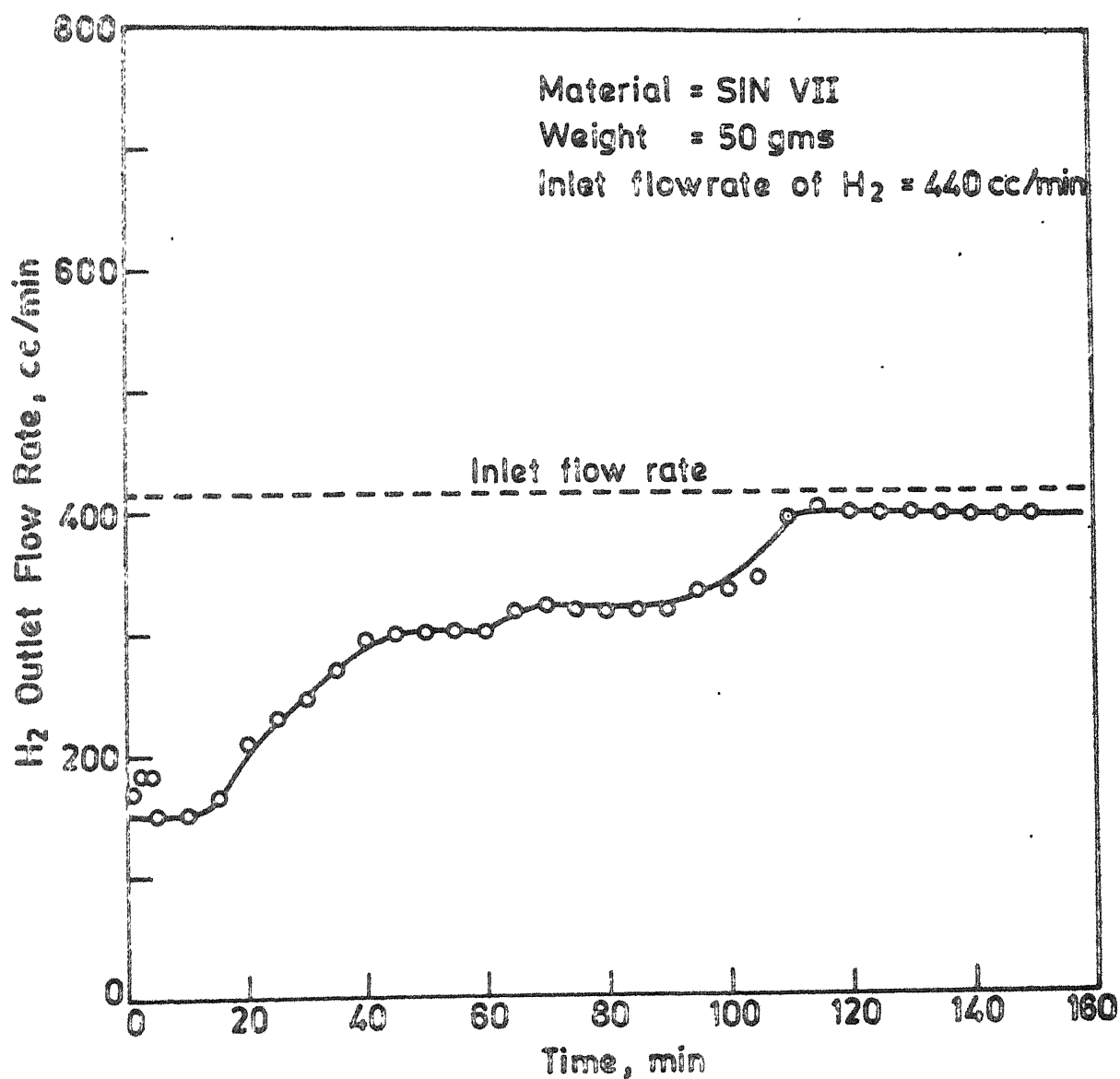


Fig. 25 Plot of outlet flowrate of H_2 in RED 7 against time

Table 8 : Shatter test results

Experiment	Wt. of the sintered mass before the test (g)	Wt. of .4.7 mm mass after the test	Strength Index	Effective yield
SIN I	630	512	31.26	40.6
SIN II	510	345	57.64	34.2
SIN III	520	445	85.57	41.2
SIN IV	500	300	60	33.6
SIN V	440	190	43.2	11.0
SIN VI	190	150	78.94	14.6
SIN VII	698	608	87.1	43.2
SIN IX	570	430	75.4	34
SIN IX	970	785	30.9	52.2

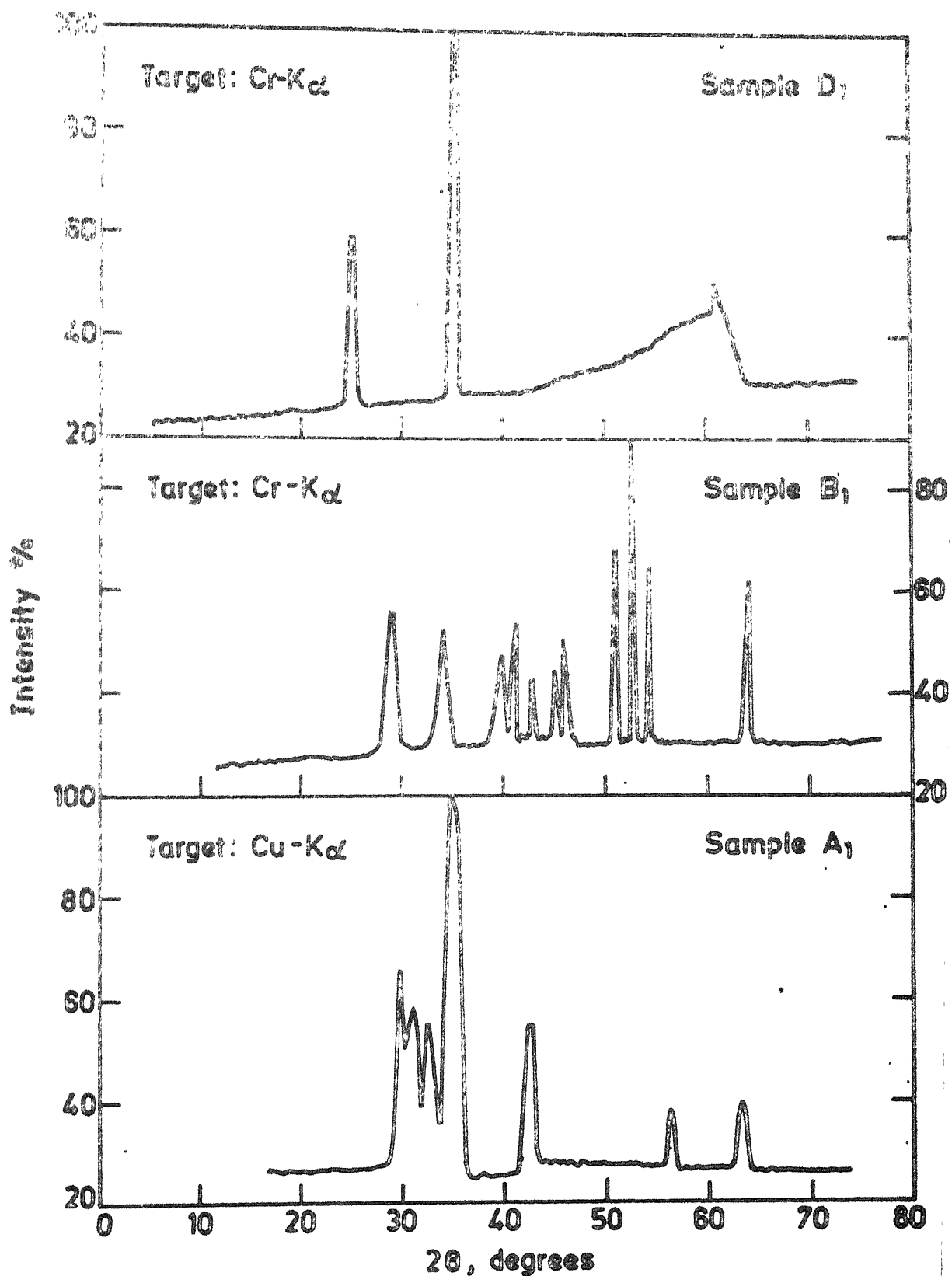


Fig.26 X-ray diffraction patterns of samples A₁ , B₁ and D₁ .

CHAPTER-VI

DISCUSSION

6.1 Effect of moisture on bulk density and permeability

Presence of water lowers the bulk density of the mix and improves the permeability of the bed. Lowering of bulk density is more pronounced in case of iron ore and (iron ore + coke breeze) mixes and the effect is small in presence of fluxes. The presence of fluxes also lower the bulk density of the iron ore.

The calculation of porosity values for different mixes is based on the following formulae :

$$\epsilon = \frac{V_o - V'}{V_o} ;$$

where, V_o = Volume of the material including voids; ϵ = porosity

V' = Volume of the material occupied by the solids or liquid

$$\text{again, } V' = \frac{V_o}{\rho_o} + \frac{p W_o}{100} \cdot \frac{1}{\rho_w} + \frac{q W_o}{100} \cdot \frac{1}{\rho_{\text{coke}}} + \frac{r W_o}{100} \cdot \frac{1}{\rho_{\text{flux}}}$$

where, W_o = Weight of iron ore taken

p = Percent of water ; q = percent of coke breeze

r = Percent of flux ; ρ_w = density of water ;

ρ_{coke} = density of coke ; ρ_{flux} = density of the flux ;

The table⁹ gives the calculated porosity values from the above equations for the experimental results in the cold model studies.

It may be seen that porosity of the green mix is not much affected by the presence of water except in one case. The presence of water thus helps to keep the solid particles apart by forming the bridges between the solid particles. The measured bulk densities of materials having water content of 4-8 pct. are in the range 1.5-1.7 g/cc compared to the reported⁵ values of 1.35-1.40 g/cc for coarse iron ore particles and 1.1 - 1.2 for the fine concentrates by Iketorp. This could be due to the large size distribution of the solid particles in the present work as the fines tend to pack in the interstitials of the big particles. Improvements in the permeability of the bed due to water additions are also much less than those reported by Iketorp. Expected increase in the bulk densities and decrease in the permeability of the bed above 6-8% moisture content were also not observed in the present work.

6.2 Forced draft sintering

6.2.1 Pressure and temperature responses : The results of the pressure and temperature responses⁵ measured were similar to those reported by Rao. Pressure drop across the bed for constant flow rate of air increased to high values as soon as the process of sintering was initiated. The pressure drop remained more or

Table 9

Table 9 : Calculated porosity values for different sinter mixes

P%	q%	r ₁ %	r ₂ %	ε %
0	0	0	0	54 .
4	0	0	0	50.85
8	0	0	0	?
0	12.5	0	0	47.17
4	12.5	0	0	51.2
8	12.5	0	0	51.68
0	12.5	20	0	53.3
4	12.5	20	0	45.74
8	12.5	20	0	45.69
0	12.5	0	20	51.29
4	12.5	0	20	43.04
8	12.5	0	20	47.1

less constant for a brief period and thereafter it started decreasing with the progress of sintering and reached a steady value at the end of the sintering of the bed. Pressure drops across the bed of green sinter mix ¹⁴ and the sintered mass were almost same as for the empty tube without any material signifying that these materials did not offer any resistance to the flow of gases.

Pressure drop response measurements across the upper portion of the bed (Man I) followed similar pattern except that it reached steady value as soon as the sinter zone moved across this region. For air flow rate of 40 lit./min, pressure drop across the whole bed during the process of sintering was of the order of 0.5-1 cm of Hg except in SIN V which was characterised by high pressure drop of 0.5-2 cm Hg (20-30 cm H_2O). For higher air flow rates of 60 lit./min the pressure drops across the bed were of the order of 1-2 cm Hg (15-25 cm H_2O) and there was rapid increase in the pressure drop in the initial stages of sintering and thereafter it decreased constantly to the steady values. Sintering of the material at high flow rates also resulted in higher peak temperatures as measured by the three thermocouples compared to those with lower air flow rate of 40 lit./min.

The increase in ^{the} resistance to the flow of gases can be attributed to the following .

1. Increase in temperature of gases resulting in higher velocities during the sintering process.
2. Expansion of solid materials on heating, thus decreasing the voids.
3. Rearrangement of the bed materials due to evaporation of moisture, calcination of fluxes, removal of fine particles etc.

Formation of a fluid slag in the sinter zone may increase the permeability as the solid shrinks on melting and voids are created. Quantity and the type of liquid slag formed is thus important. Higher temperatures of gases and solids in the vicinity of 900-1000°C without any formation of the liquid slag result in higher pressure drop across the bed as measured in experiment SIN V. The same thing could occur in the initial period of other experiments where the liquid slag might not have formed due to insufficient preheating of the air and the burden. As soon as the liquid slag is formed in the sinter zone, pressure *dr* starts decreasing due to increase in the voids caused by the fusion of materials. The sintered product on cooling is quite porous and does not offer any resistance to flow of gases.

3.2.2 Sinter quality : In the present work quantity of the sintered material in the product was observed to be around 50% only in most of the experiments except in SIN V and SIN VI in which 20-25 % material was sintered and in SINIX 65% of the material was in the sintered form. Earlier investigators have reported the yield in the order of 50-65 %. The effective yield of sinter can be defined as the material remaining above 5 mm size after dropping it once from the height of 2 m and this can be expressed in the following form :

$$EY = \text{Yield} \times (SI)$$

where, EY = Effective yield : SI = Shatter Index.

'EY' for all the experiments of sintering is shown in Fig. 27.

Where the peak temperatures recorded by ^{the 3} thermocouples are also shown therein for the comparison purposes. One can make the following observations from the effective yield data :

1. It is necessary for the bed to reach a temperature of 1150°C or so, for it to be sintered in presence of fluxes in the mix.
2. In absence of fluxes in the mix, the bed must attain a temperature of around 1300 C to get a good sintered product.
3. Dolomite in the mix decomposes faster and ahead of the sinter zone, and the maximum temperature attained by the bed are thus high and EY is satisfactory even at low flow rates of air.
4. Calcite material is known to decompose at a slow rate and if present in large quantity, it may not get calcined ahead of the sinter zone at low flow rates of air. In such cases combustion of carbon in sinter zone and calcination of fluxes occur simultaneously and ~~temperature of~~ the beds may not attain the temperature of 1150°C which ^{is} needed for fusion of slag and bond formation. Such beds give low EY values (SIN V).

The process analysis of the sintering to describe the effects of the sinter zone velocity, fuel content of mix, fluxes in the mix, moisture content etc. is given in the next chapter.

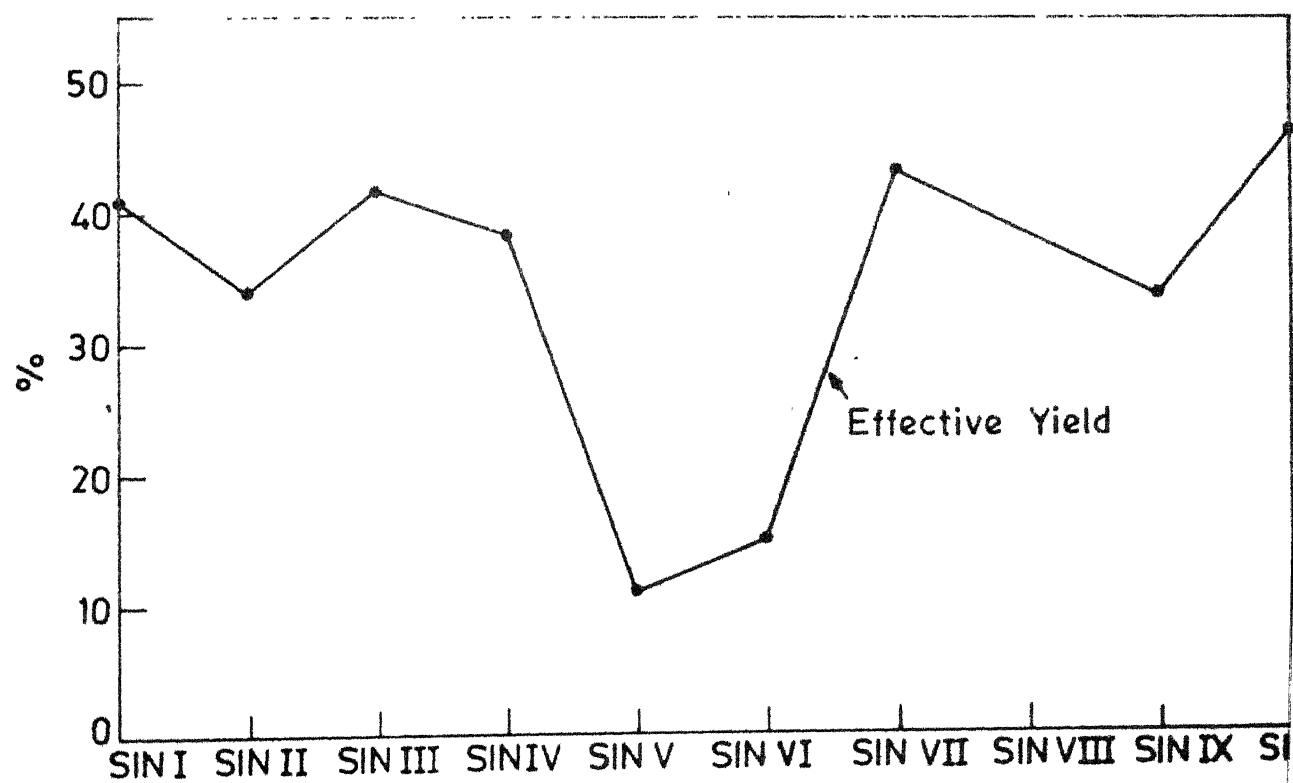
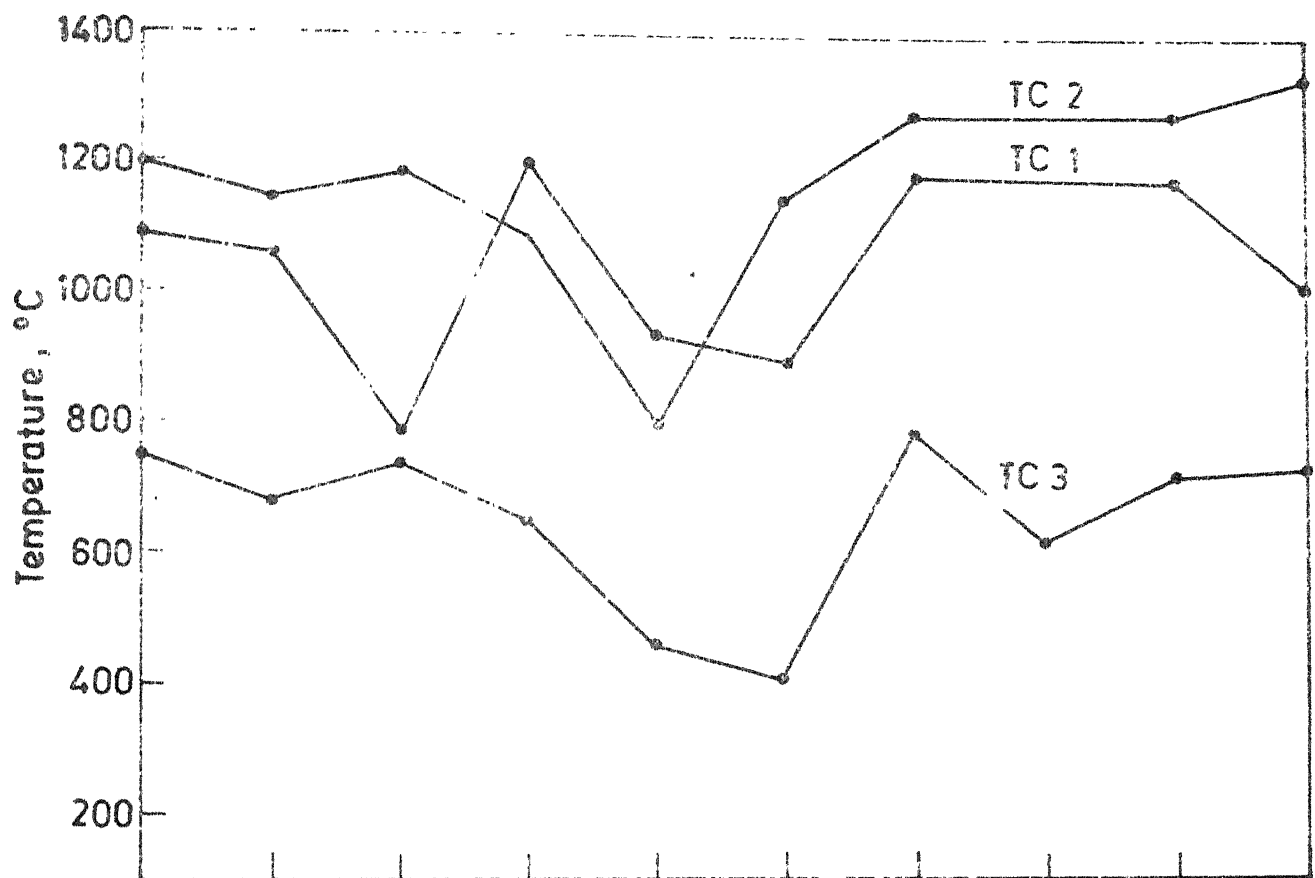


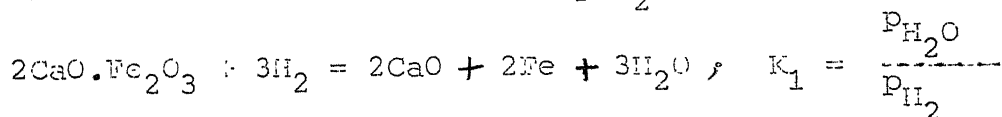
Fig. 27. Plots showing the peak temperatures in the bed and effective yield for the sintering experiments.

6.3 Reducibility of iron ore sinters

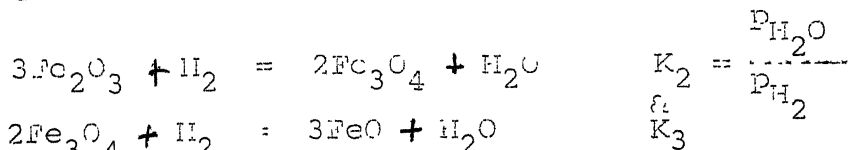
It is well known that the reducibility of the sinter is improved with increases in the sinter basicity due to the suppression of the fayalite ($2\text{FeO} \cdot \text{SiO}_2$) phase and the formation of the calcium ferrite. Reduction strength is also known to improve with the increase in CaO/SiO_2 ratio of the sinter. Presence of MgO is known to promote the formation magnesio spinel and it suppresses the formation of $\text{CaO} \cdot \text{Fe}_2\text{O}_3$ and hence it reduces the reducibility slightly. Moreover in sinters Fe_2O_3 , Fe_3O_4 or FeO may not be present in pure forms and the equilibrium Fe-C-O or $\text{Fe-H}_2\text{O}$ diagrams (Fig. 28) may not be applicable to understand their reduction behaviour.

Seth and Ross¹⁷ had proposed the following mechanism for reduction of sinter containing calcium ferrites.

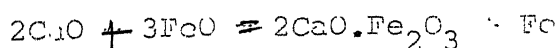
- (1) Dicalcium ferrite is reduced by H_2 as follows :



- (2) The spent gas from above, reduces any free Fe_2O_3 to FeO as follows



- (3) CaO and FeO combine to form dicalcium ferrite :



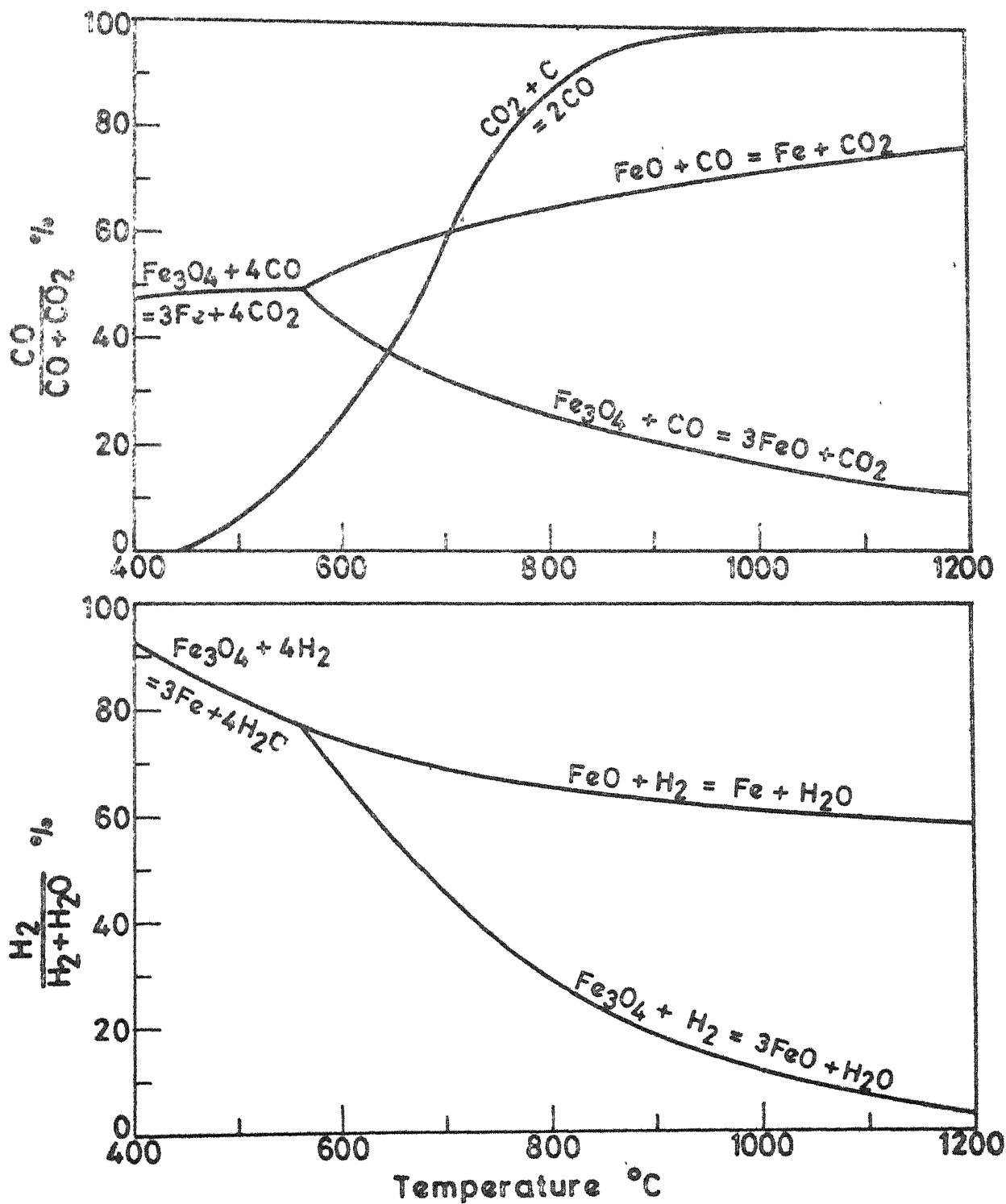


Fig. 28 Iron-Carbon-Oxygen and iron-Hydrogen-Oxygen equilibrium diagrams.

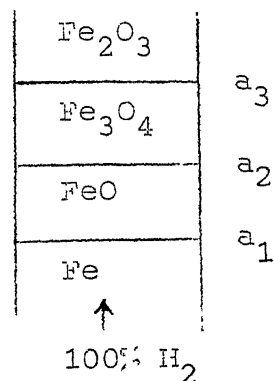
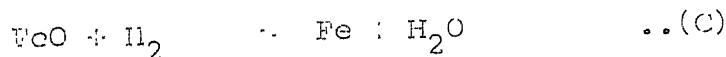
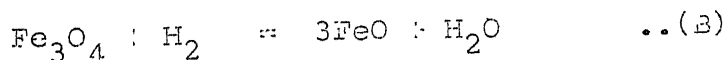
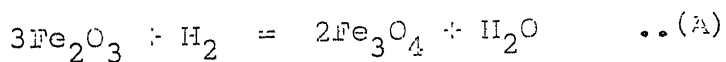
The reduction of FeO by H_2 may require higher concentration of H_2 in the gas than for the reduction of $2CaO \cdot Fe_2O_3$. Also the reduction of $2CaO \cdot Fe_2O_3$ phase may be occurring at faster rate compared to the reduction rate of FeO.

These aspects can be studied by the reduction of the material in a shaft. If a gas is passed at a slow rate, it can be expected to reach equilibrium with respect to the solid phase and the estimation of the exit gas composition can tell about the extent of the reduction occurring in the shaft.

5.4 Model for shaft reduction of iron ore.

Consider the reduction of 'n' moles of Fe_2O_3 in the shaft by passing H_2 at the rate 1 mole/min. The shaft gets divided into different zones of Fe_2O_3 , Fe_3O_4 , FeO and Fe layers depending upon the equilibrium gas composition with respect to various phases.

Let a_1 , a_2 and a_3 be the $\frac{\% H_2}{\% H_2 + \% H_2O}$ fraction at equilibrium for reduction of FeO, Fe_3O_4 and Fe_2O_3 phases respectively. Then the proportion of different oxides in the system will change as follows :



From Eq. (A)
$$\frac{d n_{\text{Fe}_2\text{O}_3}}{dt} = -3 (a_2 - a_3) ;$$

From Eq. (B) ;
$$\frac{d n_{\text{Fe}_3\text{O}_4}}{dt} = 2 (a_2 - a_3) - (a_1 - a_2)$$

& (A)

From Eq. (B)
$$\frac{d n_{\text{FeO}}}{dt} = 3 (a_1 - a_2) - (1 - a_1)$$

& (C)

$$\frac{d n_{\text{Fe}}}{dt} = (1 - a_1)$$

Time taken to reduce Fe_2O_3 completely to Fe_3O_4 is

$$t_1 = \frac{n_{\text{Fe}_2\text{O}_3}}{3(a_2 - a_3)}$$

The exit gas composition will correspond to value a_3 till time t_1 . Thereafter the gas composition will correspond to the value a_2 till time t_2 which is given as

$$t_2 = t_1 + \frac{[2(a_2 - a_3) - (a_1 - a_2)] t_1}{(a_1 - a_2)} = \frac{2(a_2 - a_3)}{(a_1 - a_2)} \cdot t_1$$

After time t_2 , the bed will consist of only Fe and FeO phases. The time for complete reduction of FeO to Fe would be given as follows

$$t_3 = \frac{2 n_{\text{Fe}_2\text{O}_3}}{(1 - a_1)}$$

For $t_2 < t < t_3$, the gas composition will remain at a_1 and thereafter H_2 will leave without taking part in any reduction reaction.

For reduction of pure Fe_2O_3 by pure H_2 at temperatures of 600, 700 and 750°C, the plots of the calculated exit gas composition versus time are shown in Fig. 19 and compared with the experimental data at 750°C. Total time for complete reduction matches with the calculated value for 600°C rather than for 750°C suggesting that the bed got cooled to 600°C or so when H_2 gas was passed through the bed. The material was heated to 750°C in the furnace before the start of the experiment but its temperature inside the quartz tube during the experiment was not measured.

6.5 Evaluation of data of reducibility tests

Let V_1 and V_2 be the amounts of H_2 passed from the bottom and H_2 collected at top. ~~all then be~~ $V = V_1 - V_2$. ^{or} where V is quantity H_2 consumed in the reduction. The flow rate of H_2 being passed is kept constant and hence V_1 can be found by knowing the flow rate and the time duration. The flow rate of H_2 gas in the outlet changes with time and V_2 can be found ~~for~~ ^{from} the area under the plot of H_2 flow rate versus time. Weight loss occurs due to the removal of oxygen atoms by H_2 . Hence weight loss from the H_2 gas flow measurements can be determined as follows .

$$\begin{aligned} W_{\text{loss}} &= \text{moles of } \text{H}_2 \text{ consumed} \times 16 \text{ gms.} \\ &= \frac{V_{\text{H}_2}^{\text{consumed}}}{22400} \times 16 \end{aligned}$$

Inlet flow rate may be corrected to match the calculated weight

loss with the actual weight loss obtained after the end of experiment. Weight of H_2O collected is due to formation of H_2O in the gas and can be determined as follows :

$$W_{H_2O} = \frac{18 V_{H_2}^{\text{consumed}}}{22400} \text{ gms.}$$

This gives an independent check on the reliability of the weight loss data. It may however be not possible to collect all the H_2O in the gas and some may be absorbed in $CaCl_2$ tube in the exit. Maximum weight loss for complete reduction of iron ore is given as

$$W_{\text{max}} = \frac{(\% \text{ Fe})_{\text{material}} W_o}{100.56} \cdot \left(\frac{O}{Fe} \right)_{\text{material}} .16$$

where, % Fe in the bed material = % Fe in iron ore $\times (f_{\text{ore}})$

f_{ore} can be obtained from the proportions of different materials in the crucible or sinter mix.

The estimated weight losses are compared with measured values in Table 10. The degree of reduction R has been obtained as follows

$$R = \frac{\text{loss(actual)} \times 100}{\text{loss(max. estimated)}}$$

Calculations show H_2 gas being passed at the rate

$$\frac{380}{22400} = 0.04 \text{ mole/min.}$$

will absorb $(0.04 \times 7 \times 600) = 168$ cal./min. for getting heated to 600°C . As the bed consists of (50 gms of Iron ore + 200 gms of preheat medium), its temperature will decrease at the rate

$$\frac{168}{250 \times 0.22} = 3.3^{\circ}\text{C/min.}$$

The bed can loose temperature by $100-200^{\circ}\text{C}$ when the gases H_2 or H_2 are passed for flushing the system ore reduction purposes. Temperature pick up by the bed for the furnace may not match with temperature loss by the bed. These experiments must be carried out over a larger size of bed or at a lower flow rate and the exact temperature of the bed should be measured simultaneously. These things could not be made possible in the present work due to the limitations posed by the diameter of the quartz tube. Additional experiments were done at low rate of about 0.02 mol/min of H_2 gas. Comparing the results of the reducibility experiments on different types of materials one can however make the following observations:

1. For dolomite and calcite based compounds of iron ore or the sinters, the initial exit gas composition is much more than zero % H_2 corresponding to equilibrium value for the reduction of Fe_2O_3 to Fe_3O_4 . In such cases, the outer layer of the particle may be coated by a solidified layer of the $\text{CaO} \cdot \text{Fe}_2\text{O}_3$ phase and this gas is never able to reach the equilibrium composition with respect to Fe_2O_3 in the solid.

2. The last stage of reduction (7-30%) of any material other than the iron ore is marked by high $H_2/(H_2 + H_2O)$ ratio in the gas of the order of 0.9 - 0.92. This could be due to either lowering of bed temperature to less than 600°C or presence of $2FeO.SiO_2$ layer in the bed which is very ~~different~~ ^{difficult} to reduce by gases. Proportion of fayalite in the bed will depend upon the type of material used in the reduction experiment. In acid sinters, %FeO is high and hence the degree of reduction achieved is less compared to the basic sinters. Low degree of reduction for RED 3 is due to insufficient period given for reduction rather than the presence of the fayalite phase.
3. Most of the sinter materials exhibit a constant exit gas composition in the range of 70-75 % for a long period of 1 hour or so. This range ^{is} also present at the start of the experiment RED 4 (fayalite) and also in RED 1 (hematite ore) for a very short period. This can be due to the presence of free FeO phase which results from the reduction of higher oxides of iron to FeO in the bed. The FeO formed during the reduction of the material at 600-700°C, does not combine with SiO_2 to form $2FeO.SiO_2$ phase and hence its reduction pattern is different from that of the pre-reduced FeO in the bed material where it will be present mostly as $2FeO.SiO_2$. The range of 70-75% H_2 in the exit gas agrees with the gas composition value at equilibrium with FeO & Fe phases at temp. 600-700°C.

Experiment	Measured inlet flow rate (cc/min.)	Corrected inlet flow rate (cc/min.)	H ₂ consumed From graph	H ₂ consumed (moles) Max. estimated	H ₂ O collected, cc.	Weight loss (gm) Max. estimated	Calculated degree of reduction R
RED 1	860	880	1.207	0.87	-	15.66	15 95.7
RED 2	450	470	0.34	0.417	4	6.6	5 76
RED 3	450	470	0.346	0.695	6	11.52	6 53
RED 4	450	435	0.123	0.183	2	2.9	2 69
RED 5	450	435	0.62	0.79	10.5	12.64	10 79.2
RED 6	450	435	0.62	0.74	10	11.84	10 84.5
RED 7	450	430	0.70	0.74	12	11.84	11 93

Table 10 : Results of reducibility tests

CHAPTER VII

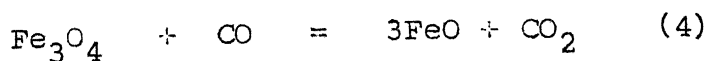
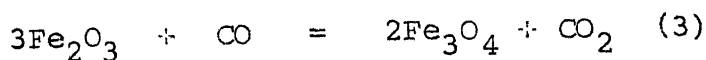
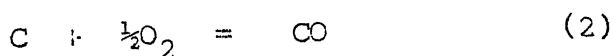
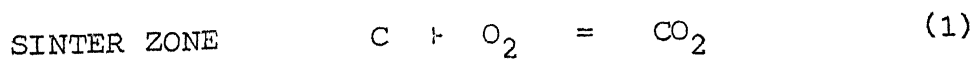
PROCESS ANALYSIS OF SINTERING

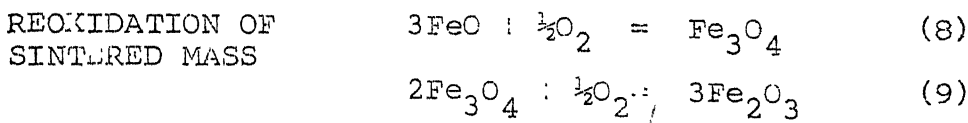
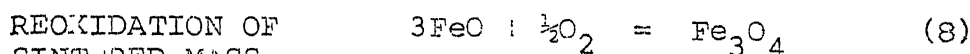
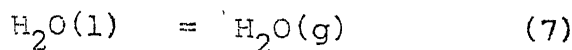
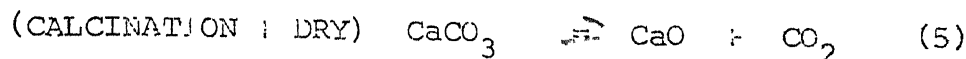
In this chapter attempts are made to analyse the sintering process by making overall material and thermal balances and by examining critically the thermal requirements of the sinter and calcination zones separately for achieving good quality sinters.

7.1 OVERALL HEAT BALANCE

The major source of heat in the sintering process is due to the combustion of carbon to CO and CO₂. A part of heat evolved is lost to the surroundings during the sintering process, a part is consumed in the evaporation of moisture and calcination of fluxes in the mix, and rest is used in raising the temperature of the sintered mass and the exit gases. The average temperatures of the gases and the solid bed are estimated from the measured temperature responses (i.e., figs. 10-18). Amounts of air passed and gases generated are theoretically determined from the combustion reactions, calcination of fluxes and evaporation of moisture as stated below.

The reactions occurring in the bed are as follows :





If n_c , n_{CaCO_3} , n_{MgCO_3} , $n_{\text{H}_2\text{O}}$ are the respective moles of carbon, CaCO_3 , MgCO_3 , H_2O in the bed and r the degree of reoxidation of the sintered mass, and carbon in the bed is assumed to produce CO and CO_2 in equal proportions by reactions (1) and (2), then overall material balances yield the following :

$$\text{Total moles of } \text{O}_2 \text{ consumed} = (0.75 + 0.25 r) n_c \quad (10)$$

$$\text{Total moles of air passed} = (0.75 + 0.25 r) n_c \cdot \frac{100}{(\% \text{O}_2)_{\text{air}}} \quad (11)$$

$$\begin{aligned} \text{Total moles of gases} \\ \text{produced} &= \left[\frac{(\% \text{N}_2)_{\text{air}}}{(\% \text{O}_2)_{\text{air}}} (0.75 + 0.25 r) \right] \cdot n_c + \end{aligned}$$

$$n_c + n_{\text{CaCO}_3} + n_{\text{MgCO}_3} + n_{\text{H}_2\text{O}} \quad (12)$$

The results of calculations for the conditions in all the sintering experiments are given in table 11. The thermal data used in making these calculations are given in Appendix. Weight of FeO in the sintered mass is calculated as follows

$$n_{\text{FeO}} = (1 - r) n_c \text{ moles}$$

where r is degree of reoxidation. It is calculated that 0.5 mole

of CO produced by 1 mole of carbon combustion reduced⁵ 0.6 moles of Fe_2O_3 to give 0.9 moles of FeO and 0.1 moles of Fe_3O_4 or 1 mole of carbon in combustion produced exactly 1 mole of Fe^{++} ions in the bed and r fraction , get reoxidised to Fe^{+++} during cooling.

Table 11 : Overall mass and heat balances in sintering experiments

Mass Balance	I	II	III	IV	V	VI	VII	VIII	IX
<u>INPUT</u>									
n_c (moles)	9.18	9.18	9.18	9.18	9.18	9.18	9.18	9.18	9.18
n_{H_2O}	6.25	6.25	6.25	6.25	6.25	6.25	6.25	6.25	6.25
n_{CaCO_3}	0.924	1.848	2.39	1.47	2.94	-	1.848	2.94	-
n_{MgCO_3}	0.67	1.37	0.67	-	-	-	1.34	-	-
r(assumed)	0.7	0.9	0.9	0.7	0.9	0.5	0.9	0.9	0.5
n_{air} (moles)	40.24	42.62	42.62	40.24	42.62	38.2	42.62	42.62	38.2
<u>OUTPUT</u>									
$n_{exit\ gases}$ (moles)	46.07	48.45	48.45	46.07	48.45	44.03	48.45	48.45	44.03
Estimated weight of sinter(g)	1620	1730	1730	1640	1730	1590	1730	1730	1590
%FeO in sinter (calculated)	12.24	3.80	3.80	12.10	3.80	20.78	3.80	3.80	20.78
<u>Heat balance</u>									
<u>INPUT</u>									
Average temp. of gas ($^{\circ}C$)	133	125	91	111	162.5	159	135	115	250
Average temp. of the bed($^{\circ}C$)	700	805	775	610	610	690	737	725	885

Table 12 : Continued

	I	II	III	IV	V	VI	VII	VIII	IX
C to CO ₂ (Kcal)	431.7	431.7	431.7	431.7	431.7	431.7	431.7	431.7	431.7
C to CO (Kcal)	120.48	120.48	120.48	120.48	120.48	120.48	120.48	120.48	120.48
Heat of reduction (Kcal)	-0.5	-0.5	-0.5	-0.5	-0.5	-0.5	-0.5	-0.5	-0.5
Heat of reoxidation (Kcal)	222.3	285.86	285.86	222.3	285.86	158.8	285.86	285.86	158.8
Total (Kcal)	773.98	837.54	837.54	773.98	837.54	710.48	837.57	837.57	710.48
<u>Heat demand</u>									
Heat of water evaporat- ion (Kcal)	71.82	71.82	71.82	71.82	71.82	71.82	71.82	71.82	71.82
Heat of flux decompo- sition (Kcal)	57.25	114.5	121	63.75	127	-	114.9	127.5	-
Sensible heat of sinter (Kcal)	268.56	324.09	271.7	230.82	245.82	251.98	295.95	291.88	325
Sensible heat of gases (Kcal)	53.1	50.7	36.33	44.94	67.6	62.46	54.76	47.84	98.2
Total (Kcal)	450.7	561.1	500.85	411.33	512.5	336.20	536.98	539.03	495.2
Heat loss by deficit (kcal)	323.28	276.47	336.72	362.65	325.07	324.24	300.59	298.5	215.26

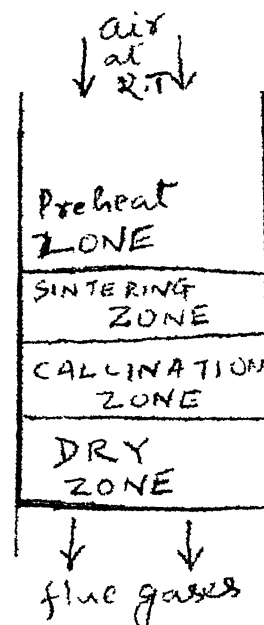
These results show that around 40% of the heat produced by the combustion reaction is retained by the bed material as its sensible heat, 5-10 % of the heat is picked up by the outgoing gases at the end of the sintering process around 9% is consumed in evaporation of the free moisture and rest is consumed in the calcination of the flux and as heat losses to the surroundings by convection or radiation. Estimation of the average temperature of the sintered mass and the flue gases may be subjected to errors and hence heat balance may not be satisfied in some cases. There are large variations in the calculated heat losses due to these reasons . Even the assumption that C reacts with oxygen to produce CO and CO₂ in equal proportions and the assumed value of the degree of reoxidation may not be correct. The overall heat balance is thus not very useful in analysing the sintering process. Attempts are made to analyse the process by making zonal balances in the following section.

7.2 Zonal balance in sintering

Cold air continuously passes through a bed of hot sinter and gets preheated to a high temperature before taking part in the combustion reaction in the sinter zone. The hot exit gases from the sinter zone cause calcination of the carbonate materials in the bed lying just below the sinter zone. The gases from the calcination zone are cooled further due to the evaporation of moisture in the mix and the heating of the dry material to the calcination temperature of the carbonate material. The water

vapour content of the gases is around 15% and its dew point would be around 50°C. Gases leaving the dry zone would cause preheating of the wet zone to the dew point due to the condensation of H_2O vapours in the wet zone.

Let the sinter zone move with a velocity $\left(\frac{dx}{dt}\right)$, cm/min., .. in the unit having cross sectional area A cm^2 , and height H cm, and the bulk density of the green mix be ρ_0 g/cm³. Let f_c , f_{CaCO_3} , f_{MgCO_3} and f_{H_2O} be the weight fractions of carbon, $CaCO_3$, $MgCO_3$ and H_2O respectively in the bed.



The rate of material being sintered = $A \frac{dx}{dt} \cdot \rho_0$ g/min

Carbon being burnt per unit time = $\dot{n} = A \frac{dx}{dt} \cdot \rho_0 \cdot \frac{f_c}{12}$ (moles/min)

7.2.1 Sinter zone heat balance

Sensible heat of incoming air to the sinter bed

$$Q_{supply}^{SZ} = \left(\frac{0.75 + 0.25 r}{0.21} \right) \dot{n} C_{p_{air}} (T_1 - 25)$$

Heat of reaction ΔH_R

$$= (-\Delta H_{CO_2} + 0.6 \Delta H_{Fe_2O_3} - 0.1 \Delta H_{Fe_3O_4} - 0.9 \Delta H_{FeO}) \dot{n}$$

Cal/min.

Sensible heat of the gases leaving the sinter zone :

$$Q_1^{SZ} = \left(\frac{0.79}{0.21} (0.75 + 0.25 r) + 1 \right) \dot{n} \cdot C_{p_{gas}} \cdot (T_2 - 25) \text{ Cal/min.}$$

Heat for raising the temperature of the solid :

$$\frac{Q_{SZ}}{2} = \frac{12 \dot{n}}{f_c} \cdot C_{p_{solid}} \cdot (T_{SZ} - T_3) \left[1 - f_{H_2O} - 0.44 f_{CaCO_3} - 0.52 f_{MgCO_3} - f_c \right] \text{ Cal/min.}$$

$$\text{Heat for fusion} = W \cdot \dot{n} \cdot \Delta H_f$$

where, r = degree of reoxidation

\dot{n} = rate of carbon burnt at any particular instant in moles/min.

T_1 = Temp. of the preheated air

T_2 = Temp. of the gases leaving the sinter zone

T_3 = Temp. of the sinter bed at the start of combustion zone

T_{SZ} = Temp. of the sinter zone bed material

$C_{p_{air}}$ = average specific heat of air in Cal/°C/mole

$C_{p_{gas}}$ = average specific heat of gas in Cal/°C/mole

The heat losses are difficult to estimate as it can lose heat by conduction in the axial directions of the steel tube as well as by convection and radiation to the surroundings.

If a part of $CaCO_3$ in the bed is left undecomposed before the sinter zone moves there, a part of $CaCO_3$ is decomposed in the zone of sintering then,

$$\text{Heat of calcination, } Q_3^{SZ} = \frac{12 \dot{n}}{100 f_c} \cdot f_{CaCO_3} \cdot g (42500 + (C_{p_{CO_2}} (T_2 - T_3)))$$

where, g is the fraction of carbonate mix decomposing in the sinter zone.

The heat balance in the sinter zone therefore is :

$$\frac{0.75 + 0.25r}{0.21} C_{p_{\text{air}}} (T_1 - 25) + \Delta H_R$$

$$= \left[\frac{0.75 + 0.25r}{0.21} + 0.25(1-r) \right] C_{p_{\text{gas}}} (T_2 - 25)$$

$$+ C_{p_{\text{solid}}} (T_{\text{SZ}} - T_3) \frac{12}{f_c} (1 - f_{\text{H}_2\text{O}} - 0.44 f_{\text{CaCO}_3} - 0.52 f_{\text{MgCO}_3} - f_c)$$

$$+ \frac{0.12}{f_c} f_{\text{CaCO}_3} \cdot g \cdot (42500 + C_{p_{\text{CO}_2}} (T_2 - T_3))$$

$$+ W \Delta H_f + \frac{Q_{\text{loss}}}{\dot{n}}$$

T_2 and T_{SZ} are high if

- (1) T_1 is high, (2) g is small, (3) W is small, (4) Q_{loss} is small, (5) f_c is large, (6) f_{CaCO_3} is small.

In the bed just above the sinter zone the liquid slag solidifies and releases its heat of fusion which is picked up by the incoming air. Hence the quantity of slag formation would not really affect the T_2 or T_{SZ} but on the other hand it will be affected by the value of T_{SZ} and the composition of the mix.

7.2.2 (Calcination + Dry) zone

Here gases enter at high temp. of T_2 but leave the zone at the dew point T_{DP} . Carbon in the bed in this zone is assumed to remain unaffected. Fluxes decompose and water gets evaporated in this zone.

$$Q_{supply}^{CD} = \dot{n} \left[\frac{0.79}{0.21} (0.75 + 0.25 r) + 1 \right] C_{p_{gas}} (T_2 - T_{DP}) + g \frac{f_{CaCO_3}}{f_c} \cdot \frac{12}{100}$$

This heat is picked by raising the temperature of solid from T_{DP} to T_3 , evaporation of moisture, calcination of fluxes besides the losses to surroundings. Assume the zone to move at the same velocity as the sinter zone.

Heat for raising the temp. of the solid is :

$$Q_1^{CD} = (1 - f_{H_2O} - 0.44 f_{CaCO_3} \cdot (1-g) - 0.52 f_{MgCO_3}) \cdot \frac{12 \dot{n}}{f_c} C_{p_{solid}} (T_3 - T_{DP})$$

Heat for calcination is :

$$Q_2^{CD} = \frac{12 \dot{n}}{f_c} \left(\frac{f_{CaCO_3}}{100} (1-g) 42500 + \frac{f_{MgCO_3}}{34} \cdot 24000 \right) \text{Cal/min}$$

42500 Cal is heat calcination of $CaCO_3$ and 24000 that of $MgCO_3$.

Heat for evaporation of moisture is :

$$Q_{CD} = \frac{12 \dot{n}}{f_c} \cdot (f_{H_2O}' \cdot 540) ; \text{Heat losses : } Q_4 = Q_{\text{loss}}$$

where, f_{H_2O}' is weight fraction of H_2O in the bed during the sintering process and it may not be same as the initial moisture content of the bed due to increased condensation of H_2O vapours.

7.2.3 Preheating of wet zone to dew point

Heat is required to raise the temperature of the bed from room temperature to T_{DP} and heat is supplied due to condensation of H_2O vapours and sensible heat of the incoming gases at T_{DP} .

$$\text{heat balance : } \frac{12 f_{H_2O}' \dot{n}}{f_c} \cdot 540 + \left(\frac{0.79}{0.21} (0.75 + 0.25) + 1 \right) \cdot$$

$$\left(\frac{f_{CaCO_3}}{100} + \frac{f_{MgCO_3}}{84} \right) C_p (T_{DP} - T_{RT})$$

$$= K C_{p_{\text{solid}}} \cdot (T_{DP} - T_{RT}) \frac{12 \dot{n}}{f_c}$$

where K is relative velocity of the preheat zone to sinter zone velocity. and

Discussion of zonal heat balances :

Calculations show that the preheat wet zone would move at a velocity 5-6 times the sinter zone velocity and hence the material should get preheated to dew point temperature of $50^\circ C$

(Contd..p.92)

Table 12 : Sample calculations for various fuel rates in the mix $f_c = 0.05$ (All the values of heats are in Kcal/mole of carbon)(Calcination
+ Dry) Zone

	(1)	(2)	(3)	(4)	(5)	(6)
	f_{CaCO_3}	f_{CaCO_3}	f_{CaCO_3}	f_{CaCO_3}	f_{CaCO_3}	f_{CaCO_3}
	=0	= 0.05	=0.1	=0.1	=0.15	= 0.15
	$g = 0$	$g = 0$	$g = 0$	$g = 0.5$	$g = 0$	$g = 0.5$
Q_{Supply}^{CD}	49.246	51.405	51.405	51.567	51.405	51.648
Q_1^{CD}	45.144	44.098	43.053	44.098	42.007	43.575
Q_2^{CD}	0	5.1	10.2	5.1	15.3	7.65
Q_3^{CD}	7.8	7.8	7.8	7.8	7.8	7.8
Q_4^{CD}	4.9	5.1	5.1	5.1	5.1	5.1
Q_{Demand}	57.82	62.074	66.153	62.102	70.207	64.125

SINTER ZONE

Q_1^{SZ}	50.158	52.357	52.357	52.357	52.357	52.357
Q_2^{SZ}	16.63	16.225	15.818	15.818	15.412	15.412
Q_3^{SZ}	0	0	0	5.64	0	8.46
Q_4^{SZ}	5.9	5.9	5.9	5.9	5.9	5.9
Q_{Demand}	72.688	74.48	74.075	79.715	73.669	82.12
$Q_{Reaction}$ (50% CO, 50% CO ₂ basis) ²	59.4	59.4	59.4	59.4	49.5 59.4	59.4

Contd....

Table 12 : Continued

	(1)	(2)	(3)	(4)	(5)	(6)
Q_{Supply}^{SZ}	0.033 (T_1^i-25)	0.035 (T_1^i-25)	0.035 (T_1^i-25)	0.035 (T_1^i-25)	0.035 (T_1^i-25)	0.035 (T_1^i-25)
T_1^i-25)	402.6	428	416	576.6	405	645
% FeO (Calculated)	15 16.6	10	3.5	3.5	3.5	3.5

$f_c = 0.06$
dry) Zone

(Calcination :
dry) Zone

Q_{Supply}^D	49.246	51.405	51.405	51.54	51.405	51.607
Q_1^{CD}	37.62	36.75	35.877	36.75	35.006	36.31
Q_2^{CD}	0	4.25	8.5	4.25	12.75	6.375
Q_3^{CD}	6.48	6.48	6.48	6.48	6.48	6.48
Q_4^{CD}	4.9	5.1	5.1	5.1	5.1	5.1
Q_{Demand}	49	52.58	55.957	52.58	59.336	54.265

SINTER ZONE

Q_1^{SZ}	50.158	52.357	52.357	52.357	52.357	52.357
------------	--------	--------	--------	--------	--------	--------

Contd...

Table 12 : Continued

	(1)	(2)	(3)	(4)	(5)	(6)
Q_2^{SZ}	13.7	13.36	13.028	13.028	12.69	12.69
Q_3^{SZ}	0	0	0	4.7	0	4.7
Q_4^{SZ}	5.9	5.9	5.9	5.9	5.9	5.9
Q_{Demand}	69.758	71.617	71.285	75.98	70.947	75.65
$Q_{reaction}$	59.4	59.4	59.4	59.4	59.4	59.4
Q_{Supply}^{SZ}	0.033	0.035	0.035	0.035	0.035	0.035
	$(T_1'-25)$	$(T_1'-25)$	$(T_1'-25)$	$(T_1'-25)$	$(T_1'-25)$	$(T_1'-25)$
$(T_1'-25)$	313.8	346	337	470	327	461.2
%FeO	20	12	4.2	4.2	4.2	4.2

$$f_c = 0.07$$

(Calcination:
dry) Zone

Q_{supply}^{CD}	49.246	51.405	51.405	51.52	51.405	51.578
Q_1^{CD}	32.245	31.498	30.75	30.75	30.005	30.005
Q_2^{CD}	0	3.64	7.285	3.642	10.928	5.464

Table 12 : Continued

	(1)	(2)	(3)	(4)	(5)	(6)
Q_3^{CD}	5.55	5.55	5.55	7.405	5.55	7.405
Q_4^{CD}	4.9	5.1	5.1	5.1	5.1	5.1
Q_{Demand}	42.69	45.78	48.655	47.64	51.533	48.97
<u>SINTER ZONE</u>						
Q_1^{SZ}	50.158	52.357	52.357	52.357	52.357	52.357
Q_2^{SZ}	11.6	11.325	11.035	11.035	10.744	10.744
Q_3^{SZ}	0	0	0	4.228	0	6.042
Q_4	5.9	5.9	5.9	5.9	5.9	5.9
Q_{demand}	67.658	69.58	69.29	73.32	69.001	75.043
$Q_{reaction}$	59.4	59.4	59.4	59.4	59.4	59.4
Q_{supply}^{SZ} ($T_1' - 25$)	0.033 ($T_1' - 25$)	0.035 ($T_1' - 25$)	0.035 ($T_1' - 25$)	0.035 ($T_1' - 25$)	0.035 ($T_1' - 25$)	0.035 ($T_1' - 25$)
($T_1' - 25$)						
% FeO	23.8	14.6	5	5	5	5

within 5-6 minutes from the start of the sintering process. Thereafter the gases of the bed would remain at dew point till the dry/calcination zone reaches there. For simplicity, the (calcination + dry) zone is assumed to move at the same velocity as the sinter zone,

Sample calculations for different terms of heat balance is the ^{sinter} outer zone as well as in the (calcination + dry) zone of the bed are shown in table 12 for varying proportions of fuels and fluxes in the bed. The (calcination + dry) zone is assumed to be separated from the sinter zone by the 950°C line. Sinter zone temp. is assumed to be 1300°C for acid sinters at 1200°C for fluxed and superfluxed sinters which ¹²~~gases~~ gases in this zone are assumed to reach temperature of 1400°C. The degree of reoxidation is assumed to be 0.5 for acid sinters, 0.7 for fluxed sinters and 0.9 for super fluxed sinters to give 15% FeO in acid sinters, 10% in fluxed and 3.5% in superfluxed sinter which seem to be of correct orders. One can make the following observation from these calculations

(1) The required carbon content of the bed comes to be around 6% by weight for acid sinters to preheat the bed ¹²~~of~~ 950°C in the dry zone for beds containing ~~0.5~~ 5 wt.% moisture and heat losses assumed as 10% of heat given by hot gases in this zone. For greater heat losses and greater consumption of water, the carbon requirement would increase.

(2) For 6 wt.% carbon in the bed for producing acid sinters, the sinter zone can reach temperature of 1300°C if air gets preheated to around 300°C before reaching the sinter zone. It will get preheated to still higher temperature by the heat released due to the solidification of the molten slag in the sinter zone. The heat requirement for the sinter zone can be met by lower fuel rate provided air get preheated to higher temperatures but then the thermal requirement of the (calcination : dry) zone will not be satisfied. If the bed material does not rise to 950°C in this zone, heat demand in the sinter zone for the bed to reach temp. of 1300°C will increase, thereby requiring extra fuel.

(3) As air gets preheated to higher and higher temperatures with progress of sintering, more heat is made available for the bed in the sinter zone and temperature may even exceed 1300°C in some cases. Dry zone temperature may also exceed 950°C and some carbon in coke would react with CO_2 to produce CO . In such cases the assumption that C burns to produce 50% CO and 50% CO_2 may be quite justified. Available carbon in the sinter zone decreases and thermal stability is restored. CO formed can result in prereduction of Fe_2O_3 to Fe_3O_4 and FeO , and FeO formed can combine with SiO_2 to form $2\text{FeO} \cdot \text{SiO}_2$ which melts at 1250°C or so. This phase is difficult to reoxidised.

4. For fluxed sinters, the amount of carbon ⁱⁿ the bed should increase to satisfy the thermal requirement of the (calcination : dry) zone. Due to presence of fluxes, the bed temperature does

not increase more than 950°C , even though the gases are at higher temperatures of 1400°C . Only when the flux has decomposed completely the bed temperature starts rising in the sinter zone. In such cases loss of C by its reaction with CO_2 will be small. Thermal requirement of the sinter zone are satisfied easily if the air gets preheated to 300°C or so before coming in contact with any liquid slag. A part of the bed material starts melting at $1150\text{--}1200^{\circ}\text{C}$ due to the formation of $\text{CaO}\cdot\text{Fe}_2\text{O}_3$ or $\text{CaO}\cdot 2\text{Fe}_2\text{O}_3$ and the bed temperature may not rise further till all lime is consumed in the formation of slag. The preheating of air is enhanced due to reoxidation of any FeO or Fe_3O_4 formed in the sinter zone. The fuel rate for fluxed sinters are mainly determined ^{by} ~~in~~ the heat requirement for the (calcination + dry) zone.

5. If gases from the sinter zone do not carry enough heat to meet the thermal requirements of the (calcination + dry) zone, the carbonate materials would not be fully decomposed in this zone. The decomposition of the remaining carbonate material would occur in the sinter zone, thereby consuming the heat. This will require extra fuel for combustion to produce heat or the material would not reach the sintering temperature of 1200°C . This phenomenon can also occur if the nature of carbonate material is such that it is difficult to decompose.

CHAPTER-VIII

8.1 Summary and conclusions

It can be concluded from the present work that the basic scientific studies on the production and testing of fluxed and superfluxed iron ore sinters can be carried out in a forced draft sintering unit. The reduction behaviour of the iron ore or the sinters can be studied to some extent by measuring the exit gas composition. This was made possible in the present work by condensation of the H_2O vapours in the exit gas and measuring the remaining volume of the H_2 gas by a soap bubble meter. The important conclusions based on the findings of the present work can be described as below.

1. Addition of water to the iron ore or sinter mixes decreases the bulk density of the material and improves the permeability of the bed. Porosity of the bed (void fraction) remains more or less constant but the bed offers less resistance to the gas flow probably because of the micro-pelletization of iron ore fines during mixing in presence of water and thereby increasing the average size of the solid particles.
2. There is a large increase in the pressure drop across the bed during the process of sintering, probably due to expansion of the gases and solids at high temperature and due to irregular

distribution of materials remaining after the evaporation of moisture, combustion of carbon and the calcination of fluxes.

3. Increase in pressure drop during sintering is much less in those beds where fusion of material occurs to form a fluid slag for bonding. This may be due to an increase in the porosity of the bed which is caused by the solid-liquid transformation.

4. The amount of liquid slag formed & hence the yield and strength of the sinter produced depend upon the maximum temperatures attained by the bed during sintering.

5. The maximum temperatures attained by the bed are more when sintering is carried out at the speed of 0.9-1.0 cm/min compared to 0.5-0.7 cm/min.

6. For acid sinter, the bed must attain temp. of 1300°C or more to make the liquid slag due to formation of fayalite whereas in fluxed sinters, good sintering can be obtained when the bed attains temperature of 1150-1200°C due to the formation of calcium ferrite phases. These observations were also confirmed by performing the crucible studies i.e. heating the oxide mixture to 1200-1300°C in a silicon carbide furnace and taking the x-ray diffraction patterns of the products.

7. Bed temperatures of 1200°C are possible only in those cases where the flux decomposes ahead of the sinter zone so that the calcination of the flux does not absorb heat during the combustion of carbon in the sinter zone.

8. Mathematical models based on overall and zonal thermal balances have been developed to describe the process variables which affect the quality and rate of sintering.

9. Calcite material decomposes at slow rate compared to naturally occurring dolomite. The peak temperatures obtained are low when calcite is present to the extent of 20% of the iron ore in the bed and the effective yield of the product is poor. The pressure drop across such beds during the sintering process are also high. Addition of 20% dolomite in the bed did not give any difficulties in the production of the sinters.

10. The ratio of the agglomerated mass to the charge remained around 0.5 in most of the experiments probably due to the material layers ⁱⁿ the upper portion of the bed and ^{at} ~~on~~ the periphery of the bed in the lower portion did not reach high temperature to cause fusion/slag bonds.

11. The effective yield (defined as the product of the actual yield to the shatter index) was of the order of around 0.40 and this depends ^{ed} greatly on the maximum temperature attained by the bed.

12. A mathematical model is developed to describe the reduction behaviour of iron ore in the shaft by H_2 gas. The model can be used to estimate the exit gas composition and the degree of reduction as a function of time.

13. Experimental results tend to match with the calculated values for the time of reduction ¹⁶ in the beds ~~there~~ are assumed to be 100-200°C below the furnace temperature. This is possible due to cooling caused by the H₂ gas ~~flowing through the bed.~~

14. The reduction patterns of the sinters show that the last 10-30% of materials get reduced with great difficulty. The equilibrium gas composition at equilibrium with the remaining material (2FeO.SiO₂) is in the range of 90-92%.

15. Reduction of hematite is marked by zero percent H₂ in the exit gas at the start of the experiment but the fluxed sinters or the crucible compounds do not exhibit this phenomenon. The exit gas always contain 30-40% H₂, probably due to the formation of the liquid CaO.Fe₂O₃ phase in the outermost layer of the iron ore.

8.2 Recommendations

There is scope for further scientific studies on the sintering of iron ore and the testing of the ore for its reducibility measurements. The following recommendations :

1. More pressure taps and thermocouples can be inserted ~~about the flow of gases~~ to understand the process more clearly.
2. Use of smaller capacity compressor could not allow the sintering to be conducted at flow rates of air higher than 60 l/min. Bigger size compressor and sintering unit are recommended to get

CHAPTER IXAPPENDIX

<u>Specific Heat</u>	<u>Cal/°C/mole</u>
----------------------	--------------------

$c_{p_{\text{gas}}}$	8.5
----------------------	-----

$c_{p_{\text{air}}}$	8
----------------------	---

$c_{p_{\text{solid}}}$	0.22
------------------------	------

$c_{p_{\text{CO}_2}}$	10
-----------------------	----

<u>Heat of formation</u>	<u>Cal/mole</u>
--------------------------	-----------------

$\Delta H_{\text{Fe}_2\text{O}_3}$	196.8
------------------------------------	-------

$\Delta H_{\text{Fe}_3\text{O}_4}$	267.3
------------------------------------	-------

ΔH_{FeO}	63.8
-------------------------	------

ΔH_{CO_2}	94.05
--------------------------	-------

ΔH_{CO}	26.4
------------------------	------

APPENDIX I

SPECIFIC HEAT AND ENTHALPY DATA FOR SPECIES USED IN THE PRESENT WORK

Species	- H ₂₉₈ ^o Heat of formation Cal/mole	C _p = a + bT - cT ⁻²		
		a	b x 10 ³ Cal/deg/mole	c x 10 ⁻⁵
C	0	4.03	1.14	2.04
CO	26420	6.79	0.98	0.11
CO ₂	94050	10.57	2.10	2.06
CaO	151500	11.67	1.08	1.56
CaCO ₃ (25-900°C)	288400	24.08	5.24	6.20
FeO	63800	11.66	2.0	0.67
Fe ₂ O ₃	196800	23.50	18.60	3.55
H ₂	0	6.52	0.78	-0.12
H ₂ O	57800	7.3	2.46	-
MgO	143700	10.18	1.74	1.48
O ₂	0	7.16	1.00	0.4
SiO ₂	217600	14.40	2.04	-
N ₂	-	6.83	0.90	-0.12
Fe ₃ O ₄	267800	21.88	48.20	-

REFERENCES

1. S. Watnabe, Agglomeration, Knepper, 1962, pp: 865-900.
2. S.C. Panigrahy et al., Iron making & Steel making, 1984, Vol. 11, No: 5, pp. 246-252..
3. S.C. Panigrahy et al., Iron making & steel making, 1984, Vol. 11, No: 1, pp: 17-22.
4. Pravin Kumar, B.Tech. Thesis, 1984, IIT Kanpur.
5. S.Eketorp, Agglomeration of Iron bearing minerals, Chipman Conference, 1962, pp: 180-199.
6. Rist, Rev. Met., 58, 17-29 (1961).
7. Fumio Matsuno, Changes of mineral phases during sintering of Fe_2O_3 - CaO - SiO_2 system, Trans. of Iron and steel Institute of Japan, (1981), Vol. 21, No. 9, p. 595-604.
8. E.J. Bagnell, Agglomeration 77, Vol. 2, K.V.S. Sastry, pp: 587.
9. E. Mazanek et al., JISI, Nov. 1968, Vol. 206, 11, pp:1104.
10. R.A. Limons et al., Journal of metals, 1967, (19), 6, pp:70.
11. S. Watnabe , Agglomeration, Knepper, 1962, p: 875.
12. Schenck et al., Agglomeration, Knepper, -O. Nyquist, p.853.
13. Panigrahy et al., Met. Trans, Vol. 15B, March 1984, p.23.
16. Rawat, Amit Chatterjee, Tisco manuscript, April 1979, p: 51-62.
15. A. Chatterjee et al., TISCO, Tech. Journal, April 1979, p. 57.
16. B. Sridhara Rao, M.Tech. Thesis, 1983, IIT, Kanpur.
17. Seth & Ross, Reduction of Iron Ores, Bogdandy, p.181-183.